Mantle Geochemical Geodynamics

Chapter for 'Treatise on Geophysics' volume edited by D. Bercovici
by Paul J. Tackley, Institut für Geophysik, ETH Zürich, Switzerland

February 9 2007

Abstract. Geochemical observations offer one of the most important constraints on mantle structure and evolution, yet interpretations of these have often been in apparent contradiction with geophysical constraints. Thus, a major focus of research has been to understand the interaction between geodynamical processes, particularly mantle convection, and chemical variations, and thus what controls the resulting observed geochemical signatures. Here is presented a review of this field of research. The review first covers the mechanisms by which chemical heterogeneities originate, and geochemical observations and constraints. Then, the physics of the stirring and mixing of passive heterogeneities is presented, including both mathematical theory and experimental results. Chemical layering of the mantle features in many conceptual models, so the dynamics and evolution of layered convection is then discussed. Next, the review turns to dynamical models that track specific trace elements, and finally new concepts that may result in a revision of traditional geochemical interpretations, and the outlook for the future.

1. OBSERVATIONS AND THE ORIGIN OF HETEROGENEITY

1.1 Introduction

Geochemical constraints on mantle heterogeneity are thoroughly reviewed in several papers (e.g., (Graham, 2002; Hilton and Porcelli, 2003; Hofmann, 2003)), but as they are so important for understanding this chapter, it is appropriate to briefly summarize here the basic observations and 'traditional' interpretations. New interpretations are discussed section 6. It is noted that with modern analysis techniques, particularly MC-ICPMS machines, the number of isotopes that geochemists are measuring has increased, and while many isotope systems are consistent in their behavior, additional complexity in interpretation is introduced by isotope systems that are affected by additional processes.

This review starts with models of the bulk silicate Earth composition, then constraints on the variations of composition, which fall into three main categories: (i) mass balance arguments based on the inferred composition of the MORB source and continental crust, (ii) noble gas constraints, and (iii) end-member components identified by analysis of the trace-element isotopic compositions of ocean island basalts (OIB) and mid-ocean ridge basalts (MORB). This section also reviews geophysical constraints on chemical heterogeneity and mantle structure, and the major types of mantle conceptual model that have been proposed to explain geochemical and/or geophysical observations.

1.2 Bulk Earth and Bulk Silicate Earth models

The bulk composition of the whole Earth (i.e., core + mantle +crust) is estimated using a variety of constraints as reviewed in (Palme and O'Neill, 2003), particularly the composition of the Sun, meteorites and upper mantle-derived rocks. The relative abundance of refractory elements is thought to be basically chondritic (i.e., solar), while non-refractory to volative elements show increasing degrees of depletion. The composition of the silicate part, i.e., bulk silicate Earth (BSE) is further influenced by core extraction, which enriched the mantle in non-siderophile elements but depleted it in siderophile elements. A commonly-used compositional BSE model is that of (McDonough and Sun, 1995), but a more depleted model was recently proposed by (Lyubetskaya and Korenaga, 2007a). Knowledge of the trace element content of the bulk silicate Earth is important in making 'mass balance' arguments summarized later, as is knowledge of the composition of the continental crust (e.g., (Rudnick, 1995; Rudnick and Fountain, 1995; Taylor and McLennan, 1995)). A recent review concludes, however, that Earth's composition is unlike any meteorite (Drake and Righter, 2002). The reader is referred to the above cited literature for further detailed arguments.

1.3 Fractionation of Major and Trace Elements

When solid and liquid coexist in equilibrium with each other in a multi-component material such as mantle silicates, the composition of the solid and liquid components are different in both major and trace elements. The two main situations for solid-liquid equilibration are are pressure-release partial melting and the crystallization of a magma ocean.

A crude way of viewing major element fractionation is that different minerals have different melting temperatures- for example in the shallow mantle garnet and clinopyroxene melt at a lower temperature than olivine. Thus, partial melting followed by melt segregation and eruption causes both the crust that forms from the resulting melt, and the residual solid, to have a different composition from the original rock. In a cooling magma ocean, this results in the solid crystals that form having a different composition from the remaining liquid, which might allow them to settle to the top or bottom due to related density differences. Indeed, density differences that result from

differences in major element composition may well play an important role in mantle dynamics, as discussed in later sections.

Trace element partitioning between solid and liquid is expressed in terms of partition coefficients *d*, which describe the equilibrium concentration of the element in the solid divided by the concentration in the liquid.

$$d = \frac{C_{solid}}{C_{liquid}} \quad (1)$$

where C_{solid} and C_{liquid} are the concentration of the element in the solid and liquid respectively. A partition coefficient << 1 means that the element preferentially enters the melt, and is known as an incompatible element. Conversely, a partition coefficient >> 1 indicates that the element is compatible and stays in the solid. The partition coefficient depends on the element (because different elements have difference sizes and electronic properties), which results in trace elements being fractionated during melting, i.e., the ratio of their concentrations changes. Partition coefficients may also depend on pressure (depth), oxygen fugacity and, of course, the minerals present. Different isotopes of the same element have partition coefficients that are almost the same, and can be treated as identical for the situations discussed in this chapter. For more information see (Righter and Drake, 2003; Wood and Blundy, 2003) and (Wood, Treatise vol. 2).

This fractionation of trace elements plays a key role in the evolution of isotope ratios of interest in mantle geochemistry. In a simple radioactive decay system in which a parent isotope radioactively decays to a daughter that is a different element, the parent to daughter ratio (P/D) will change as a result of melting and crustal formation, whereas the ratio of the daughter to a stable isotope of the same element (D/D_S), will not change. This change in (P/D) affects the future rate of change of (D/D_S). By analyzing the (D/D_S) ratio in two or more samples that have experienced fractionation in a single event, it is possible to derive the elapsed time since the fractionation event, and this is the principle of radiogenic dating. The specific example of Pb-Pb dating is more complicated because it combines two decay systems, but this also makes it more robust (for details see, e.g., (Stacey, 1992)).

The concentration of trace elements in the melt depends not only on the partition coefficient but also the melt fraction. For example a highly incompatible element essentially all enters the melt, which means that its concentration in the melt is inversely proportional to melt fraction. In the more general case, it is straightforward to derive an equation for the equilibrium concentration of a trace element in the melt (Shaw, 1970):

$$C_{liquid} = \frac{C_0}{F + d(1-F)} \quad (2)$$

where F=melt fraction and C_0=concentration in the total (bulk) system. Thus the enrichment of a magmatic product in trace elements relative to its source can be used to estimate the melt fraction.

1.4 Trace Element Budgets of the Crust and Mantle

The trace element composition of the continental crust and the inferred composition of the MORB source are often compared to the composition of the bulk silicate Earth discussed earlier. This comparison indicates that the continental crust is strongly enriched in incompatible trace elements- by a factor of ~50-100 in the most incompatible elements, whereas the MORB source is depleted. Furthermore, the patterns of enrichment and depletion (i.e., as a function of elements) appear to be complementary. The enriched continental crust and the depleted MORB source region have thus long been thought to be complementary in their trace element signature, implying that the MORB

source region is the residue from melting that produced the continental crust (e.g., (Hofmann, 1988)). Mass balance calculations have been used to estimate the fraction of the mantle that must be depleted to make the continental crust (e.g., (Jacobsen and Wasserburg, 1979; O'Nions et al., 1979; Davies, 1981; Allegre et al., 1983a; Hofmann, 1988)) with estimated depleted reservoir size ranging between 30-97% of the mantle and the rest of the mantle being primitive, i.e., roughly chondritic. Even with the latest constraints there is a considerable range in the estimated depleted reservoir size: 50-80% of the mantle (Hofmann, 2003). A curious feature of this calculation is that the degree of melting required to produce continental crust is small, e.g., ~1% (Hofmann, 2003)--about an order of magnitude lower than the 8-10% melting thought to produce present-day MORB. This indicates that incompatible trace elements must be scavenged from a large volume and concentrated into a small volume in order to produce the concentrations observed in continental crust, as discussed in section 1.5.2.

Reservoir of 'missing' elements. The above mass balance calculation implies the existence of a primordial reservoir of primitive (i.e., bulk silicate Earth) composition containing the trace elements that are 'missing' from the continental crust plus depleted (MORB source) mantle. This inferred reservoir of volume 20-50% of the mantle is often argued to be important in explaining the mantle's heat budget, as it would contain a large amount of heat-producing elements, and the concentration of heat-producing elements in the MORB source appears to be too low to explain the mantle's heat budget. The reservoir appears to be 'hidden', in the sense that it produces no observed geochemical signature, except perhaps that of high $^{3}He/^{4}He$. As an alternative to a primitive reservoir, it has also been proposed that the 'missing' trace elements are contained in a smaller, enriched reservoir (e.g., (Coltice and Ricard, 1999; Tolstikhin and Hofmann, 2005; Boyet and Carlson, 2006; Tolstikhin et al., 2006)).

1.5 Origin of Heterogeneities

Chemical variations inside the mantle could arise either from primordial differentiation of the Earth, through subsequent magmatism, or through possible minor reactions with the core, and these are discussed in this section. Quantitative models of either process require a knowledge of the bulk composition of the mantle, which was discussed in section 1.2.

1.5.1 Primordial (fractionation of magma ocean, core formation, early atmosphere)

The extent to which the mantle might have started off layered due to fractional crystallization of a magma ocean has been hotly debated over the years. Key issues are whether a deep magma ocean existed, and if so whether its cooling would result in a fractionation due to crystal settling, or whether it would instead solidify into a chemically homogeneous mantle. This depends on various factors such as type of transient atmosphere present, grain size, viscosities, convection mode, etc. (Solomatov and Stevenson, 1993a; Solomatov and Stevenson, 1993b; Abe, 1997). The existence of a deep magma ocean has previously been argued against because the geochemical signature of the mantle is inconsistent with wholesale fractionation (e.g., (Ringwood, 1990a)), but if magma ocean convection is vigorous enough that crystals do not settle (Tonks and Melosh, 1990; Solomatov et al., 1993; Solomatov and Stevenson, 1993b), then this difficulty vanishes. Furthermore, models of Earth formation predict collisions with planetesimals the size of the Moon or even Mars (the latter of which offers the most popular explanation for the formation of the moon), which would inevitably result in large scale melting and a deep terrestrial magma ocean (e.g., (Benz and Cameron, 1990; Melosh, 1990)). Another possibly important aspect of magma ocean evolution is its interaction with the primordial atmosphere, through which it might have absorbed volatile elements (e.g., (Ballentine, 2002)), although (Ballentine et al., 2005) suggests that this was not important for primitive volatile (particularly He/Ne) acquisition.

While there is therefore much uncertainty about magma ocean evolution, a recent synthesis by (Solomatov, 2000) offers a scenario that is consistent with both geochemical and dynamical constraints. In this, following a giant impact the lower mantle solidifies rapidly (i.e., <1000 years) and undifferentiatedly, leaving a shallow magma ocean in which fractionation and much slower cooling occur. This is consistent with the earlier work of (Abe, 1997), who also found that following a giant impact, lower mantle differentiation is uncertain whereas upper mantle differentiation is likely, and a shallow magma ocean could remain for 100-200 Myr.

Another chemically-important process is the separation of the metal core from the remaining silicate. Metal-silicate separation is likely to have occurred in (at least) two environments (Stevenson, 1990; Karato and Murthy, 1997): small metal droplets falling through a magma ocean, where separation would occur rapidly (Tonks and Melosh, 1990; Solomatov, 2000; Rubie et al., 2003; Hoink et al., 2006), and large metal diapirs sinking through solid silicate or primitive material. The details of these strongly influences the partitioning of trace elements between the mantle and core as well as the extent to which the core and mantle are chemically equilibrated in general. Specifically, chemical equilibration is efficient in a magma ocean, but is ineffective for large sinking diapirs, leading to the view that metal-silicate equilibration last happened at temperatures and pressures relevant to the base of the magma ocean (Murthy and Karato, 1997). Such mechanisms are relevant to questions such as whether the core contains potassium or noble gases, as well as whether reactions between the mantle and core take place.

In summary, at the present moment the consensus from geochemical constraints combined with dynamical considerations is that primordial chemical stratification in the deep mantle is unlikely, whereas primordial upper mantle chemical stratification is likely. Partitioning of elements between the mantle and core is sensitive to poorly-known processes that occurred during core-mantle separation.

1.5.2 Formation of continental and oceanic crust

It is clear that much differentiation has taken place due to melting subsequent to Earth's formation. The most obviously manifestations of this are (i) the formation of the continental crust, which is strongly enriched (by a factor of up to 50-100) in incompatible trace elements compared to bulk silicate Earth models and can survive over billions of years, and (ii) the formation of the oceanic crust, which is less enriched and gets subducted back into the mantle after 100-200 Myr possibly to get mixed again (see later discussion). A thorough review of crustal formation and its geochemical consequences was given in (Hofmann, 2003); here the main points relevant to the discussion in this chapter are summarized.

Continental crust. As discussed above, the (enriched) continental crust is typically thought to be complementary to the depleted mantle, with an implied degree of melting of ~1%. This is very low, and suggests that continental crust is produced by more complex process than simple partial melting (by ~1%) and eruption- indeed, melting experiments carried out on peridotite produce magmas that do not resemble (i.e., are less 'evolved' than) the continental crust in their major element composition (Hirose and Kushiro, 1993; Rudnick, 1995). Various possibilities have been proposed, as reviewed by (Rudnick, 1995). Modern continental crust is produced either by the intraplate volcanism (i.e., flood basalts on continents, or accretion of oceanic plateaus) or at convergent margins, for which an important process is dehydration of subducted crust and removal and transport of incompatible elements by the resulting fluid in the subduction wedge, followed by metasomatism and melting to produce new crust. Processes generating continental crust may have different in the Archaean (e.g., (Rudnick, 1995; Taylor and McLennan, 1995)): possibilities include melting of subducted oceanic crust, weathering of surface rocks leading to depletion in MgO. Furthermore the growth history of continents is highly uncertain, and reflects a balance between processes of production of new continents and entrainment of delamination of old continental material, with several different models proposed (e.g., (Reymer and Schubert, 1984; Taylor and McLennan, 1995)). Recent zircon data implies that continents already existed 4.4-4.5 Gyr before

present and were being rapidly recycled into the mantle (Harrison et al., 2005). According to (Rudnick, 1995), anywhere between 40-100% of the present mass of the continents may have existed since the Archaean. New material is still being added.

Oceanic crust. While continental crust formation is generally considered to be the dominant influence on the trace element abundances in the mantle (the present-day oceanic crust is much less enriched and smaller in volume), a large fraction of the mantle has passed through the melting ("processing") zone beneath mid-ocean ridges, and thus the production and recycling of oceanic crust has had a major influence on mantle heterogeneity. The rate at which this happens is somewhat uncertain and is discussed in detail in the next section. Regardless of the exact rate of processing, subducted MORB is clearly a volumetrically-significant component in the mantle and should not be ignored in calculating mantle geochemical evolution.

1.5.3 Processing rate of mid-ocean ridge melting

The exact volume of material that has been processed by MOR melting is quite uncertain, because of differing estimates of the present-day rate of processing and uncertainty about how this changed in the past over billions of years. One measure of the processing rate is the 'residence time', which for random sampling of the mantle is equal to the length of time taken for the mass of the mantle to pass through the processing zone. At present rates of seafloor spreading, estimates of this processing time or residence time have varied widely, from 2.9-10 Ga. Example estimates are: 4 Gyr (O'Connell and Hager, EOS 61, 373, 1980, as referenced in (Davies, 1981)), 10 Gyr (Gurnis and Davies, 1986b), 5.7 Gyr (Kellogg and Wasserburg, 1990), 3-6 Gyr (Davies, 2002), 9.5 Gyr (Phipps Morgan, 1998), 4.5 Gyr (Xie and Tackley, 2004b), or 2.9 Gyr (Coltice, 2005). It is worth analyzing why there is such a large variation in these estimates. The processing rate, expressed as the volume of mantle processed per year is given by:

$$P = Ad\rho \quad (3)$$

where A is the area of oceanic seafloor produced per year, d is the depth of onset of melting beneath spreading centers, and rho is the density of the processed material. Observations of the age distribution of ocean floor (e.g., summarized in (Phipps Morgan, 1998)) indicate that A=2.7 km^2/year for seafloor produced in the last 1 Ma, or A=2.9 km^2/year based on an average over the last 100 Ma, the latter being similar to the 3.0 km^2/year estimated by (Stacey, 1992). Other authors have preferred to use 'back of the envelope' estimates, for example (Davies, 2002) assumed a ridge length of 40,000 km and spreading velocity of 5-10 cm/year (giving A=2-4 km^2/year) and (Coltice, 2005) assumed a ridge length of 60,000 km and plate velocity of 5 cm/year (A=6 km^2/year). Regarding onset depth of melting d, (Phipps Morgan, 1998) assumed that the oceanic crustal thickness of 6.5 km was produced with 10% melt, ($d = 65\rho_{crust}/\rho_{mantle}$ km), whereas (Davies, 2002) assumed d=100 km and (Coltice, 2005) assumed d=150 km. Using the observationally-constrained A=2.9 km/year together with, for example, d=80 km and peridotite density = 3000 kg/m^3 leads to P=6.96×10^{14} kg/year, which gives a timescale of 5.74 Gyr to process the mantle mass of 4×10^{24} kg. Thus, estimates of processing time as low as 3 Gyr should be regarded as extreme lower limits. Estimates of the present-day processing time based on geochemical fluxes (Albarède, 2005b) range from 4-9 Gyr, bracketing the geophysical value discussed above; this estimate is further discussed in section 2.5.

It is likely that the rate of seafloor spreading and hence crustal production was considerably higher in the past when the mantle was hotter, which would greatly reduce the processing/residence time in the past (Gurnis and Davies, 1986b). In addition, the depth of melting would have been larger due to the hotter mantle, as considered by (Tajika and Matsui, 1992; Tajika and Matsui, 1993; Davies, 2002), further increasing processing rate. The appropriate increase of seafloor spreading in the past is not known: in simple, internally-heated convection in secular equilibrium the surface velocity scales as (radiogenic heat production)^2 (Davies, 1980), and (Phipps Morgan,

1998) gave detailed arguments why this also applies to plate tectonics. It is, however, likely that the early Earth did not have plate tectonics as it exists today because the thicker oceanic crust and younger oceanic plates (when they reach subduction zones) would make plates difficult to subduct (Vlaar, 1985; Davies, 1990; Davies, 1992), and perhaps because the mechanical oceanic lithosphere was thicker because water depletion, which causes an increase in viscosity, occurred deeper (Korenaga, 2003). Thus, the most likely increase in crustal production rate lies between constant and H^2, where H=radiogenic heat production rate.

To give some quantitative examples of the influence of faster processing in the past: (i) (Xie and Tackley, 2004b) calculated the volume of oceanic crust produced over the age of the Earth to be ~10% of the mantle mass if the present day production rate applied to whole Earth history, 54% if the H^2 law of (Davies, 1980) applied, or 82% if the increase in depth of melting due to higher mantle temperatures were additionally taken into account. In the latter two cases, this clearly implies that the same material melts two or more times, as it is not possible to produce this amount of MORB from the residue of continental crust production. (ii) (Davies, 2002) calculated that the H^2 law leads to 4 times the amount of processing over geological time, which he expressed as being equivalent to 18 Gyr of constant-rate processing. This means that 98.6% of the mantle is processed if the present-day residence/processing time is 4.2 Gyr

1.5.4 Reactions with the core

Some researchers have studied the possibility of an iron-rich layer forming above the CMB caused by reactions with the core. There is some geochemical evidence (based on the Os-Pt system) for mass exchange between the mantle and core (Walker et al., 1995; Brandon et al., 1998; Brandon et al., 2003; Humayun et al., 2004), but this is controversial (Schersten et al., 2004; Brandon and Walker, 2005).

Experiments indicate that iron reacts with silicate perovskite to form iron oxide and silica (Knittle and Jeanloz, 1989; Knittle and Jeanloz, 1991). Experiments with liquid iron and solid silicate show that the silicate becomes depleted in Fe and O (Goarant et al., 1992). Liquid iron also reacts with Al_2O_3 at CMB pressures (Dubrovinsky et al., 2001) but not with silica (Dubrovinsky et al., 2003). Using thermodynamic calculations, (Song and Ahrens, 1994) determined that the observed reactions are thermodynamically possible. Thus, core-mantle reactions are expected from an experimental standpoint, although it is possible that the presence of water inhibits them (Boehler et al., 1995; Poirier et al., 1998).

It appears difficult to generate significant mantle heterogeneity this way, because the thickness of the reaction zone is relatively small. (Poirier and Le Mouel, 1992; Poirier, 1993) find that liquid Fe can penetrate 1-100 m into the mantle along grain boundaries if it reacts with the silicate. (Knittle and Jeanloz, 1991) proposed that the Fe ascents by a capillary action driven by surface tension. However, a much more efficient mechanism is a suction mechanism in areas of downwelling (where the CMB is depressed) may entrain Fe of order ~1 km into the mantle with fractions of up to 10%, depending on parameters such as the effective bulk viscosity (Stevenson, 1988; Kanda and Stevenson, 2006). (Petford et al., 2005) also proposed a dynamically-assisted Fe transfer mechanism assuming that the D" region behaves as a poro-viscoelastic granular material with dilatent properties, but the required strain rates are rather high (10^{-12} s^{-1}). Thus, it appears that Fe might be able to infiltrate up to ~1 km at significant volume fractions, but this needs further study.

If Fe does infiltrate the mantle in some regions in a thin (<=1 km) layer and react to form dense products, the question is then whether the continual flux of new mantle material through this reaction zone is sufficient, over geological time, to affect a volumetrically significant amount of mantle material. (Knittle and Jeanloz, 1991) suggested that the material would not be raised far into the mantle because of its increased density, and could accumulate into a ~few 100 km thick D" layer, but this needs to be tested using detailed modeling. Numerical models of this performed to date have parameterized core reactions as an effective chemical diffusivity, which may not

correctly capture the process. The most advanced model is that of (Kellogg, 1997), who parameterized the infiltration of Fe using a chemical diffusivity 100-1000 times smaller than the thermal diffusivity, and found that large density contrasts (B=10) result in a thin (<100 km) layer that slows further growth, whereas lower density contrast (B=1) result in an undulating layer several 100s km thick that piles up under upwellings, as is observed in earlier calculations (Hansen and Yuen, 1988). If a metal –bearing layer does build up, it could have a thermal conductivity an order of magnitude higher than that of silicates (Manga and Jeanloz, 1996), which could further influence mantle convection.

It has been proposed that silicate melt (partial melt fractions up to 30%) exists in some areas at the core-mantle boundary (CMB) as an explanation of seismically-observed Ultra Low Velocity Zones (ULVZs) (Williams and Garnero, 1996; Lay et al., 2004). Such areas of partial melt could have interesting geochemical consequences. Firstly, they might facilitate reactions between the mantle and the core due to the larger flux of mantle material that comes into contact with the core. Secondly, incompatible trace elements would be redistributed between melt and different solid phases with different partition coefficients. If they were still incompatible then the melt could act as a reservoir of such elements; however, (Hirose et al., 2004) found that large ion lithophile (LIL) elements partition into the solid calcium-perovskite phase rather than the melt, which should result in measurable geochemical signatures for plumes. Lateral variations in the occurrence and/or thickness of partially-molten zones could be due to lateral variations in bulk composition, or possibly to the interplay between upwellings, downwellings and melt migration. In the past, the CMB temperature was higher and so such regions of partially molten silicate would have been larger and/or more prevalent, or at least, more likely.

1.6 MORB and OIB Trace Element Signatures

1.6.1 Noble gases

The most common noble gases considered in mantle geochemistry are the isotopes of He and Ar, with Ne and Xe also sometimes considered.

^{3}He/^{4}He ratios. The two isotopes of Helium are ^{3}He, which is primordial, and ^{4}He, which is produced by the radioactive decay of U and Th. Histograms of the ratio of ^{3}He/^{4}He for mid-ocean ridge basalts (MORBs) and ocean island basalt (OIBs) show clear differences. MORBs have a relatively constant ^{3}He/^{4}He ratio with a mean value of 1.16×10^{-5}, which is a factor of 8.4 higher than the atmospheric value (Kurz et al., 1983; Allegre et al., 1995; Graham, 2002). The range of ^{3}He/^{4}He ratios between 7 and 9 is thus taken as representative of the depleted upper mantle. OIB ^{3}He/^{4}He ratios are, in contrast, extremely heterogeneous, extending to both higher and lower values than MORB, with the highest ratios measured (at Baffin Island) about 50 times atmospheric (Stuart et al., 2003).

There are several possible explanation for the high ^{3}He/^{4}He material. The 'traditional' interpretation is that this component comes from an undegassed, 'primitive' source, because noble gases are highly incompatible and volatile, and are thus expected to enter any melt and be heavily out gassed prior to or during eruption (Allegre et al., 1983b; Farley et al., 1992; Porcelli and Wasserburg, 1995) (note that outgassing requires CO_2 bubbling, which occurs at depths less than 60 km). This component has traditionally been identified as the lower mantle, consistent with the need to keep it intact for billions of years, with other arguments for the lower mantle being primitive, and with the idea of plumes sampling the lower mantle and spreading centers sampling the upper mantle. However, the actual volume and location of this component is not constrained. If the 'primitive' interpretation is correct, one might expect the absolute concentration of He in OIB to be higher than that in MORB, but this is not observed, perhaps because magma chamber processes cause loss of He (Farley and Neroda, 1998).

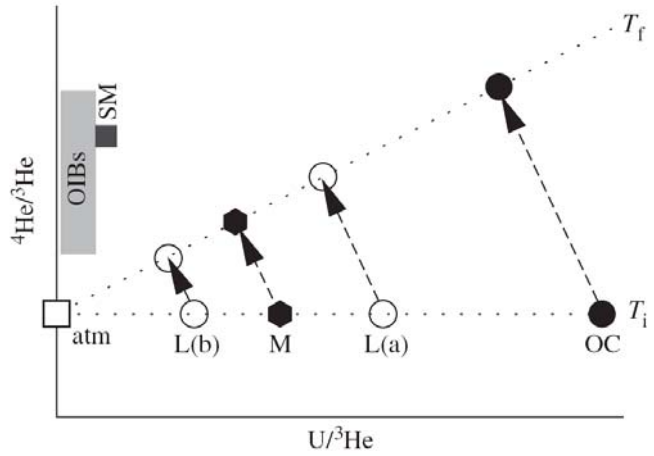

Figure 1. Schematic diagram showing the Helium isotope evolution of different mantle components, from (Coltice and Ricard, 2002). M=mantle, L=lithosphere, atm=atmosphere, OC=oceanic crust. When M melts it produces oceanic crust, lithosphere (a) or (b) depending on the relative partition coeffients of U and He, and some He is lost to the atmosphere. Between melting events, U decays and produces ^{4}He, so U/^{3}He decreases and ^{4}He/^{3}He increases. The shallow mantle (SM) is a mixture of recycled lithosphere and oceanic crust, so recycled lithosphere will always have lower ^{4}He/^{3}He (high 3He/4He) than the average, regardless of the relative partition coefficients. With successive melting events, the mantle average ratios move to the right due to He outgassing.

The leading alternative explanation for high ^{3}He/^{4}He is that it is associated with recycled depleted oceanic lithosphere (Albarède, 1998; Anderson, 1998; Coltice and Ricard, 1999; Ferrachat and Ricard, 2001; Coltice and Ricard, 2002). This is based on the fact that as high ^{3}He/^{4}He simply requires high ^{3}He/(U+Th) because decay of U and Th produce ^{4}He. Therefore, an alterative to high [^{3}He] is low [U+Th], which is found in material that has been depleted in incompatible trace elements due to melting. The evolution of He ratios is illustrated in Figure 1. Note that ^{3}He/^{4}He decreases with time in all 'reservoirs' due to the radiogenic ingrowth of ^{4}He. If the ratio ^{3}He/(U+Th) is changed in different components due to fractionation (during which ^{3}He/^{4}He remains the same), then with time, it will evolve ^{3}He/^{4}He that is higher or lower than the original material. If He is less incompatible than U and Th (e.g., (Graham et al., 1990), and as found in recent laboratory experiments (Parman et al., 2005)), then ^{3}He/(U+Th) is higher in the depleted residue and after some time its ^{3}He/^{4}He will be higher than that of the original material. However, (Anderson, 1998; Coltice and Ricard, 1999; Ferrachat and Ricard, 2001; Coltice and Ricard, 2002) showed that it is not necessary for He to be less incompatible if the residuum is stored for substantial time periods while the rest of the mantle becomes increasingly outgassed. To understand this, note that in the crust, ^{3}He/(U+Th) is extremely low due to degassing of He and concentration of U and Th, so the crust will have much lower ^{3}He/^{4}He regardless of the exact relative He and U partitioning. If the mantle has almost all differentiated, such that to first order it is made of a mixture of subducted crust and depleted residue, then the average mantle ^{3}He/^{4}He will inevitably be inbetween the ratios in residue and subducted crust, making residue ^{3}He/^{4}He appear to be high.

Another proposed explanation of the "primordial" helium component is that it comes from the core. However, the only measurements of noble gas partitioning between silicate melt and iron melt under pressures up to 100 kilobars indicate that the partition coefficients are much less than

unity and that they decrease systematically with increasing pressure (Matsuda et al., 1993). These results suggest that Earth's core contains only negligible amounts of noble gases if core separation took place under equilibrium conditions at high pressure, although the uncertainties are too great to rule out the core as a potential mantle ^{3}He source (Porcelli and Halliday, 2001).

Finally, it has been proposed that a large amount of ^{3}He has delivered to the Earth's surface by cosmic dust, and then recycled to the mantle (Allegre et al., 1993; Anderson, 1993). Several arguments have been made against this proposal (Farley and Neroda, 1998); in particular, the dust flux is several orders of magnitude too low to account for the ^{3}He flux out of the mantle, and ^{3}He is expected to be degassed from the dust particles during subduction.

Heat – Helium imbalance: The present-day flux of ^{4}He out of the mid-ocean ridge system has been estimated by measuring the concentration of ^{4}He in ocean water. (O'Nions and Oxburgh, 1983) pointed out that this ^{4}He flux is only a small fraction of what would be expected from the concentration of ^{238}U, ^{235}U and ^{232}Th in MORB and even lower than U and Th in bulk silicate Earth, which has led to the term "heat-Helium imbalance". The 'traditional' explanation of this is that the radiogenic sources are trapped in the lower mantle, from which heat can escape by conduction across a thermal boundary layer, but ^{4}He cannot. It has been suggested that the concentration of ^{4}He might be misleading because this is influenced by short-timescale processes, whereas the concentration of U and Th is a long-timescale process. Possible solutions to this are discussed in later sections 4.1.1 and 5.1.

Argon outgassing. Argon has three stable isotopes, the two of most interest being 'primitive' ^{36}Ar, and 'radiogenic' ^{40}Ar. There is virtually no primordial ^{40}Ar in the Earth (Ozima and Kudo, 1972), it being entirely produced by the decay of ^{40}K. As Ar does not escape from the atmosphere (unlike He) due to its large atomic mass, the amount of ^{40}Ar in Earth's atmosphere represents the total amount of argon degassed from the Earth's interior over the age of the Earth. This atmospheric ^{40}Ar budget, when combined with an estimate of the total ^{40}K content of the Earth, implies that approximately half of all ^{40}Ar produced within Earth since its formation is retained within the solid Earth (Allegre et al., 1996; O'Nions and Tolstikhin, 1996), which gives a constraint on the fraction of the mantle that has been processed through mid-ocean ridge or other melting environments. There is some uncertainty in this figure due to uncertainty in the amount of ^{40}K in the mantle and a fairly small uncertainty in how much of the ^{40}Ar in continental crust has actually outgassed. The uncertainty in total amount of K arises because in the planetary formation process K is moderately volatile, so the total amount of K is usually calculated from the total amount of (refractory) U assuming some a particular K/U ratio, estimates of which range from a widely-accepted value of 12,700 (Jochum et al., 1983) to as low as 2800 (Stacey, 1992). The continental crust contains ~1/3 to 1/2 of the K budget (Rudnick and Fountain, 1995) and for the above mass balance calculation is usually assumed to be completely outgassed in the resulting ^{40}Ar, which may not be the case (see e.g., discussion in (Phipps Morgan, 1998)). The linkage between K assimilation by the continental crust and ^{40}Ar crust and mantle outgassing can be used to constrain the relative amounts of K in the crust and Ar in the atmosphere (Coltice et al., 2000a). In any case this "50% outgassing" constraint is commonly misinterpreted to mean than 50% of the mantle is undegassed- in fact, because Earth's ^{40}Ar was continuously produced over geological time from a negligible initial concentration, the mantle could have almost entirely degassed early in its history, and still match the Ar constraint. In other words, early or accretionary degassing events do not influence ^{40}Ar outgassing. Quantitatively, for a constant convective vigor (van Keken and Ballentine, 1999) show that outgassing 50% radiogenic ^{40}Ar implies outgassing 72% of primordial, nonradiogenic species. If the convective vigor were higher in the past then the latter fraction can be much higher. (Phipps Morgan, 1998) showed that the outgassing constraint is perfectly compatible with whole-mantle convection, even if the processing rate is much higher in the past: for example assuming that the present-day processing time is 9.6 Gyr and was faster according to (heating rate)^2 in the past, one obtains 93% outgassing of primitive ^{36}Ar but only 58% outgassing of radiogenic ^{40}Ar, or 98% primitive outgassed while retaining 31% of radiogenic Ar. A better expression of this

constraint is "50% of the mantle has been undegassed *since the ^{40}Ar was produced in it*" (Phipps Morgan, 1998).

The Argon paradox. A more problematic constraint arises from the concentration of Ar in the MORB source region, which is much lower than what would be expected if the ^{40}Ar remaining in the mantle were evenly distributed (Turner, 1989). This has traditionally been interpreted to mean that the additional, 'missing' ^{40}Ar must be 'hidden' in the lower mantle, which should have about 50 times the ^{40}Ar concentration of the upper mantle (Allegre et al., 1996). It has been argued that this difficulty could be resolved if the amount of ^{40}K in the mantle were lower than commonly estimated (Albarède, 1998; Davies, 1999). Another reconciliation is that this, as well as the heat-Helium imbalance and the apparent need for a deep ^{3}He reservoir, could be reconciled if the estimate of ^{40}Ar in the shallow mantle, which comes from measured short-term ^{3}He fluxes into the oceans, were too low by a factor of 3.5 (Ballentine et al., 2002). It is important to note that the proposal of K in the core does not help with this paradox, because it is the imbalance between mantle Ar and K that is the problem.

Neon, Xenon, Krypton. Far less attention has been paid to isotopes of these elements, largely because of atmospheric contamination problems (Farley and Neroda, 1998; Ballentine and Barford, 2000; Ballentine, 2002), but some recent work has important implications for mantle processes. Neon has three isotopes (atomic weights 20,21,22), of which ^{21}Ne is radiogenic and ^{20}Ne and ^{22}Ne are primordial. Recent measurements of ^{20}Ne/^{22}Ne in magmatic CO_2 well gases (Ballentine et al., 2005) provide the first unambiguous value for the convecting mantle noble gas abundance and isotopic composition, and indicate that the upper mantle has a ^{20}Ne/^{22}Ne similar to that of solar wind irradiated meteorites (~12.5, so-called Neon-B), which is significantly lower than ^{20}Ne/^{22}Ne of the solar nebula (13.6-13.8). This Neon-B value is reproduced in samples from Iceland and Hawaii (Trieloff et al., 2000) and Reunion (Hopp and Trieloff, 2005). Some studies (e.g., (Honda et al., 1999; Dixon et al., 2000; Moreira et al., 2001), have argued for a solar component based on extrapolating plots of ^{20}Ne/^{22}Ne vs. ^{21}Ne/^{22}Ne but their measured ^{20}Ne/^{22}Ne values are not higher than the Neon-B value. However, some samples from Iceland (Harrison et al., 1999) and the Kola peninsular (Yokochi and Marty, 2004) appear to have ^{20}Ne/^{22}Ne>12.5, which if verified would represent a minor component.

These measurements imply that the convecting mantle is dominated by Neon gained by solar wind irradiation of accreting material (Neon-B), but that another "solar" component might exist, sometimes sampled by plumes, associated with early-accreted material with a solar nebula composition. The latter might be in the deep mantle or core (Ballentine et al., 2005). Alteration by recycled material appears to have played a minimal role. While measured Xe and Kr ratios generally appear air-like (Ballentine, 2002), evidence for 'solar' Xe has also been detected in CO_2 well gases by (Caffee et al., 1999). A recent analysis suggests that the mantle content of 'heavy' noble gases (i.e., Xe,Kr,Ar) is dominated by ocean water subduction (Holland and Ballentine, 2006), consistent with the finding of (Sarda et al., 1999) that a significant amount of mantle Ar is recycled.

1.6.2. The end member "zoo"

Analysis of the varying trace-element isotopic compositions of ocean island basalts (OIB) and mid-ocean ridge basalts (MORB), particularly those of Sr, Nd, Hf and Pb suggest that they are the result of mixing between several "endmembers", which are typically referred to as DMM, HIMU, EM1 and EM2 (White, 1985; Zindler and Hart, 1986; Carlson, 1994; Hofmann, 2003). Additionally considering He data leads to a further component, commonly referred to as C or FOZO. The common interpretations of these are as follows:

DMM (Depleted MORB mantle). This endmember represents the most depleted MORB. Most MORBs are not as depleted as DMM, but plot on the DMM – HIMU trend.

HIMU (High-μ). μ is the ratio $^{238}U/^{204}Pb$. As U and Th decay into ^{207}Pb and ^{206}Pb with time, high μ leads to high ratio of radiogenic to primordial lead, i.e., $^{206}Pb/^{204}Pb$ - a 'radiogenic' signature. This component is typically interpreted to be recycled oceanic crust (Chase, 1981; Hofmann and White, 1982; Allegre and Turcotte, 1986; Hofmann, 1997). However, as U and Pb are approximately equally compatible (or U is slightly more incompatible) when making oceanic crust, some additional mechanisms must be invoked to fractionate U and Pb to make the HIMU signature. The invoked mechanisms are hydrothermal removal of Pb from the subducted slab into subduction-related magmas (Hofmann, 1988) and enrichment of the oceanic crust in continental U carried by eroded sediments.

EM (Enriched Mantle) 1 and 2. These signatures are observed in OIBs, but their origin remains controversial. Leading explanations are (Carlson, 1994; Hofmann, 2003): EM1 may originate from either recycling of delaminated subcontinental lithosphere or recycling of subducted ancient pelagic sediment, while EM2 may be recycled oceanic crust with a small amount of sediment, melt-impregnated oceanic lithosphere, or sediment contamination of plume-derived magmas as they pass through the crust.

FOZO (Focus zone). Components that are essentially the same as FOZO (Hart et al., 1992; Hilton et al., 1999) have also been named C (Hanan and Graham, 1996), PHEM (Farley et al., 1992), PREMA (Zindler and Hart, 1986) and HRDM (Stuart et al., 2003). This corresponds to the high $^{3}He/^{4}He$ component, and in other isotopes has a composition on the DMM-HIMU trend, although in the definition of (Stracke et al., 2005) it lies off the DMM-HIMU trend when considering the Sr-Rb system. Samples from many OIB associations appear to form linear trends that radiate from FOZO to various enriched compositions.

Isotopic "Ages". As discussed earlier, isotope ratios evolve along separate paths in different materials due to fractionation of radiogenic parent and daughter elements during melting and subsequent radiogenic ingrowth of daughter isotopes. The resulting slopes on isotope diagrams indicates an age of fractionation and are widely used to date geological processes. Even though the mantle has undergone continuous differentiation rather than a single differentation event, plots of $^{207}Pb/^{204}Pb$–$^{206}Pb/^{204}Pb$ from MORB and OIB samples display a coherent line, or "pseudo-isochron", from which an ''effective age'' can be calculated. The Pb system has the advantage that Pb isotopes do not fractionate from each other on melting, which is a disadvantage with, for example, the Sm-Nd system. Pb-Pb plots display a trend from DMM to the highly radiogenic HIMU endmember. The Pb-Pb pseudo-isochron ages for various MORB and OIB groups correspond to effective ages of 1.5 to 2 Gyr [Hofmann, 1997], although the exact meaning of these ages is not straightforwardly interpretable (Hofmann, 1997; Albarède, 2001). A recent mathematical analysis reveals that for ongoing differentiation the Pb-Pb 'pseudo-isochron' age is generally much larger than the average age of crustal differentiation (Rudge, 2006).

Lead paradoxes. Another constraint is that all oceanic basalts and most MORB plot to the high $^{206}Pb/^{204}Pb$ side of the geochron, implying that the mantle has experienced a net increase in μ, and implying that there is a hidden reservoir of unradiogenic (low μ) material. This problem is still unresolved and is discussed in more detail in (Hofmann, 2003; Murphy et al., 2003). A second lead paradox, often called the kappa conundrum, is related to the discrepancy between measured $^{208}Pb/^{206}Pb$ ratios and the ratio of their parents, $\kappa=^{232}Th/^{238}U$. A layered-mantle 'steady-state' solution to this was proposed by (Galer and O'Nions, 1986), with a more recent layered solution proposed by (Turcotte et al., 2001). Other recent work has focused on reconciling it with whole-mantle convection; a reasonable resolution is starting to recycle uranium into the mantle ~ 2.5 billion years ago (Kramers and Tolstikhin, 1997; Elliott et al., 1999).

1.7 Lengthscales: Geochemical and Seismological

Of primary interest for understanding mantle mixing processes and the preservation of chemical endmembers is the lengthscale distribution of chemical heterogeneity in the mantle, so this section

reviews constraints from geochemical and seismological observations. In general, it is observed that heterogeneity exists at all scales, but quantitative constraints on the spectrum are minimal.

Geochemical. Chemical heterogeneity is observed at all scales (Carlson, 1987; Carlson, 1994; Meibom and Anderson, 2004), even within the relatively uniform MORB source. For example, at the smallest scale (i.e., melt inclusions in olivine phenocrysts), Pb isotope ratios in OIB span a large fraction of the global range (Sobolev and Shimizu, 1993; Sobolev, 1996; Saal et al., 1998; Sobolev et al., 2000; Hauri, 2002), while Nd ratios in the Ronda peridotite massif in Spain exceed the global OIB Nd ratio variation (Reisberg and Zindler, 1986). According to (Sobolev et al., 2000), extreme heterogeneity of trace element patterns in olivine phenocrysts at Hawaii indicate that the isotopic signature is maintained up to crustal magma chambers, limiting the scale of heterogeneities in the source region to a few kilometers or less. At the centimeter to meter scale, mantle rocks outcropping in peridotite massifs have been observed to contain centimeter to decimeter thick isotopically-enriched pyroxenite veins embedded within a mostly depleted peridotite matrix (Polve and Allegre, 1980; Reisberg and Zindler, 1986; Suen and Frey, 1987; Pearson et al., 1993). Such variations have inspired the proposal of a ''marble cake'' or "plum pudding" style of chemical variation in the mantle, in which small volumes of enriched material reside within a matrix of depleted MORB mantle (Allegre and Turcotte, 1986), a concept that has been the topic of much recent investigation as discussed in later sections. At the longest scale, there is also abundant evidence for compositional heterogeneity at scales of >1000 km in the form of the Dupal anomaly (Schilling, 1973; Dupre and Allegre, 1983; Hart, 1984; Klein et al., 1988) (Hart, 1984; Castillo, 1988), a $\sim 10^8$ km^2 region centered in the Indian ocean that stretches in an almost continuous belt around the Southern hemisphere between the equator and 60°S and is characterized by its anomalous Sr and Pb ratios.

Limited information exists about the spectrum of geochemical heterogeneity from sampling variations in isotope ratios along mid-ocean ridges. An early compilation of $^{87}Sr/^{86}Sr$ data from MORB and ocean island basalts (Gurnis, 1986b) seemed consistent with a flat or "white" spectrum, but the wealth of data that has been gathered since then reveals more complex patterns. The spectrum of $^{3}He/^{4}He$ for 5800 km of the southeast Indian ridge displays periodicities of 150 and 400 km (Graham et al., 2001), which was interpreted to be indicative of upper mantle convection. Using new high-resolution MC-ICPMS data, (Agranier et al., 2005) plotted the spectra of various isotope ratios along the mid-Atlantic ridge, finding two distinct signals: a 6-10° lengthscale signal visible in Pb, Sr and He ratios and the principle component 1 and associated with the Iceland hotspot, and a power-law spectrum with a slope of -1 visible in Nd, Hf ratios and principle component 2, perhaps indicative of dynamic stretching processes discussed later. (Graham et al., 2006) found a bimodal distibution of hafnium isotope ratios along the southest Indian ridge, which appears to indicate compositional striations with an average thickness of ~40 km in the upper mantle.

Seismological. The long-wavelength spectrum of heterogeneity is revealed by global seismic tomographic models, but much of the heterogeneity at this wavelength is thermal. There have, however been attempts to separate thermal and chemical components to the seismic velocity variations (e.g., (Ishii and Tromp, 1999; Forte and Mitrovica, 2001; Romanowicz, 2001; Trampert et al., 2004)). Particularly notable are those studies that use normal mode splitting data because these are sensitive to density variations, providing an additional constraint. In particular, at the longest wavelengths of 1000s km, (Ishii and Tromp, 1999) and (Trampert et al., 2004) found that a substantial fraction of the shear wave heterogeneity in the deepest mantle is due to compositional variations, and that the two low-velocity "megaplumes" seen in global tomographic models seem to have dense material at their bases. Short wavelength heterogeneity is constrained by scattering: short-period precursors to PKP reveal the presence of small ~8 km, weak (1% rms.) velocity perturbations throughout the mantle (Hedlin et al., 1997). There are strong regional differences in scattering strength (Hedlin and Shearer, 2000), with strong scattering beneath South and Central America, eastern Europe, and Indonesia, and some correlation with large-scale anomalies revealed by seismic tomography including the African superplume and Tethys trench. Other types of seismic

observation find structure with a gradient in velocity that is too large to be explained by diffusive thermal structures, including a dipping low-velocity layer in the mid lower mantle (Kaneshima and Helffrich, 1999) and sharp sides to the deep mantle "superplumes" beneath Africa and the Pacific (Ni et al., 2002). In summary, while there is ample seismic evidence for chemical heterogeneity in the mantle, it is not sufficient at this point to constrain the spectrum over all wavelengths, and in particular not to the sub-kilometer wavelengths to which subducted MORB is expected to be stretched.

The spectrum of heterogeneity expected from stirring theory is discussed in the later section 2.7.

1.8 Geophysical Constraints in Favor of Whole-Mantle Convection

A number of types of geophysical evidence argue that mantle convection is not completely layered at the 660 km discontinuity, which is in conflict with the models based on mass balance of Ar and other trace elements discussed earlier.

Firstly, seismological observations have long favored penetration of slabs into the lower mantle. While arguments initially revolved around interpreting travel times (Creager and Jordan, 1984; Creager and Jordan, 1986), subsequent three-dimensional regional or global seismic tomographic models (Fukao, 1992; Fukao et al., 1992; Grand, 1994; Van der Hilst et al., 1997; Masters et al., 2000) clearly show slabs penetrating immediately in some areas, or penetrating after a period of stagnation in other areas, although it has also been argued that thermal coupling in a two-layered convection could produce similar features (e.g., (Cizkova et al., 1999)). Significant flow stratification should lead to a strong decorrelation in global tomographic models across 660 km depth, which is not observed (Jordan et al., 1993; Puster and Jordan, 1994; Puster et al., 1995; Puster and Jordan, 1997). Recent tomographic models have also revealed some upwelling plumes that appear to be continuous across the whole depth of the mantle (Montelli et al., 2004), although there is an active debate on this topic.

Several types of geodynamic evidence also favor penetration of flow into the lower mantle. Firstly, if the 660 km discontinuity were a total barrier to convection, then there would a strong thermal boundary layer at the base of the upper mantle, and all of the heat coming from the lower mantle would be carried by strong upwellings in the upper mantle. As demonstrated by (Davies, 1988), such pervasive strong hot upwellings would violate constraints based on the topography and geoid of the ocean floors, which instead appear to be passively spreading. Identifiable hotspot swells assumed to be caused by upwelling plumes only account for 6-10% of the global heat flow (Davies, 1988; Sleep, 1990). Secondly, modeling the global geoid and dynamic topography using driving forces derived from seismic tomography indicates a better fit to observations with whole-mantle flow than with layered flow (Hager et al., 1985; Ricard et al., 1988; Hager and Richards, 1989; Ricard et al., 1989), although some successful fits are possible with layered models (Wen and Anderson, 1997). A third line of evidence comes from correlating global tomographic models with the spatial locations of subduction zones in the past 140-180 Ma (Richards and Engebretson, 1992; Scrivner and Anderson, 1992; Kyvalova et al., 1995): past subduction appears to match well with lower mantle tomography, implying that the subducted slabs are in the lower mantle. Extending this approach, 3D mantle structure models have been constructed by combining historical plate reconstructions with a global flow solver, and the results show a reasonable match to fast structures observed in global tomographic models (Deparis et al., 1995; Megnin et al., 1997; Bunge et al., 1998). Finally, numerical convection models indicate that the endothermic phase transition at 660 km depth is too weak to completely layer the flow at present-day convective vigor- only intermittent regional layering is plausible (Christensen and Yuen, 1985; Machetel and Weber, 1991; Peltier and Solheim, 1992; Tackley et al., 1994; Bunge et al., 1997), although this does not rule out chemical layering per se, as chemical layering with a large enough density contrasts is additive to the phase change buoyancy effect (Christensen and Yuen, 1984).

While complete layering at 660 km depth seems ruled out, there is evidence in favor of chemical layering in the lowest ~few hundred km of the mantle, perhaps localized in certain regions. Firstly, the D" region has long been found to be seismically highly heterogeneous (e.g., (Lay and Garnero, 2004)), which might require compositional variations to explain. Second, long-wavelength seismic tomographic models robustly find two large regions of low seismic velocity underneath Africa and and Pacific. While these might plausibly be smeared-out groups of narrow plumes (Schubert et al., 2004), seismic evidence indicates that these are not purely thermal in origin, including (i) 'anomalous' scaling between P-wave and S-wave velocities (Kennett et al., 1998; Masters et al., 2000; Bolton and Masters, 2001) (ii) a positive density anomaly, according to some models that use normal mode splitting data (Ishii and Tromp, 1999; Trampert et al., 2004), (iii) sharp sides, which are difficult to maintain with a diffusive thermal field (Luo et al., 2001; Wen, 2001; Wen, 2002). Some thermo-chemical convection models discussed later produce structures that are consistent with these seismological observations.

It has also been argued that geophysical evidence favors a ~1300 km deep, highly undulating layer in the deep mantle (Kellogg et al., 1999; van der Hilst and Karason, 1999). The boundary of this should, however, produce strong observable signatures (heterogeneity and scattering) that have not presently been found (Vidale et al., 2001; Tackley, 2002; Castle and van der Hilst, 2003b; Castle and van der Hilst, 2003a). At the present time, the evidence favors a deeper layer that is probably not global.

1.9 Overview of Geochemical Mantle Models

Before discussing the geophysical findings regarding thermo-chemical convection, it is useful to give an overview of the major models that have been proposed to explain geochemical observations and reconcile geochemical and geophysical observations. Some of these are discussed in more detail in the final section. Rather than discuss a large number of proposed models, some of which have similarities, it is useful to discuss the two main characteristics that differ amongst models, and which tend to be the aspects that models focus on. Figure 2 schematically represents the main models.

1.9.1 Vertical layering

Layered at 660 km. The traditional layered model is chemically and dynamically stratified at the 660 km discontinuity (e.g., slabs do not penetrate), with the upper mantle being a depleted, degassed region that is the complement of the continental crust, and the lower mantle being primitive- the repository for 50% of the bulk silicate Earth's Argon, for the high $^{3}He/^{4}He$ component, and for other trace elements that are missing from the (MORB source + continental crust) according to mass balance calculations (Allegre et al., 1996). Variations on this model include intermittent breakdown of layering (Stein and Hofmann, 1994), the idea that this layering broke down in recent history (Allegre, 1997), and the model of (Anderson, 1995), in which the upper mantle is divided into an enriched shallow layer (the source of OIBs) and a depleted transition zone (the source of MORB). This model is contradicted by a number of geophysical observations, as discussed in section 1.8.

Deep, highly undulating layer (hidden anomalous layer). This model, proposed by (Kellogg et al., 1999), is conceptually similar to the traditional layered model except that the layer boundary is moved downwards to approximately 1300 km above the CMB, undulating by ~1000 km. Recycled components reside on top of the layer. The layer is 'hidden' because the seismic wave velocity anomalies caused by the different composition and higher temperature cancel out. While this proposal has been thought-provoking and has stimulated increasing progress towards findings a unified model, it should produce a seismic signature that is not found, as discussed in section 1.8.

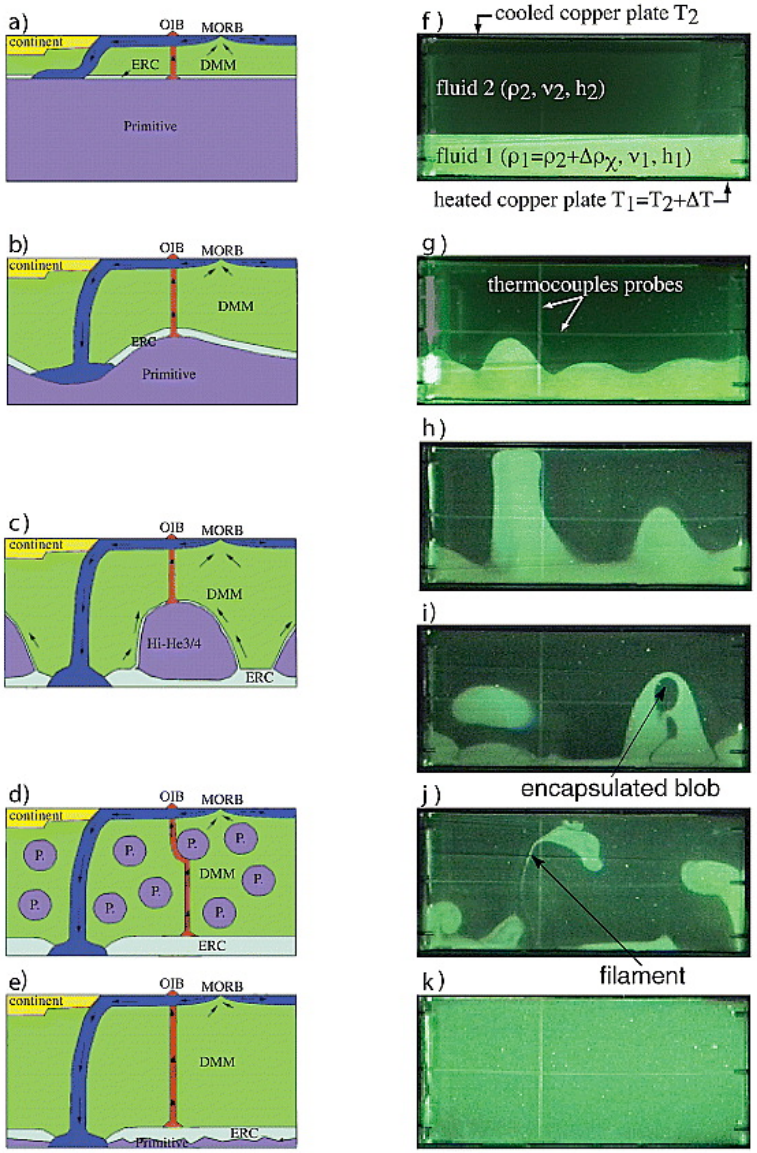

Figure 2. Various mantle models proposed to explain geochemical observations compared to results from a laboratory experiment at different times in its evolution, taken from (Le Bars and Davaille, 2004b). Cartoons in the left column are from (Tackley, 2000). (a) Layered at the 660 km discontinuity, (b) deep, high-topography hidden layer (Kellogg et al., 1999), (c) 'piles' (Tackley, 1998) or 'domes' (Davaille, 1999a), (d) primitive blobs (Davies, 1984; Manga, 1996; Becker et al., 1999; du Vignaux and Fleitout, 2001), (e) whole-mantle convection with thin dense layer at the base.

Thin layer (D" region). A ~few hundred km thick layer above the CMB, perhaps highly undulating and/or localized into certain areas, and which could potentially contain primitive material, recycled material, or some mixture of the two, is a possibility. It has long been proposed that such a layer could contain recycled oceanic crust that provides the HIMU signature (Hofmann and White, 1982). Such oceanic crust contains a higher concentration of incompatible trace elements than primitive material so could also account for the 'missing' trace elements (about 1/3 of the total inventory of heat-producing elements according to (Coltice and Ricard, 1999)). Whether such a layer could exist depends on the density contrast of MORB at these high pressures and temperatures, as discussed in section 3.3.2. It has recently been argued that this enriched layer may have formed shortly after Earth's accretion process (Tolstikhin and Hofmann, 2005; Tolstikhin et al., 2006). Another proposal is that the layer preferentially contains oceanic crust containing oceanic plateaus, with normal oceanic crust not reaching this depth (Albarède and van der Hilst, 2002). Seismological observations support the existence of a thin and perhaps intermittent layer, as discussed in section 1.8.

1.9.2 Distributed heterogeneity

Instead of, or as well as, radial stratification, lateral compositional heterogeneity is typically though to exist. An early justification for this was that mantle rocks outcropping in peridotite massifs have been observed to contain centimeter to decimeter thick isotopically-enriched pyroxenite veins embedded within a mostly depleted peridotite matrix (Polve and Allegre, 1980; Reisberg and Zindler, 1986; Suen and Frey, 1987; Pearson et al., 1993). Such variations have inspired the proposal of a ''marble cake'' or "plum pudding" style of chemical variation in the mantle, in which small volumes of enriched material reside within a matrix of depleted MORB mantle (Allegre and Turcotte, 1986), a concept that has been the topic of much recent investigation as discussed in later sections, with several variations and refinements proposed. At the larger scale, it has been proposed that very large (~100 km scale) blobs may exist (Becker et al., 1999). Seismic scattering supports distributed heterogeneity, as discussed in section 1.7. Dynamically, key issues are how rapidly distributed heterogeneity gets mixed (see section 2), which will be influenced by any composition-dependence of viscosity (section 2.3.5).

1.10 Mantle-Exosphere (Biosphere) Interactions

Cycling of volatiles (particularly water and carbonate) between the interior and fluid envelope of a terrestrial planet could play a major role in the evolution of the fluid envelope, and hence the long-term habitability of the surface environment. The mantle influences the fluid envelope by volatile outgassing associated with volcanism, and by volatile recycling back into the interior. Indeed, a long term cycle associated with carbonate recycling and reoutgassing may provide a critical feedback mechanism that maintains surface temperature in a habitable range (Kasting et al., 1993b; Sleep and Zahnle, 2001). Volatile recycling also affects the redox state of the mantle, which, through outgassing, influences the redox state of the atmosphere (Kasting et al., 1993a; Lecuyer and Ricard, 1999; Delano, 2001), and may have been responsible for the rapid rise in atmospheric oxygen ~2 Gyr ago (Kump et al., 2001). Crucial to recycling is the existence of plate tectonics, through which carbonate, water and other volatiles are subducted into the mantle (e.g., (Ruepke et al., 2004); note, however, that until recently it was widely accepted that a 'subduction barrier' existed that prevented volatiles from being recycled into the mantle (Staudacher and Allegre, 1989) and even recent mass balance calculations (Hilton et al., 2002) indicate that the mass of water erupted by arc volcanics far exceeds the unbound water subducted). Thus, the existence of plate tectonics on Earth may be important for long-term habitability. Multiple feedbacks exist in the fluid envelope-mantle-core system. Water strongly affects the viscosity of the mantle (Hirth and Kohlstedt, 1996), so water exchange between the mantle and exterior may have had important influences on the evolution of the coupled system. Furthermore, water greatly reduces the strength

of the lithosphere through its effect on faults and the yield strength, and is thus commonly thought to be necessary for plate tectonics to exist. The convective regime and heat flow out of the mantle are strongly affected by the fluid envelope through the influence of water on mantle viscosity and plate tectonics. Recent analysis indicates that subducted seawater accounts for about 50% of the unbound water presently in the convecting mantle (Holland and Ballentine, 2006).

2. MANTLE STIRRING AND MIXING OF PASSIVE HETEROGENEITIES

2.1 Stirring, Stretching, Mixing and Dispersal

It is important to distinguish between different concepts that are all sometimes loosely referred to as "mixing". Strictly speaking, "mixing" involves homogenization of the chemical differences by a combination of stirring and chemical diffusion. Stirring involves stretching, which is the process by which an initial 'blob' of chemically-distinct material is elongated into a thin tendril or lamella by strain caused by the convective flow. This greatly increases the surface area of the heterogeneity and decreases its width, facilitating chemical diffusion. Chemical diffusion of most elements is extremely slow, acting over lengthscales of centimeters to meters over geological time, thus it is necessary to stretch heterogeneities to this scale before they can be mixed. As discussed later, however, observed MORB or OIB compositions probably involve averaging over a volume that is larger than this, so stretching to diffusion scales may not be necessary to eliminate the signature of an individual heterogeneity during melting.

"Dispersal" refers to the dispersal of initially close heterogeneities evenly around the mantle. While this occurs partly by similar processes to stretching (i.e., the increasing separation of two initially very close points), effective dispersal involves material transport across convective "cells". It is possible in some flows for rapid stretching to occur within a cell, but for inter-cell transfer to be slow. Conversely, as discussed later, high viscosity blobs undergo very slow stretching, but may get rapidly dispersed around the domain.

Many of the concepts introduced in this section are illuminatingly illustrated in the review of (van Keken et al., 2003). See also the Chapter of Ricard (this volume).

2.2 Stretching Theory: Laminar and Turbulent Regimes

2.2.1 Finite deformation tensor

The mathematical description of finite deformation was presented by (McKenzie, 1979) following (Malvern, 1969). We are interested in the deformation tensor relating the vector $\mathbf{y}'(t)$ which joins two particles in a fluid element at positions $x_1'(t)$ and $x_2'(t)$ to y, the vector joining the same two particles at t=0.

$$\mathbf{y}'(t) = \mathbf{F}(t)\mathbf{y} \quad (4)$$

The **F** matrix is initially the unit matrix and evolves according to:

$$D_t F_{ij} = L_{ik} F_{kj} \quad (5)$$

where D_t is the Lagrangian time derivative and **L** is the velocity gradient tensor:

$$L_{ij} \equiv \frac{\partial v_i}{\partial x_j} \quad (6) \quad \text{(can also be written in the material frame (Farnetani et al., 2002))}$$

which is a combination of the strain rate tensor (symmetric part of **L**) and the vorticity tensor (antisymmetric part of **L**).

As the **F** tensor has 9 components in three dimensions, or 4 components in two dimensions, it is desirable to extract a simpler quantity to describe the stretching. In two dimensions a convenient scalar measure is the logarithm of the aspect ratio of the strain ellipse (McKenzie, 1979), i.e.,

$$f(t) = \log_{10}(a/b) \quad (7)$$

where a and b are the major and minor axes of the ellipse, respectively, and a/b can be found from the second invariant of the **F** tensor, i.e.,

$$a/b = \gamma + \left(\gamma^2 - 1\right)^{1/2} \quad ; \quad \gamma = \tfrac{1}{2} F_{ij} F_{ij} \quad (8)$$

Some authors prefer to measure the change in the semi-major or semi-minor axis of the strain ellipse, which is the square root (or one over the square root) of (a/b). In two dimensions, (Kellogg and Turcotte, 1990) show how a complete description of the total deformation of a heterogeneity can be obtained by tracking only two quantities for each tracer, the aspect ratio ($a/b \equiv e$) and orientation θ of the strain ellipse. In three dimensions, the strain ellipse becomes an ellipsoid and a method of tracking that is simpler than the above equation has not yet been proposed.

2.2.2 Asymptotic stretching rate

Two types of shear flow, simple shear and pure shear, result in two different asymptotic stretching behaviors termed laminar and turbulent respectively (see Figure 3). The theory is described by (Olson et al., 1984b; Olson et al., 1984a) based on previous theory by (Batchelor, 1952; Batchelor, 1959; Corrsin, 1961), and is briefly summarized here; see also (Ricard, Ch 2, this volume).

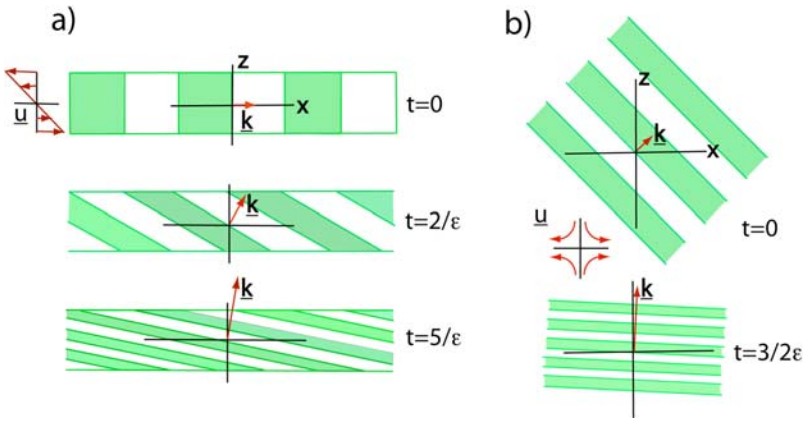

Figure 3. Diagrams illustrating the evolution of a single Fourier component of a passive anomaly for (a) uniform laminar shear flow, and (b) stagnation point flow, based on Figures 4 and 5 of (Olson et al., 1984b). The velocity field **u** is sketched for each case. In a uniform shear flow (a), the Fourier component is rotated into the direction of shear while its wavelength decreases, such that the wave number magnitude |**k**| grows at a rate $\dot{\varepsilon}$, the Lagrangian strain rate. Near a stagnation point (b) the Fourier components also become rotated, this time into the direction of compression, but the wave number magnitude grows at a rate that is proportional to time, i.e., $\dot{\varepsilon} t$.

Laminar mixing (Figure 3a) occurs in a simple shear flow and involves a linear increase in the cumulative strain ε with time t:

$$\varepsilon = \dot{\varepsilon} t \quad (9)$$

where $\dot{\varepsilon}$ is the average strain rate experienced by the heterogeneity. A linear decrease with time occurs for the component of the wave number vector that is perpendicular to the velocity,

$$k_x(t) = k_x(0) \;\; ; \;\; k_z(t) = k_z(0) + k(0)\dot{\varepsilon} t \quad (10)$$

for a shear flow described as $\mathbf{u} = -\dot{\varepsilon} z \hat{\mathbf{x}}$. This effectively describes a cascade of heterogeneity to shorter wavelengths, with 'blobs' being stretched into thin strips aligned with the direction of flow velocity. In the absence of diffusion, the Fourier amplitude of the heterogeneity does not change, it simply moves to higher k. For the case with diffusion see below.

Turbulent mixing is associated with pure shear (also known as normal strains (Olson et al., 1984a; Olson et al., 1984b)), which occurs at stagnation points in convective flows (Figure 3b). In this case, the velocity is proportional to the distance from the stagnation point ($\mathbf{u} = \dot{\varepsilon} x \hat{\mathbf{x}} - \dot{\varepsilon} z \hat{\mathbf{z}}$), so the cumulative strain increases exponentially with time:

$$\varepsilon = \exp(\dot{\varepsilon} t) \quad (11)$$

with wavenumbers evolving exponentially in both directions:

$$k_z(t) = k_z(0)\exp(\dot{\varepsilon} t) \;\; ; \;\; k_x(t) = k_x(0)\exp(-\dot{\varepsilon} t) \quad (12)$$

As turbulent mixing is far more rapid than laminar mixing, it is important to establish which regime is most appropriate to characterize flows associated with mantle convection, so this has been a major focus of research. This issue has been investigated theoretically and for kinematically-driven flows and for convectively-driven flows. The general findings are (i) that the type of mixing can be quite sensitive to exact flow, although greater time-dependence results in a greater tendency towards turbulent mixing, and (ii) that different 'blobs' may undergo substantially different rates of stretching in the same flow depending on their location in that flow. This is discussed in the next section.

Some semantic issues are worth noting: Firstly, the very high Prandtl number flow that the mantle undergoes should actually be termed laminar due to the unimportance of intertial terms; nevertheless it can lead to the turbulent stretching regime. Secondly, turbulent mixing is often referred to as chaotic mixing, and laminar mixing is often referred to as regular mixing.

2.2.3 Measures of stretching

Most measures of stretching are based on the elongation of an infinitesimal strain ellipse, i.e., the ratio of the major axis to its original value (a/a_0), calculated using the equations in section 2.2.1, and tracked using infinitesimal tracer particles distributed throughout the domain. The width of the strain ellipse is the inverse of this value. Values of (a/a_0) exhibit a considerable spread, so it is important to consider the range in values as well as the average. When the time-averaged stretching rate increases exponentially with time, the appropriate average to take is the median (Christensen, 1989a) or the geometric mean, which is related to the mean in logarithmic space. In this approach, the strain ellipse is always considered to be infinitesimal in size even if it reaches 10^{10} or larger, so

these measures are not appropriate for estimating the separation of two initially closely-spaced points, which cannot get larger than the size of the domain.

Other than the median or geometric mean stretching, it is useful to consider quantities that convey information about the distribution of strains. The statistical distribution of stretching can be plotted in various ways, for example (Kellogg and Turcotte, 1990) plot the probability distribution of strain (a/a_0 versus number of tracers), the cumulative distribution (a/a_0 versus fraction of particles exceeding (a/a_0)), and the time-dependence of strain evolution (time versus a/a_0 with different lines for the percentage of tracers exceeding a/a_0). An example of the latter quantity is the size reduction exceeded by 90% of tracers plotted by (Christensen, 1989a).

Often the goal is to determine what fraction of heterogeneities have 'mixed', in the sense of being stretched to less than the diffusive or sampling lengthscale. (Kellogg and Turcotte, 1990) plotted as a function of time the fraction of tracers that have been completely homogenized. (Gurnis and Davies, 1986b) were interested in heterogeneities that remained relatively intact, so plotted as a function of time the fraction that have strain less than 5.

Lyapunov exponents

The Lyapunov exponent is the exponential coefficient for the rate at which two initially close heterogeneities are separated. This can be written as

$$\lambda(P,\vec{y}) = \lim_{\substack{t\to 0 \\ y\to 0}} \left[\frac{1}{t} \ln\left(\frac{y(t)}{y} \right) \right] \quad (13)$$

where y is the length of separation vector $\vec{y}$ located at position P, and y(t) is its length after a time t. This is zero for laminar stretching and positive or negative for exponential stretching. The value depends on the direction of $\vec{y}$ relative to the velocity gradient tensor, so λ has maximum and minimum values. (Kellogg and Turcotte, 1990) use the maximum Lyapunov exponent and the minimum Lyapunov exponent to quantify the stretching (Wolf, 1986), and these are straightforwardly related to $\overline{\alpha}_e$, the average strain rate measured from the numerical experiments, by:

$$\lambda_{\max} = \frac{\overline{\alpha}_e}{\ln 2} \quad (14)$$

where

$$\overline{\alpha}_e = \frac{1}{\tau} \ln\left(\frac{a}{a_0} \right) \text{ or } \; a = a_0 \exp(\overline{\alpha}_e \tau) \quad (15)$$

In numerical applications it is often more convenient to calculate the Lyapunov exponent using finite rather than infinitesimal time difference t, or finite separation y, for example by considering the motion of nearby tracers. Lyapunov exponents calculated using these finite quantities are referred to as finite time or finite size Lyapunov exponents, respectively, and have been used in the mantle dynamics literature (Ferrachat and Ricard, 1998; Ferrachat and Ricard, 2001; Farnetani et al., 2002; Farnetani and Samuel, 2003).

In general, for finite quantities we can write using the above equations above that:

$$\frac{y(t)}{y(0)} = \frac{|\mathbf{F}(t)\mathbf{y}|}{|\mathbf{y}|} = \left(\frac{\mathbf{y}^T \mathbf{F}^T(t)\mathbf{F}(t)\mathbf{y}}{\mathbf{y}^T \mathbf{y}} \right)^{1/2} \quad (16)$$

The maximum and minimum eigenvalues of the right Cauchy-Green strain tensor $\mathbf{F}^T\mathbf{F}$ can then be used to calculate the maximum and minimum finite-time Lyapunov exponents (e.g., (Farnetani and Samuel, 2003)):

$$\lambda_{\max} = \frac{1}{t}\ln\sigma_{\max} \;;\; \lambda_{\min} = \frac{1}{t}\ln\sigma_{\min} \quad (17)$$

In 2-D incompressible flow, $\lambda_{\min} = -\lambda_{\max}$.

The hyperbolic persistence time method is a method to analyze stable or unstable material trajectories (unstable meaning that nearby particle trajectories separate from it), and was introduced to the mantle community by (Farnetani and Samuel, 2003). Readers are referred to this paper for more details.

2.3 Stretching: Numerical Results

2.3.1 General discussion

A convective flow includes both stagnation points (e.g., at the corners of a "cell"), which will be associated with pure shear and exponential stretching, and laminar regions (away from corners), which will be associated with simple shear and linear stretching. It is therefore likely that a heterogeneity will experience linear stretching most of the time, with the occasional episode of exponential stretching. Which regime dominates the long-term behavior depends on the details of the flow. If the flow is steady-state and two-dimensional, then most of the heterogeneities never pass close to a stagnation point, so the average stretching rate follows a linear stretching law (McKenzie, 1979; Olson et al., 1984b). If the flow is highly unsteady, then the stagnation points move around and new ones are generated, allowing essentially all heterogeneities to pass close to stagnation point at some point, and giving on average an exponential stretching rate. The overall behavior is, however, highly sensitive to the details of the time-dependence, and this has been studied by a variety of models ranging from purely kinematic flows to purely convective flows (e.g., (Christensen, 1989a)). As all heterogeneities are not stretched at the same rate, it has proven important to study the range of stretching rates as well as the average. Most of the research has been done in two dimensions, so three-dimensional studies are discussed in a later section.

2.3.2 Steady-state 2D flows

Steady-state 2-D Bénard convection cells follow the laminar stretching law, whether kinematic (Olson et al., 1984b) or convective (McKenzie, 1979). The fit to theory is reasonable for both non-diffusive and diffusive heterogeneity (Olson et al., 1984b). It is instructive to understand the resulting stretching regime as a baseline for more interpreting more complex flows. Heterogeneities are stretched into spirals of lamellae that are locally oriented subparallel to the streamlines, because different streamlines are rotating at a different rate. For example, near the top of the domain the lamellae are locally sub-horizontal. In a completely heated-from below steady-state Bénard convection cell the interior of the cell (far from the boundaries) undergoes almost rigid-body rotation with an associated low stretching rate, but near the boundaries, where heterogeneities pass close to stagnation points in the corners, the cumulative strain can increase substantially (e.g., the aspect ratio of the strain ellipse (a/b) by a factor of 1000) over one rotation (McKenzie, 1979). It is interesting to note that strain does not increase monotonically, but rather as large oscillations with a

superimposed linear trend (McKenzie, 1979). The parts of these oscillations where the strain decreases have been termed "unmixing". The addition of internal heating makes the situation more complex as there is no uniformly-rotating area in the middle, but again the cumulative strain (a/b) undergoes considerable oscillation and near the edge of the "cell" can reach a factor of 100 over one rotation (McKenzie, 1979). The highest strain rates (hence velocity gradients) occur near the downwelling. For finite-sized bodies (initially cylinders), (Hoffman and McKenzie, 1985) found that for pure basal heating the amount of stretching was rapid for a blob initially situated near the edge of the flow, but with internal heating the blob became deformed but not greatly stretched in one revolution.

Steady corner flows relevant to mid-ocean ridges and subduction zones have also been studied (McKenzie, 1979). The most severe strain (a/b~30) was experienced in the corner above a subducting slab, with the principle axis of the strain ellipse aligned subparallel to the streamline. Again, strain does not necessarily increase monotonically with time.

2.3.3 Time-dependent 2D flows

Various types of 2D flow have been studied, including purely kinematic flows, purely convective flows, and convective flows with kinematic upper boundary conditions. This has led to the identification of three main stirring regimes (Christensen, 1989a): a regime in which all particles are undergoing exponential stirring, a 'slow' regime similar to the laminar regime, and a hybrid regime in which some particles/regions are undergoing turbulent stretching while some are undergoing slow laminar stretching. Fully time-dependent convection with no kinematic constraints has always been found to give turbulent mixing, whereas controlling the flow with a kinematic upper boundary condition or fully kinematic description may lead to the 'slow' or hybrid regimes, though some kinematic flows lead to the turbulent mixing regime (e.g., (Kellogg and Turcotte, 1990)). More discussion of the factors that lead to these regimes now follows.

Slow stirring. In this regime, most heterogeneities are stretched into long streaks, but clumps exist where the streaks get folded, leading to the simultaneous existence of tendrils with average stretching rate and blobs with very slow stretching (Gurnis, 1986c) which can survive for up to tens of transit times. This regime has been observed in kinematically-prescribed flows consisting of two counter-rotating cells with a boundary that moves smoothly and periodically with time (Gurnis, 1986c; Gurnis and Davies, 1986b; Christensen, 1989a). While visually the system may look reasonably well mixed, the average stretching rate is slow compared to the other regimes, and lies somewhere between exponential and linear with time (Gurnis, 1986c; Christensen, 1989a). (Gurnis and Davies, 1986b) also obtained a regime visually similar to this with a combination of convection and kinematic plates, but the asymptotic stretching rate was not analyzed.

Exponential stirring. In this regime, all heterogeneities experience exponential stretching, although at different rates. There are no unmixed islands or persistent large blobs. All fully time-dependent purely convective (i.e., with no kinematic control) 2D flows in the mantle convection literature that have been suitably analyzed are in this regime, including those in (Hoffman and McKenzie, 1985; Christensen, 1989a). So are kinematic flows in which there is an oscillation between a single cell and three cell structure, like those of (Kellogg and Turcotte, 1990) and simplified versions in (Christensen, 1989a). A characteristic that this kinematic flow shares with time-dependent convection is the creation of new cell boundaries, which can occur due to plume formation, sub-lithosphere convection or delamination, or new subduction zone formation. In some cases it can also be obtained by two-cell kinematic flow with the boundary motion containing more than one frequency component (Christensen, 1989a).

It is important to note that the effective stretching rate that goes into the exponential stretching law (sometimes called the Lagrangian strain rate (Coltice, 2005)) is much lower than the mean strain rate of the flow- approximately 10-30 lower according to (Christensen, 1989a). In two-dimensional convective flows with internal heating up to $Ra=10^{10}$ and with basal heating up to

Ra=10^9 (Coltice, 2005) found that the Lagrangian strain rate scales in proportion to the convective velocity, i.e., $Ra^{1/2}$ and $Ra^{2/3}$ respectively, even though the higher Ra flows are more time-dependent, implying that the stretching rate is simply proportional to the rate at which material is moving, provided the flow is time-dependent. This finding also applied to cases with a 100 or 1000 fold viscosity jump at mid depth.

Hybrid stirring. In this regime, most of the flow is exponentially stirred but there exist unmixed regions or 'islands' in the flow; the histogram of strain distributions can exhibit a bimodal distribution with one peak at very low strains (Christensen, 1989a). In the experiments of (Christensen, 1989a) this was found in relatively few cases- in two of the kinematic flows with more than one driving frequency. Nevertheless, it is a mode that is commonly observed in mixing experiments performed outside the solid Earth science community (see (Metcalfe et al., 1995) and references therein). The wide range of stretching rates observed in this mode and the 'slow stirring' mode above indicate the importance of considering the range rather than only the median or mean.

The statistical range of heterogeneity stretching in the turbulent mixing regime was studied by (Kellogg and Turcotte, 1990) using a chaotic kinematic flow with time-dependence driven by the Lorenz equations. Specifically, the flow had two cells, and the boundary between moved smoothly but chaotically such that sometimes there was only one cell. Into this they injected a large number of particles with different starting positions, in order to obtain robust statistics regarding their stretching. Naturally, exponential (turbulent) stretching was obtained, but the amount of strain experienced by different tracers varied very widely, such that after, for example, five overturns, the semi-major axis of the strain ellipse divided by its initial radius (a/a_0) averaged 10^4 but varied between $\sim 10^1$ and $\sim 10^7$ (1st to 99th percentile) or $\sim 10^2$-$\sim 10^6$ (10^{th} to 90^{th} percentile). In other words, the (logarithmic) variation in cumulative strain is as large as the average cumulative strain. It is thus not meaningful to talk about a precise quantities such as "mixing time" based on average stretching; everything must be qualified in terms of probability distributions. The effective strain rate for this stretching was found to be 13% of the maximum strain rate that occurred at the stagnation point in the corner of the cell.

2.3.4 3-D flows

It is expected that mixing in three-dimensions is quantitatively different from that in two dimensions, but so far studies have been few and appear contradictory about the sign of the change. Two key concepts are relevant:

(i) **Toroidal motion**. 3-D flows can have toroidal motion- the component of motion associated with rotation about a vertical axis and strike-slip motion, whereas 2-D flows (in a vertical plane) cannot. In steady-state 2-D flows the streamlines (particle paths) are always closed, but in 3D the presence of toroidal motion can cause chaotic, space-filling particle paths, even if the flow is stationary in time (Ottino, 1989). One way of viewing this, as discussed by (Ferrachat and Ricard, 1998), is that toroidal motion increases by one the number of degrees of freedom of the Hamiltonian, for which one degree of freedom gives regular mixing and two degrees of freedom gives chaotic flow. For steady-state flows driven by an upper boundary condition mimicking a spreading center with a transform offset this effect was demonstrated by (Ferrachat and Ricard, 1998). Areas of rapid, turbulent mixing, as well are islands of laminar mixing, were identified based on Poincare sections and maps of finite time Lyapunov exponents. Quantitatively, a 3D flow with zero toroidal component was found to give similar Lyapunov exponent to 2D flow, while the addition of a toroidal component increased the exponents by a factor of ~2. A large lower mantle viscosity tends to confine toroidal motion to the upper mantle (Gable et al., 1991; Ferrachat and Ricard, 1998).

(ii) **Plumes versus sheets**. Because 3D upwellings (and downwellings if slabs are not included) can be columnar plumes rather than infinite sheets, they have a smaller effect on disrupting the flow pattern and causing inter-cell mixing. This was apparent in time-dependent, constant-viscosity

convection at Rayleigh numbers up to $8x10^5$ calculated by (Schmalzl et al., 1996): after several overturns tracers had dispersed efficiently within individual cells (as indicated by histograms of tracer vertical positions), but dispersal between cells was much slower in 3-D than in equivalent calculations in 2-D. A recent suite of calculations comparing 2-D and 3-D (poloidal only) flows up to much higher Rayleigh numbers found, however, that 2-D and 3-D flows have approximately the same Lagrangian strain rate (Coltice and Schmalzl, 2006).

In summary, if the results of (Coltice and Schmalzl, 2006) are validated for flows with more complex physics, then overall mixing efficiency in 3-D is likely to be similar to (if poloidal-only) or greater than (if toroidal motion is present) 2-D flows with the same parameters.

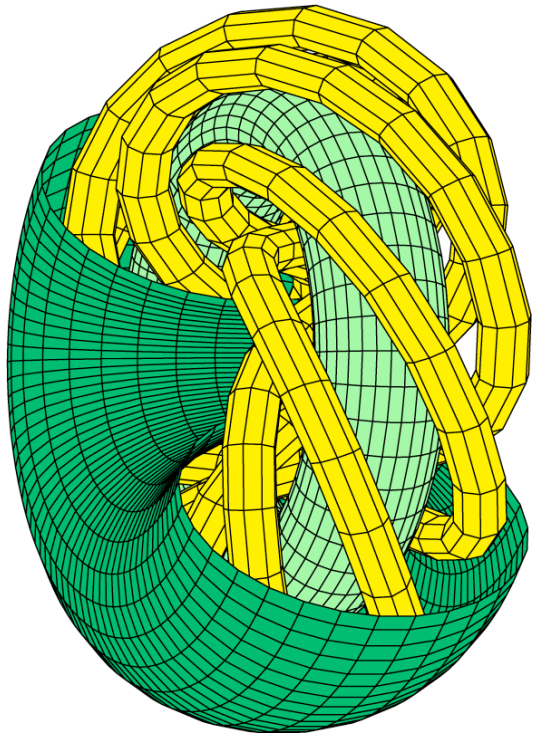

Figure 4. The topology of the pathlines for 3-D flow that is purely poloidal, extracted from a figure from (Ferrachat and Ricard, 1998). Individual tracer paths are restricted to tubes or tori, which they spiral round. Adding increasing amounts of toroidal motion breaks up the tubes, then the tori.

It is worth considering the particle trajectories in 3-D flows. In steady-state 3D convection with zero toroidal component, inter-cell transfer is zero because individual flow lines lie on a two-dimensional distorted (but closed) toroidal surface (Schmalzl et al., 1995). Individual streamlines are generally not closed in small number of orbits around the torus, but rather the surface is progressively filled by the trace of a single streamline. Extreme shear strains can occur but mixing is in 2D. This is illustrated in Figure 4. With the addition of time-dependence, boundary layer instabilities perturb these "toroidal" structures, allowing for cross-cell mixing (Schmalzl et al., 1996). Here it is important to note that the "toroidal paths" followed by particles in a steady-state

flow are completely different to the "toroidal motion" caused by surface rotation and strike slip motion- indeed toroidal motion breaks up the tori found with purely poloidal motion (Ferrachat and Ricard, 1998). The only relevant laboratory experiments were the steady-state experiments of (Richter et al., 1982) in which for convective rolls, blobs were smeared out into spiral sheets or corkscrews if a superimposed lateral motion, with more complicated topologies for spoke pattern convection, but still within individual cells and not cross-cell.

The analysis of mixing in steady-state 3-D flows was extended to spherical geometry by (van Keken and Zhong, 1999), using a flow intended to be similar to the flow in the present-day mantle, generated by buoyancy from a slab model combined with an approximate plate rheology. As with the simple flow of (Ferrachat and Ricard, 1998), only limited regions exhibited laminar mixing, with most other regions containing corkscrew-like particle tracks and probably chaotic mixing: the areas with highest stretching rates are those with high toroidal motion. Long-range dispersal was also studied, as discussed in a later section.

2.3.5 Effect of viscosity variations

Depth-dependent viscosity. For some time it was thought that if the lower mantle has a substantially higher viscosity, then motion would be so sluggish that chemically-distinct material could be retained for long periods of time (e.g., (Davies, 1983)). Numerical studies have, however, found that the effect of higher lower mantle viscosity on stirring and residence times is relatively small, and that it cannot provide an explanation for long-lived heterogeneities per se. These numerical studies, which all study passive tracers, are discussed in this section.

Somewhat confusingly, the earliest study to address this issue (Gurnis and Davies, 1986a) did appear to show very slow stirring in a 100 times higher-viscosity lower mantle, even though the heterogeneities were passive, i.e., had no density anomaly to keep them in the lower mantle. The circulation in these cases was however extremely sluggish, and was arguably driven mainly by a prescribed plate-like boundary condition rather than convection. (Although the authors were careful to make the prescribed surface velocities consistent with convection for constant-viscosity cases, this was not the case for depth-dependent viscosity cases (Christensen, 1989a; Christensen, 1990)).

With a much higher convective vigor more relevant to the Earth and free slip upper boundary, a lower mantle viscosity up to a factor of 100 higher than the upper mantle viscosity does not prevent large-scale mixing of the mantle (van Keken and Ballentine, 1998). The latter's calculations tracked Helium degassing and ingrowth by radioactive decay, and it was found that the horizontally-averaged %degassed and $^3He/^4He$ ratio were approximately constant with radius even for high viscosity lower mantle cases, indicating good vertical mixing, although lateral heterogeneity was observed. Curiously, higher lower mantle viscosity seemed to cause higher outgassing rates- this was because the viscosity of the upper mantle was decreased in order to maintain the same surface heat flux in all cases, which led to higher velocities in the shallow mantle, hence more rapid outgassing. Subsequent models (van Keken and Ballentine, 1999) demonstrated that temperature-dependent viscosity and an endothermic phase change at 660 km depth also do not result in chemical stratification, even when the mantle starts out layered in trace element content, although again, there was a significant amount of lateral heterogeneity (i.e., $^3He/^4He$ varies from 0 to a maximum value of 36-72).

Regarding stretching rate, a 100-fold viscosity jump was found by (Coltice, 2005) to make no difference to the average Lagrangian strain rate for internally-heated convection, but for basally-heated convection it decreased strain rate by a factor of ~4, probably because plumes from the lower boundary are affected by the viscosity jump, but instabilities from the upper boundary are not. In these calculations, the upper mantle viscosity and Rayleigh number were held constant.

Processing (residence) time was found to be insensitive to a viscosity jump, regardless of heating mode (Coltice, 2005). Consistent with random sampling and the He ratio results of (van Keken and Ballentine, 1998), (Hunt and Kellogg, 2001)found that the a 100-fold viscosity jump at 660 km depth did not cause any age stratification. Seemingly inconsistent with (Coltice, 2005),

(Hunt and Kellogg, 2001) found that the mean particle age increased by a factor of ~2, but this could be because they removed particles not only when they were sampled by melting, but also when they became widely dispersed from other particles that were introduced at the same time, which means that the mean age cannot be interpreted as a simple residence time. The viscosity jump does, however, make a substantial difference to the ability of tracers to migrate laterally from their starting positions, because the flow is more steady, and this is something that should be studied further.

A non-convective, steady-state flow, driven by top boundary forcing and assumed idealized density anomalies due to downwelling slabs was studied by (Ferrachat and Ricard, 2001), who found that a 100-fold viscosity jump at mid-depth increased the lower mantle mixing time (using a modified version of (Olson et al., 1984a) definition based on even dispersion across boxes) by a factor of ~5, and that the finite-time Lyapunov exponents increased by a factor ~2-3. It is not clear how much such an idealized flow applies to the real Earth, however.

Composition-dependent viscosity. If a blob of compositionally-distinct material has a higher viscosity than its surroundings, then the rate at which it gets stretched is considerably reduced. Simple theory predicts that in pure shear, the deformation rate is proportional to $1/(\lambda+1)$, where λ is the viscosity contrast (Spence et al., 1988; Manga, 1996). In a steady-state 2-D convective flow, (Manga, 1996) found that the deformation rate of extremely large (diameter ~1000 km) blobs was dramatically reduced with only a factor of ~10 viscosity increase, whereas if the viscosity of the blob is lower than its surroundings then it rapidly gets stretched into tendrils. (Manga, 1996) also found that these large high-viscosity blobs tend to aggregate, raising the possibility that they could combine into even larger blobs.

For time-dependent convection (with a prescribed time-dependent top velocity condition) (du Vignaux and Fleitout, 2001) showed that stretching rate is more highly dependent on viscosity ratio than in simple shear, and that the stretching is exponential with time, consistent with the turbulent mixing regime. Specifically, they found that:

$$e_m \equiv \frac{d\ln(a^*/a_0)}{dt} = \frac{C}{(1+\lambda)^2} \qquad (18)$$

where e_m is the mixing efficiency, a* is the mean distance between two points initially at separation a_0, and C is a constant. The quantity a* is commonly used in mixing studies as a measure of stretching (Ottino, 1989) and is related to, but not the same as, the semi-major axis of the strain ellipse *a* (du Vignaux and Fleitout, 2001). This equation is valid for viscosity contrast λ of ~an order of magnitude or more. This scaling can be explained using an analytic theory of a blob experiencing repeated pure shear events in random directions (du Vignaux and Fleitout, 2001). While one might intuitively expect repeated shear in random directions to average out, or at least add like a random walk, the fact that when the major axis of the ellipse is at an angle like 45º to the pure shear direction the stretching increases regardless of its orientation, means that the overall effect is one of exponentially increasing strain.

Thus, differing viscosity of components can have a dramatic effect on the rate at which they get stretched and hence mixed. It is quite likely that chemically-different components have different viscosities. Subducted basaltic crust in the upper mantle has a large proportion of garnet, which has a relatively high viscosity (Karato et al., 1995). The presence of water can reduce viscosity by up to ~two orders of magnitude (Hirth and Kohlstedt, 1996), which will increase the viscosity of depleted residue and possibly decrease the viscosity of primitive material, which is rich in volatiles. In the lower mantle, magnesiowüstite likely has a higher viscosity than perovskite (Yamazaki and Karato, 2001), so assemblages that have different proportions of these minerals will have differing viscosity.

Non-Newtonian viscosity. Mineral physics results suggest that a substantial part of the upper mantle is undergoing non-Newtonian dislocation creep (Karato and Wu, 1993), yet very few studies have addressed the influence of non-Newtonian power-law rheology on mixing. In a series

of papers, (Ten et al., 1996; Ten et al., 1997; Ten et al., 1998) compared the mixing properties of highly time-dependent Newtonian and non-Newtonian flows of similar vigor, in 2-D models that also had temperature- and pressure-dependent viscosity. Their basic finding is that mixing is less efficient in non-Newtonian flows, with unmixed 'islands' persisting for long time periods, both in plumes (Ten et al., 1996) and global convection (Ten et al., 1997; Ten et al., 1998). The local patterns of mixing were quite different between the different rheologies, with a greater richness in the scales of spatial heterogeneities in the non-Newtonian case (Ten et al., 1997). Non-Newtonian rheology causes chemical heterogeneity to persist for longer, implying that original chemical heterogeneities can remain unmixed for a long period and may be concentrated at certain depths (Ten et al., 1998). These results suggest that Newtonian models underestimate the mixing time in the upper mantle, something that warrants further study.

2.4 Dispersal

2.4.1 Measures of dispersal

Based on sampling cells

One class of measure for measuring the dispersal of initially close particles through the domain is based on dividing the domain into sampling cells and using statistical measures based on the number of particles in each cell. Initially, all the tracers will be in one cell, but when they are completely dispersed, the distribution of number of particles per cell will be indistinguishable from a random distribution.

Measures that have been used include the fraction of sampling bins with 0 tracers (Christensen, 1989a) or the fraction of sampling bins with >5 times the average number of tracers (Christensen, 1989a) (both measures decrease with time), or the fraction of cells with >1 tracer, which increases with time (Schmalzl et al., 1996). (Schmalzl et al., 1996) plot statistics for each of several initial blocks, and derive a 'rate of mixing' from the slope.

The statistics of #particles/call can also be used to directly calculate a 'mixing time' (Olson et al., 1984a), which is the decay time for reduction of the variance, as described in section 2.6.1.

Based on separation

Given a distribution of particles, the **two-particle correlation function** H(r) gives the fraction of pairs of particles with separation less than r (Schmalzl and Hansen, 1994). To calculate H(r), all pairs of particles, i.e., N(N-1)/2 combinations, must be considered. H(0) is zero, then H(r) increases with r, reaching a maximum at either the size of the domain or the size of the tracer cloud (if smaller than the domain). The initial increase can generally be approximated as $H(r) \sim r^{\alpha}$, where α is the **correlation dimension**, and gives information about the dimensionality of the tracer cloud. In particlar, $\alpha = 1$ corresponds to tracers spread into a line, $\alpha = 2$ to well-mixed 2-D convection, and $\alpha = 3$ to well-mixed 3-D convection. In spherical geometry, a random distribution of heterogeneities has a correlation dimension that depends on length scale, rising to a maximum of 2.8 at ~4000 km, falling monotonically to ~2 at ~7500 km then plunging to 0 by 10,000 km (Stegman et al., 2002).

The **root-mean square dispersion index** was introduced by (Hoffman and McKenzie, 1985) to quantify long-wavelength dispersion. It is defined as the square root of the second moment of the autocorrelation of the density distribution, the general form of which is:

$$R_2 = \frac{\left(\iint r^2 dV_1 dV_2\right)^{1/2}}{\left(\iint dV_1 dV_2\right)^{1/2}} \quad (19)$$

where r is the separation of two volume elements dV_1 and dV_2 of the same body. To study the one-dimensional horizontal dispersion of a body represented by N tracers in a 2-D domain this is simplified to:

$$R_2 H = \frac{1}{N}\left(\sum_{i=1}^{N}\sum_{j=1}^{N} x_{ij}^2\right)^{1/2} \quad (20)$$

there x_{ij} is the horizontal separation of two particles i and j, and this measure reaches an asymptotic value (for perfectly random mixing) of

$$R_2 H(\infty) = \left[1/6(N^2 - 1)\right]^{1/2} \quad (21)$$

Other

Other quantities that have been used are the time spectrum of a tracer's vertical position, which gives the 'overturn time' of the convection (Schmalzl et al., 1996), and Poincaré sections (Schmalzl et al., 1995; Ferrachat and Ricard, 1998), i.e., 2-D slices of a 3-D volume showing where the particle paths intersect it. These are useful for identifying whether motion is restricted to closed 2-D surfaces as in (Schmalzl et al., 1995), or is chaotic (Ferrachat and Ricard, 1998).

2.4.2 Numerical results

Many discussions of "mixing" actually refer to the dispersal of heterogeneities around the domain, rather than the process of stretching and diffusion previously discussed. This dispersal is often studied by placing an array of tracers in one part of the domain, and studying how rapidly they spread out and become evenly distributed. A common observation in laboratory and numerical experiments (e.g., [*Richter, et al.*, 1982](Schmalzl and Hansen, 1994)) is that dispersal (and mixing) occur rapidly inside a convective cell, but much more slowly between one cell and another, i.e., long-range lateral dispersal can be a relatively slow process. Another way of expressing this is that "mixing" properties depend on spatial scale. The rate of cross-cell dispersal depends on how time-dependent the flow is, for example how time-dependent upwellings and downwellings at the cell boundaries are, and whether and how often the cell pattern reorganizes. In the limit of steady-state flow, inter-cell dispersion is zero in 2-D flows and in 3-D flows with only poloidal motion, but non-zero if toroidal motion is present, as discussed later.

Intra-cell dispersal. The dispersal of tracers within a cell scales similarly to stretching. In the experiments of (Christensen, 1989a) using a variety of kinematic and convective flows as discussed earlier, stretching-related diagnostics and dispersion-related diagnostics were compared, and found to obey similar behaviors, including the delineation of three regimes of mixing.

Inter-cell dispersal. For time-dependent 2-D flows, several numerical studies have studied the rate of lateral dispersion as a function of parameters. Convection that is completely internally-heated is typically highly time-dependent with no long-lived cells, and (Richter et al., 1982) found that at $Ra=1.4 \times 10^6$ tracers were fairly rapidly (e.g., in 0.1 diffusion times) dispersed across a box of aspect ratio 8 in what visually resembles a diffusion process. Using an analytic time-dependent flow they argued that rapid long-wavelength dispersal requires that the convective pattern change on a timescale comparable to the overturn time. Basally-heated convection tends to have a steadier cellular pattern. (Hoffman and McKenzie, 1985) presented a series of calculations, also in an 8x1 box at $Ra=1.4 \times 10^6$, with either 100% internal heating or 50% basal and 50% internal, and found that the flows with basal heating produced slower lateral dispersal, although it was still quite rapid. Completely heated from below flows were investigated by (Schmalzl and Hansen, 1994), who

found that at range Ra=10^6-10^8 heterogeneities within one cell are destroyed rapidly while two adjacent cells can remain unmixed for substantially longer, although at Ra=$3x10^6$ particles were well-dispersed by nondimensional time 0.02. They found the particle correlation function H(r) and corresponding correlation dimension to be effective measures of long-wavelength dispersion, with a value of 2 corresponding to a perfectly dispersed field. Higher Rayleigh number flows are more time-dependent such that the increase in the rate of laterally dispersion with Ra is higher than the increase in velocity with Ra (Schmalzl and Hansen, 1994).

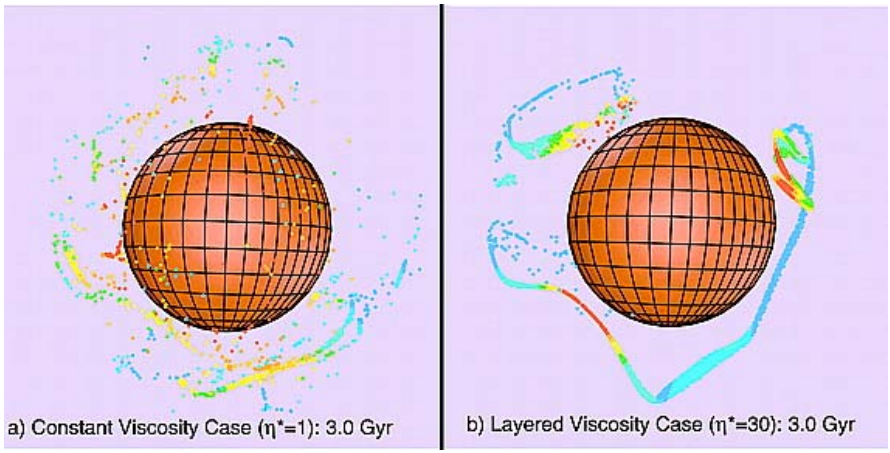

Figure 5. Dispersal of an initial 125 km radius cluster of tracers around the mantle after 3 Gyr, from (Stegman et al., 2002). Mantle flow is driven entirely by plate-like boundary conditions. Comparing the the two panels show the effect of a 30* viscosity increase at the 660 km discontinuity. In the lower mantle the heterogeneity is stretched into a ribbon-like structure, but this is more rapidly destroyed in the upper mantle, or in an isoviscous mantle, where toroidal flow is more prominent.

3-D spherical results. Results regarding inter-cell dispersal in cartesian 3D flows were mentioned in a previous section. Long-range dispersal in steady-state 3-D spherical flows was studied by (van Keken and Zhong, 1999), using a flow intended to be similar to the flow in the present-day mantle, generated by buoyancy from a slab model combined with an approximate plate rheology. They found that that particles could be efficiently transported far from their source: after 4 billions years of motion in this steady-state flow, pairs of particles initially 10 km apart were dispersed around the mantle with an almost flat probability distribution (i.e., number versus separation). This suggests that dispersal in the actual mantle is relatively efficient. (Stegman et al., 2002) extended such 3-D spherical modeling in order to determine whether dispersal is reduced by higher lower-mantle viscosity (see Figure 5). Using the correlation dimension to measure dispersion, they found that in a model with 100 times higher lower mantle viscosity and driven by a slab model and present-day plate motions, the correlation dimension reached after a few billion years is only of order 1, which is normally indicative of stretching into a line. A representative structure can be seen in Figure 5. They also found that in a model with 100 times higher lower mantle viscosity and driven by a slab model and present-day plate motions, the upper mantle became mixed about 60% faster than the lower mantle, which mixing is determined by the correlation dimension. They conclude that this is insufficient differential mixing to explain the difference between the relatively high heterogeneity of OIBs and relatively low heterogeneity of MORBs, although it could be argued that the latter is related to the small-scale structures in the melting region, whereas the correlation dimension is quantifying variations at ~1000s km lengthscales.

2.4.3 Eddy diffusivity?

In the atmospheric community, long-wavelength lateral dispersal is commonly treated using an "eddy diffusivity", although it has been found to be dependent on the initial lengthscale (separation) being considered: larger separations lead to larger estimates of effective eddy diffusivity (Richardson, 1926; Richter et al., 1982). It is interesting to know whether this concept could be applied to the mantle. (Olson et al., 1984b) studied whether an effective diffusion could be used to parameterize mixing within a convecting cell (an 'eddy'), and concluded that it could not, because the effective diffusion coefficient would need to be larger for larger heterogeneity size. However, the two studies that have attempted to fit lateral dispersal across convective cells with an effective "eddy" viscosity do appear to had reasonable success.

For internally-heated convection at Ra=$1.4x10^6$, (Richter et al., 1982) use the distance-neighbor approach of (Richardson, 1926) to estimate an eddy diffusivity for the large-scale dispersal of heterogeneities at a scale length several times that of the depth, and estimated a value of 30 times the thermal diffusivity, i.e., ~0.003 m^2/s, independent of initial separation. In similar experiments but with varying heating modes, (Hoffman and McKenzie, 1985) estimated a value of 25 times the thermal diffusivity for internally-heated convection, and 20 times the thermal diffusivity for 50% internal heated convection, by fitting the time evolution of the horizontal rms. dispersion index with a diffusion curve, i.e.,

$$R_2 H = \sqrt{\kappa t} \quad (22)$$

The slight difference from the almost identical experiment of (Richter et al., 1982) is probably due to difference in estimation technique and is not meaningful. and they find that their numerical experiment agrees this square root of time curve, so that eddy diffusivity is a good approximation for large scales of over 3 times the layer depth, and they get 20 times the thermal diffusion coefficient rather than 30 times. Based on these two studies, an eddy viscosity seems to offer a reasonable parameterization of lateral dispersal over distances greater than ~3 times the layer depth in a simple 2D convective system, but the application to more complex situations and as a function of convective parameters remains to be determined.

2.5 Residence Time

The concept of residence time plays a central role in geochemical theory (e.g., (Albarède, 1998)), and is something that can be investigated in numerical calculations of stirring and mixing processes. Residence time is defined as the length of time a heterogeneity (tracer) stays in the specified reservoir or other container. In geochemical box modeling, it may be applied to how long (on average) an isotope stays in a reservoir such as the continental crust, lower mantle, etc. In numerical modeling of mantle evolution it usually means the average length of time before a tracer is sampled by melting, either from the beginning of the calculation or, if tracers are being continually introduced at subduction zones, the average length of time before they are next sampled (melted). For whole-mantle convection in statistical equilibrium, this is equal to the time taken for one mantle mass to pass through the mid-ocean ridge processing zone, the quantitative value of which was discussed earlier in section 1.5.3, and is probably around 6 Gyr at the present processing rate, but could have been much faster (i.e., lower) in the past, which (Phipps Morgan, 1998) showed can easily match the "50% Argon outgassing constraint" as discussed in section 1.6.1.

From a chemical perspective, the residence time for lithophile elements was calculated by (Albarède, 2005b) by dividing the amount of the element in a mean mantle model (i.e., bulk silicate Earth – continental crust) model by the current rate at which the element is extracted into the ocean crust. Residence times in the range 4-9 Gyr were obtained, which bracket the geophysically-constrained value of ~6 Gyr discussed in section 1.5.3. Again, it is likely that processing was

substantially faster in the past, as is required to match the Argon outgassing constraint (Phipps Morgan, 1998).

In geochemical box modeling it is commonly assumed that a reservoir is randomly sampled, i.e., the probability of melting each atom or tracer in the reservoir is equal regardless of how long they have been in the reservoir, in which case the overall process is analogous to radioactive decay. Thus, if a reservoir starts off with N_0 atoms or tracers of a particular isotope, the rate of sampling is given by:

$$\frac{dN}{dt} = \frac{N}{\tau} \quad (23)$$

where τ is the residence time. Hence the number left after time t is given by:

$$N = N_0 \exp(-t/\tau) \quad (24)$$

The random sampling assumption is valid if tracers are effectively dispersed through out the domain in question by time-dependent flows, and as discussed in section 2.3.3, fully time-dependent free convection (i.e., without kinematic constraints) experiments have always displayed chaotic mixing, which effectively disperses tracers. In steady-state 2D flows, tracers are instead restricted to individual streamlines, so only streamlines that intersect the sampling area are sampled and the sampling increases linearly with time until all tracers on the those streamlines have been sampled (Coltice, 2005). Viscosity stratification has only a minimal effect, as discussed elsewhere. If heterogeneities are anomalously dense they may preferentially reside near the base of the domain, reducing the number in the sampling area which can increase average residence time.

The earliest study to check residence times was (Gurnis and Davies, 1986b), who investigated a low-Ra flow driven by internally-heated convection at Ra=10^5 and "organized by" a kinematic plate-like surface velocity condition. Tracers were introduced at the simulated moving trench, and it was found that the length of time tracers spend in the box before being sampled was easily predicted by the applied volumetric sampling rate and the rate of introduction of new tracers, consistent with the random sampling assumption. For free convection, (Coltice, 2005) confirmed that random sampling applies when the mixing is chaotic.

Effect of chemical density. In a related study (Gurnis, 1986a), the effect of the heterogeneity being denser than surrounding material was studied, and found to have a fairly small effect, despite chemical buoyancy ratios as large as 2. However, with a more Earth-like model setup, this conclusion is modified (Christensen and Hofmann, 1994; Davies, 2002). (Davies, 2002) adopted a similar model setup, but at the correct convective vigor for Earth, and with a chemical buoyancy ratios of up to 0.8, and also obtained residence times consistent with random sampling. While the mean age of tracers was only slightly increased (from a scaled 2.42 to 2.52 Ga), some dense basaltic tracers settled into piles at the base, and their mean age increased by 32% from 2.57 to 3.38 Ga. If tracers are truly randomly sampled, then the distribution of ages should have a particular probability distribution that depends on the source function. (Davies, 2002) showed that tracers settling the base of the domain have a probability density function (PDF) that is dramatically different from those in the MORB sampling region, which implies that random sampling does not apply to all tracers even though the average residence time may not change much. An appropriate description is probably that a different residence time applies to material that settles above the CMB, and (Christensen and Hofmann, 1994) calculated such a quantity for their calculations in which somewhat more basalt settling was obtained. They obtained residence times in the dense basal layer of between 0.36 and 1.62 Ga depending on parameters. For the whole system, they did not calculate the "mean age" but rather the lead-lead pseudo-isochron age; changing the buoyancy ratio from 1.0 to 2.25 while keeping other parameters constant changed the Pb-Pb age from 1.37 to 2.66 Ga. Thus, if density contrasts cause a layer to form, it is important to study residence times in the layer, and not just the average of the whole system.

Effect of viscosity stratification. The effect of viscosity stratification and heating mode on residence time was determined by (Coltice, 2005). When the Ra is high enough for the flow to effectively disperse the tracers, the residence time scales with the theoretical prediction based on fraction of the mantle sampled per unit time, independent of viscosity contrast. This is consistent with works that have studied the effect of viscosity stratification on the depth distribution of mean age (van Keken and Ballentine, 1998; Hunt and Kellogg, 2001)- the effect is minimal.

2.6 Mixing Time

2.6.1 Background

Several definitions of "mixing time" have been used, which, together with sensitivity of stirring rate to the exact type of assumed flow, has led to a wide variety of estimates for mixing time in the mantle. Some estimates have been based on stretching, while others have been based on dispersal. As discussed previously, "mixing" (dispersal) across several convective cells can be far slower than "mixing" in a single convective cell. In any case, a key quantity is the lengthscale of interest, which could be the diffusion lengthscale, or sampling lengthscale.

The strictest definition of mixing time is the time required for the heterogeneities to get stretched thin enough to be homogenized by diffusion, which requires stretching down to sub-meter lengthscales for silicate rocks. It is questionable, however, whether such small-scale variations can be observed in geochemical observations (see later discussion) so an important concept is that of sampling volume (or, in 2-D, sampling area) (Richter and Ribe, 1979), which can be re-expressed as a sampling lengthscale by taking the cubed (or square) root (Olson et al., 1984b; Olson et al., 1984a). This sampling volume describes the region over which heterogeneities are homogenized by the sampling process, such as partial melting and extraction and mixing of magmas with each other and with the rock through which they are passing. While this has often been assumed to be ~tens of kilometers, some of the geochemical observations discussed in section 1.7 indicate that shorter-lengthscale heterogeneity can be preserved in the resulting rocks. When calculating compositional heterogeneity in models, heterogeneity should be integrated (averaged) over the sample volume. In summary the mixing time is the time required for heterogeneity to get stretched to the sampling size or the diffusion lengthscale, whichever is larger.

It has been usual to scale estimates of mixing time to either upper mantle convection or whole-mantle convection, which generally results in rather small estimated timescales for upper mantle mixing. These are probably irrelevant to the present-day mantle, as it is now clear that the upper mantle is not convecting independently as a simple heated-from-below Rayleigh-Bénard system, but instead the convective regime is dominated by whole-mantle flow and the plates impose a long-wavelength organization to the upper mantle. It is possible that small-scale convection below the plates exists in the upper mantle, but this would be less vigorous than assumed in the 'upper mantle' mixing estimates and its effect on mixing has not yet been evaluated.

Some important statistical measures of heterogeneity are now introduced, following (Olson et al., 1984a). The two-point correlation function is given by:

$$R(\mathbf{r},t) = \left\langle \theta(\mathbf{x}')\theta(\mathbf{x}'+\mathbf{r}) \right\rangle \quad (25)$$

where $\theta(\mathbf{x})$ is the compositional field, $\mathbf{x}$ is the position vector, $\mathbf{r}$ is the separation vector and the angle brackets denote the volume average. Its Fourier transform, the energy spectral density (Olson et al., 1984a) in n spatial dimensions is given by:

$$E(\mathbf{k},t) = \left(\frac{1}{\pi}\right)^n \int_0^\infty R(\mathbf{r},t)\exp(-i\mathbf{k}\cdot\mathbf{r})\mathbf{dr} \quad (26)$$

and the related variance of composition σ^2 is given by

$$\sigma^2 = R(0,t) = \int_0^\infty E(\mathbf{k},\mathbf{t})\mathbf{dk} \qquad (27)$$

If heterogeneity is not created or destroyed but only changes wavelength, the variance remains constant with time (see Ricard, ch.2, this volume). However, if there is a sampling wavelength below which heterogeneity can no longer be detected, then it is appropriate to use the corresponding wavenumbers as the upper limit for the integration, leading to the sampling variance:

$$\overline{\sigma}^2 = \int_0^{k_s} E(\mathbf{k},\mathbf{t})\mathbf{dk} \quad (27)$$

which will decrease with time due the cascade of heterogeneity to shorter wavelengths if heterogeneity is not replenished at long wavelengths. This has led to one definition of the mixing time (Olson et al., 1984a),

$$\tau_{mix} = \int_0^\infty \frac{\overline{\sigma}^2(t)}{\overline{\sigma}^2(t_0)} dt \qquad (28)$$

the physical meaning of which is the time needed to reduce the sample variance of the composition significantly. A modification of this should be made when calculating $\overline{\sigma}^2$ numerically using a finite number of sampling cells containing a finite number of tracer particles, as described by (Ferrachat and Ricard, 2001). In this situation, $\overline{\sigma}^2$ does not tend asympotically to zero, so the integral does not converge. Instead, the statistical limit is:

$$\lim_{t\to\infty} \frac{\overline{\sigma}^2(t)}{\overline{\sigma}^2(t_0)} = \frac{s-1}{n} \quad (29)$$

where s is the number of sampling cells and n is the number of particles. Thus, (Ferrachat and Ricard, 2001) introduce a definition for mixing time that includes this and does converge:

$$\tau_{mix} = \int_0^\infty \left(\frac{\overline{\sigma}^2(t)}{\overline{\sigma}^2(t_0)} - \frac{s-1}{n}\left[1 - \exp(-t/\tau_{mix})\right] \right) dt \qquad (30)$$

The mixing time is expected to depend on sampling lengthscale, as discussed elsewhere. To test this, the number of sample cells *s* can be varied, as was done by (Olson et al., 1984a; Ferrachat and Ricard, 2001). (Ferrachat and Ricard, 2001) found that the mixing time increases regularly with 1/lengthscale, with a moderate increase in mixing time for decreasing cell size – approximately a factor of 4-5 for factor 32 decrease in lengthscale.

2.6.2 Laminar flows

A heterogeneity is stretched until it is either homogenized by diffusion or has a width of less than the sampling lengthscale. The balance between diffusion and sampling lengthscale in controlling the mixing time was analyzed by (Olson et al., 1984b) for idealized flows, then compared to numerical results of a steady-state Rayleigh-Bénard convection cell in which the stretching rate is laminar with time. Substituting the spectral expansion of a heterogeneity into the above equation led to the mixing time for non-diffusive laminar stirring being proportional to initial lengthscale / sampling lengthscale , i.e.,

$$\tau_{mix} \approx \frac{\pi}{\dot{\varepsilon} k_0 \Delta z} = \frac{\lambda_0}{2\dot{\varepsilon}\Delta z} \qquad (31)$$

where λ_0 is the initial wavelength of heterogeneity (if a localized heterogeneity, twice its size) and Δz is the sampling lengthscale. If, however, diffusion is rapid enough to homogenize the heterogeneity before it reaches the sampling lengthscale, a different expression is obtained:

$$\tau_{mix} \approx \left(\frac{\lambda_0^2}{4\kappa\dot{\varepsilon}^2} \right)^{1/3} \qquad (32)$$

where κ is the diffusivity. There is a smooth transition between these types of behavior.

(Olson et al., 1984b) tested these equations using a single Bénard convection cell, and found that the results fitted reasonably well, for both non-diffusive and diffusive heterogeneity. Scaled to the Earth with an assumed $\dot{\varepsilon} = 3 \times 10^{-15}\, s^{-1}$, an initial anomaly wavelength equal to the depth and a sampling lengthscale of 5 km, this leads to mixing time of 2.3 Gyr for upper mantle convection or 10 Gyr for whole mantle convection.

In the convective+kinematic internally-heated (Ra=10^5) flows of (Gurnis and Davies, 1986b), long-lived clumps (folded strips of crust) that persisted over tens of transit times were observed, even though most tracers were well dispersed. Based on qualitative measures the authors estimated the survival time of the clumps to be 2.4 Gyr, or 1.4 Gyr if faster processing in the past is taken into account.

2.6.3 Turbulent regime

For turbulent mixing, the equivalent result for non-diffusive flow is logarithmic and thus more rapid (Olson et al., 1984b):

$$\tau_{mix} \approx \frac{1}{\dot{\varepsilon}} \ln\left(\frac{2\lambda_0}{\Delta z} \right) \qquad (33)$$

An important point to note is that effective strain rate $\dot{\varepsilon}$ that goes into this equation can be more than an order of magnitude smaller than the average (e.g., root mean square) strain rate of the flow and depends on the details of the flow. For the convective flows investigated by (Christensen, 1989a) at Rayleigh numbers in the range 10^5-10^6, the effective strain rate was a factor of 10-30 less than the mean strain rate of the flow. The effective strain rate scales in proportion to convective velocity over a wide range of Rayleigh number for both basally-heated and internally-heated flows (Coltice, 2005).

As for mixing time, (Christensen, 1989a) assumed the mantle well mixed when >90% of the heterogeneities had been reduced to less than 1/50th of their original size, and scaled his numerical results to the Earth using the transit time. This led to an estimate of 200-300 Ma for upper mantle convection, or 1500-2000 Myr for whole-mantle convection with a reasonable viscosity increase with depth. There are two points to note. This mixing criterion involves stretching oceanic crust down to 100 m thickness, which is larger than what other estimates have assumed: if instead the mixing is taken to meter scale, this timescale estimate is ~doubled to 3-4 Gyr for whole-mantle convection. Secondly, there is a wide distribution in stretching rates, so that even when the "mixed" criterion is met, there are still heterogeneities that are substantially larger and could influence isotopic signatures.

(Hoffman and McKenzie, 1985) also estimate mixing time from the scaling relationships that they found for small-scale stretching and large-scale dispersion. They estimated that "any reasonable body" experiencing upper mantle convection will be thinned to 10^{-3} layer depths (700 m) in 400 Myr and 10^{-6} layer depths (0.7 m) in 700 Myr; for whole mantle convection these timescales are 1.0 Gyr (for 3 km) or 1.5 Gyr (for 3 m). However, lateral dispersion takes much longer: for half the circumference of the Earth and whole mantle convection the timescale is 4.6 Gyr, similar to the age of the Earth.

The mixing time for subducted oceanic crust in a kinematic chaotic flow was calculated by (Kellogg and Turcotte, 1990). They assumed that a heterogeneity must be stretched thin enough for diffusive homogenization to take place based on the model of (Kellogg and Turcotte, 1986), which gives an equation for mixing time of:

$$t_h = \frac{12h}{\pi u_{sm} \overline{\alpha}_e} \ln\left[4b_0\left(\frac{\pi u_{sm}\overline{\alpha}_e}{12Dh}\right)^{1/2}\right] \quad (34)$$

where D is the chemical diffusivity (assumed to be 10^{-19} m^2s^{-1} based on (Hofmann and Hart, 1978; Sneeringer et al., 1984)), h is the depth of the convecting layer, b_0 is the initial heterogeneity size (assumed to be 6 km), u_{sm} is the average surface velocity (assumed to be 10 cm/year) and $\overline{\alpha}_e$ is the effective strain rate from the numerical experiments. With these assumptions t_h was calculated to be 240 and 960 million years for upper mantle convection or whole mantle convection respectively, which is the time for 50% of the heterogeneities to be homogenized by diffusion and corresponds to 9 overturns. The diffusive homogenization lengthscale for this is less than 1 cm for both cases, and the amount of thinning is 6 to 7 orders of magnitude. Due to idealizations in their model, however, these times must be interpreted as lower limits. One idealization is that this is not a real convective flow, and it is not clear how representative the effective strain rate will be of the real mantle. For example, in the real mantle the viscosity increases with depth, which will reduce the strain rate in the deep mantle and increase the "overturn time", a concept which itself is not well defined for flow in the actual mantle. An obvious quantitative issue is that the assumed average surface velocity of 10 cm/year is approximately three times larger than Earth's actual mean poloidal surface velocity, the poloidal component of which is around 3.5 cm/year (Lithgow-Bertelloni et al., 1993). If the times are recalculated with this value, they change to 660 and 2630 million years, respectively, the latter of which may well be consistent with geochemical evidence for survival of geochemical heterogeneity over 2 billion year timescales.

In the actual mantle, heterogeneity is continuously introduced at the same time as 'old' heterogeneity is destroyed by stirring and diffusion, so (Kellogg and Turcotte, 1990) also consider the fraction of the mantle that is completely homogenized by the present day when oceanic crust is continuously introduced into the mantle over geological time. For this it is first necessary to assume an equation for crustal production vs. time, and they assume that oceanic crustal production in the past scales with radiogenic heat production in the mantle with a 1/e decay time of 2.5 Gyr (Turcotte and Schubert, 1982), that the present rate of production is 2.8 km^2/year,and that the processing depth under mid-ocean ridges in 60 km, assumptions that lead to half of the mantle being processed in 800 Myr for layered convection or 2200 Myr for whole mantle convection. Combining this melting model with their mixing model, they derive an expression for F(d), the fraction of particles narrower than d. Hence setting d to the diffusion lengthscale of 10^{-7}, they obtain a curve for the fraction of particles that have been completely homogenized, in terms of the mixing time. For their estimated whole-mantle mixing time of 960 Myr, 67% of the mantle is perfectly mixed, but for the adjusted mixing time of 2.6 Gyr as discussed above, this fraction is 28%, i.e., over 70% of the present-day mantle is still in the form of strips of varying thickness. Thus, they predict substantial chemical heterogeneity even with the relatively rapid mixing in their experiments.

(Kellogg and Stewart, 1991) estimate the effective strain rate and mixing time for a chaotic flow using the same method, but this time the flow is the nonlinear interaction of a single

convection roll with a single spatial subharmonic and the obtained mixing times are about a factor of 2 smaller.

2.6.4 Summary of different "mixing time" estimates

Table 1 summarizes the various estimates of mixing time for whole mantle convection, as discussed above. As far as the author is aware these are all the published estimates given in dimensional time units, although it might be possible to obtain additional estimates by scaling nondimensional results from other studies. Estimates vary by an order of magnitude, from 1 to 10 Gyr, because of different assumptions about the lengthscale to which heterogeneities should be stretched, the type of flow, and the flow velocity. (Gurnis and Davies, 1986b) were concerned with the survival of large clumps, so their estimate is not directly comparable to the other estimates. The estimate of (Olson et al., 1984b) is large because they assumed laminar flow, whereas it is now established that time-dependent convective flows tend to give turbulent mixing, as occurred in the last three estimates. The estimate of (Kellogg and Turcotte, 1990) should be at least tripled because their assumed velocity was too large, as discussed above. The estimate of (Christensen, 1989a) refers to stretching oceanic crust to ~100 m thicknes, and should be at least doubled for comparison with the (Kellogg and Turcotte, 1990) estimate. The estimate of (Hoffman and McKenzie, 1985) was made before it was established that the lower mantle is probably a factor of ~30 more viscous than the upper mantle (they assumed a factor of 3), so should be at least doubled when this is taken into account. When such scaling is done, estimates are better agreement, in the 3-4 Gyr range for stretching crust to the sub-meter lenthscale. If an equivalent table were constructed for upper mantle convection estimates then the times would be much shorter, but as argued earlier, geophysical constraints indicate that the dominant mode of convection in the present Earth is whole-mantle, and the effect of possible 'small-scale' convection beneath the oceanic plates has not yet been evaluated.

Table 1. Summary of mixing time estimates.

Study	τ_{mix} *(Ga)*	*Lengthscale (inner)*	*Notes*	*Rescaled* τ_{mix} *(Gyr)*
(Gurnis and Davies, 1986b)	2.4	Visible clumps	Survival time	
(Olson et al., 1984b)	10	Diffusion	Laminar stretching	
(Christensen, 1989a)	1.5-2.0	1/50 (~100 m)	90% reduced to this size	3-4
(Hoffman and McKenzie, 1985)	1.0	3 km	only 3* viscosity increase with depth	>3
	1.5	3 m		
(Kellogg and Turcotte, 1990)	0.96	diffusive	50% homogenized	~3

2.7 Spectrum of Chemical Heterogeneity

As was discussed in a section 1.7, our knowledge of the spectrum of chemical heterogeneity in the mantle is far from perfect but some useful information does exist. Geochemical observations show the existence of heterogeneity at all lengthscales, from the scale of melt inclusions to thousands of kilometers, and quantitative information regarding the spectrum is becoming available. As also discussed earlier, seismological information points to the existence of scatterers throughout the lower mantle, with the amount of scattering varying from place to place. The longest wavelengths are constrained by seismic tomography but separating thermal from compositional contributions has major uncertainties. This section reviews the dynamical theory about the expected lengthscales of heterogeneity.

Mantle heterogeneity is introduced at long wavelengths by subduction (and possibly, primordial layering). If subducted material segregates into a layer then this acts to increase its wavelength, but if it remains in the convective flow then it is progressively stretched until it reaches small enough lengthscales to be homogenized by diffusion. Thus, as discussed by (Olson et al., 1984a), the spectrum of mantle heterogeneity undergoing stirring is expected to display three regions with increasing wavenumbers (decreasing wavelength): a 'source' region corresponding to the spectral characteristics of the source, a "cascade" region in which the heterogeneities are being stretched to shorter wavelengths, and a "dissipation" region, in which chemical diffusion acts to eliminate heterogeneity at the shortest scales. It is useful to consider the spectrum that is obtained in statistical equilibrium, in which heterogeneity is introduced at a constant rate and the total spectrum does not change with time. This depends on the stretching regime in the cascade region: For laminar stirring the wave number k of an individual heterogeneity increases linearly with time, which leads to a flat ("white") spectrum for all heterogeneities in statistical equilibrium (Olson et al., 1984a). In contrast, for turbulent stirring the wave vector of an individual heterogeneity increases exponentially with time, i.e., the rate of increase is proportional to its present value, which leads to a statistical equilibrium spectrum that scales as 1/k. This at first seems inconsistent with the with the -5/3 slope obtained by (Metcalfe et al., 1995) for a kinematic chaotic stirring of a laboratory fluid, but as this system was not in statistical equilibrium the slope reflects a transient regime.

Geochemical observations, as discussed in Section 1.7, can be compared to these theoretical slopes. The early analysis of (Gurnis, 1986b) using $^{87}Sr/^{86}Sr$ data from MORB and ocean island basalts appeared to be consistent with a "white" laminar mixing spectrum, but the more highly constrained spectrum of isotope ratios along the mid-Atlantic ridge obtained by obtained by (Agranier et al., 2005) instead indicates the turbulent, 1/k regime, consistent with expectations from mantle mixing theory discussed earlier.

Such theory also successfully predicts the smaller scales of heterogeneity observed in peridotite massifs in Beni Bousera (Kellogg and Turcotte, 1990). They derive that the probability of finding a strip of material larger than size d is given by $1/d\left(1-F(d)\right)$, which, when evaluated for scales between 1 and 100 cm gives a slope close to –1, indicating that the $(1/d)$ term is dominating and $(1\text{-}F(d))$ doesn't change very much over this range. Field samples match this slope reasonably well.

In any case, it is clear that because thermal heterogeneity diffuses rapidly whereas chemical heterogeneity does not, short wavelength mantle heterogeneity is dominantly chemical in origin, while thermal heterogeneity should be important, and perhaps dominant, at long wavelengths, although recent seismological studies argue for a large chemical component (Trampert et al., 2004; Deschamps et al., 2005). These expectations are confirmed in the thermo-chemical convection calculations of (Nakagawa and Tackley, 2005b), in which the slope of the chemical heterogeneity at long wavelengths also appears to be consistent with a $1/k$ scaling, although they do not study how this scales at short wavelengths.

3. MANTLE CONVECTION WITH ACTIVE (BUOYANT) CHEMICAL HETEROGENEITY

This section considers thermo-chemical mantle convection in which the composition affects density. Studies have typically considered what happens with a pre-existing dense layer, or the development of a layer over time by settling of dense material or reactions with the core. Because the chemical diffusivity in the mantle is orders of magnitude lower than thermal diffusivity, it is typically assumed that the chemical field is non-diffusive, although if the field is being treated as a continuous field then some numerical diffusion is typically introduced in order to stabilize the advection. The Lewis number gives the ratio of chemical to thermal diffusivity:

$$Le = \frac{\kappa_T}{\kappa_C} \quad (35)$$

Its value is quoted as $\sim 10^8$ by (Hansen and Yuen, 1989), but the chemical diffusivity quoted by (Kellogg and Turcotte, 1986) would lead to $Le=10^{13}$.

Attention has generally focused on two cases: compositional layering at the 660 km interface, or a relatively thin composition layer above the CMB corresponding to D".

3.1 Stability and Dynamics of Chemical Layering in a Convecting Mantle

3.1.1 The balance between chemical and thermal buoyancy

If a layer of dense material is present, the parameter that most strongly influences its dynamics and evolution is the ratio of chemical density contrast to thermal density contrast, i.e., the buoyancy ratio, here written as B:

$$B = \frac{\Delta\rho_C}{\Delta\rho_T} = \frac{\Delta\rho_C}{\rho_0 \alpha \Delta T} \quad (36)$$

where $\Delta\rho_c$ is the density contrast due to composition, $\Delta\rho_T$ is that due to temperature, ρ_0 is the density, and ΔT is the temperature contrast. If ΔT represents the total thermal contrast available in the system, then it has been found that the layering displays long-term stability with a fairly flat interface if B is greater than some critical value of order 1, and undergoes either large-topography layering or various shorter-lived behaviors that end in mixing and whole-mantle convection, if B<1 (Richter and Johnson, 1974; Richter and McKenzie, 1981; Olson and Kincaid, 1991; Montague et al., 1998; Davaille, 1999a; Montague and Kellogg, 2000; Le Bars and Davaille, 2004a). The behaviors of short-lived modes were systematically mapped out as a function of B, viscosity contrast and layer thickness using laboratory studies (Davaille, 1999a; Davaille, 1999b; Le Bars and Davaille, 2004b; Le Bars and Davaille, 2004a) supplemented by mathematical analysis (Le Bars and Davaille, 2002), and are generally consistent with earlier laboratory and numerical studies, as follows, and as illustrated in the domain diagram of Figure 6:

(i) B>1 stable stratification, both layers convecting with slow entrainment
(ii) B>1 but thin, non-convecting lower layer
(iii) 1>B>0.5: layered but with large topography
(iv) 0.3<B<0.5, layer thickness between 0.2 and 0.7: doming, for and, #pulsations increases rapidly with viscosity contrast,
(v) B<0.2: rapid overturn and mixing of layers.

If the two layers initially have the same temperature, then additional transient behavior occurs as a temperature difference develops across the layers, thereby decreasing the total (i.e., thermal+chemical) density contrast. In this case, layers that should be unstable according to the above criteria may initially be stable, as in, for example, the calculations of (Samuel and Farnetani, 2003). B may decrease with time due to the entrainment of each layer into the other layer, as discussed below. Indeed, in laboratory experiments of (Le Bars and Davaille, 2004b) (Figure 2), the experiment evolved through several different regimes as the density difference between the layers decreased. Another initial condition that causes transient behavior is a linear compositional gradient throughout the domain and constant temperature, as studied by (Hansen and Yuen, 2000), who found that after some time the system developed a stable but large-topography layer. After that, the evolution discussed in the remainder of this section applies.

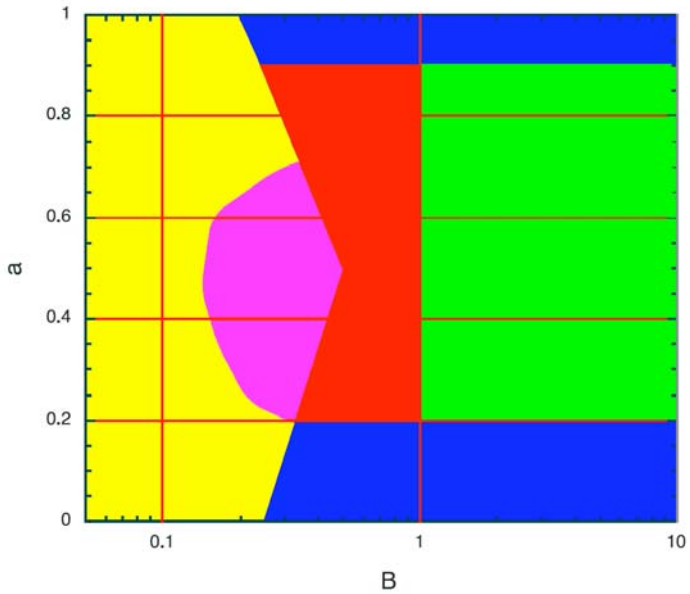

Figure 6. Domain diagram for the behavior of thermo-chemical convection as a function of buoyancy ratio B and initial depth of dense layer a, as determined by laboratory experiments (Davaille, 1999b; Davaille et al., 2002; Le Bars and Davaille, 2002; Le Bars and Davaille, 2004a; Le Bars and Davaille, 2004b). Green=flat layers, red=large topography layers, pink=transient oscillating domes, blue=thin non-internally convecting layer progressively entrained by thermo-chemical plumes, yellow=rapid overturn. Adapted from (Le Bars and Davaille, 2004b)

In the mantle, the relevant physical properties (α, ρ_0) vary with depth, and the above criteria are most valid if values of the physical properties close to the chemical boundary area considered, although some studies have used, for example, reference or 'surface' values and thus require careful interpretation. Scaling to the Earth, the appropriate ΔT is the superadiabatic temperature drop between surface and CMB, which might be 2500 K. For layering at around 660 km depth, α~2.5x10^{-5}, so the critical $\Delta\rho_c/\rho_0$~6.25%, whereas at the CMB α~1.0x10^{-5} , so $\Delta\rho_c/\rho_0$~2.5%. These are rough estimates, as it has been found that other characteristics such as the viscosity contrast between the two layers (a combination of intrinsic viscosity contrast and temperature-dependent contrast) , the thickness of the dense layer, and the thermal conductivity of the dense layer also play a role, as discussed later.

The detailed dynamics have been investigated variously by laboratory and numerical experiments with some mathematical analyses, with laboratory experiments having the advantage of physical correctness, which is particularly important because entrainment rates are difficult to accurately measure numerically (van Keken et al., 1997; Tackley and King, 2003), whereas numerical experiments have the advantage that the variation of physical properties (viscosity, thermal expansivity, conductivity) with pressure and temperature can be more realistically ascertained and full information about the various fields is available for analysis. Experiments (both numerical and laboratory) with layering are often initialized in a way that is far from a steady-state (e.g., temperature is isothermal instead of higher in the lower layer), which results in a transient behavior. Furthermore, layered experiments are intrinsically transient in that the layering evolves with time, and this may result in the final state retaining a memory of the initial conditions. Further discussion of laboratory experiments can be found in (Davaille, this volume).

3.1.2 Initially stable layering: pattern and dynamics

Flat, thick, internally-convecting layers. For thick, convecting layers, layered convection occurs and a thermal boundary layer builds up over the interface, with heat transport accomplished by thermal diffusion, substantially reducing the global heat flow and affecting Earth's thermal evolution (Montague and Kellogg, 2000). For layers of approximately equal thickness and viscosity, as in the laboratory and numerical experiments of (Richter and McKenzie, 1981), the temperature difference between the layers is $\Delta T/2$ (Richter and McKenzie, 1981), but this varies as the viscosity contrast and thicknesses are changed. The pattern of convection in the upper and lower layers are coupled. When the layers are of similar viscosity, mechanical coupling dominates such that upwellings in one layer match with downwellings in the other layer (Richter and McKenzie, 1981; Cserepes and Rabinowicz, 1985). When there is a large viscosity contrast exceeding a factor of ~100 (Cserepes and Rabinowicz, 1985), however, thermal coupling dominates, in which upwellings in the lower layer underlie upwellings in the upper layer. Intermediate viscosity contrasts, such as 25-30, result in a mixture of thermal and mechanical (viscous) coupling, as show by 3-D calculations (Cserepes et al., 1988; Glatzmaier and Schubert, 1993). In this mixed regime, the flow direction of rolls in the upper layer was observed to become perpendicular to those in the lower layer by (Cserepes et al., 1988). Entrainment occurs at cusps in the interface, as discussed later.

If one layer is substantially more viscous, the form of upwellings or downwellings forming at the interface is also different (Davaille, 1999b), with 2-D sheets forming in the more viscous layer but 3-D plumes forming in the less viscous layer, which have different entrainment rates as discussed below.

Thin, non-convecting lower layer. In this case the lower layer is embedded within the lower thermal boundary layer of the main convection, and the dense material gets swept by the convection, forming a spoke pattern of ridges on top, with plumes at the junctions of the ridges, and entrainment takes place there, as shown by 3-D numerical experiments (Tackley, 1998) and laboratory experiments (Olson and Kincaid, 1991; Davaille et al., 2002). The numerical experiments show that this dense layer acts like a rigid boundary, reducing the horizontal wavelength of convective planform relative to a free-slip lower boundary (Tackley, 1998), and that if the layer internally convects (Montague et al., 1998; Montague and Kellogg, 2000), as would be the case if its viscosity is low enough (Solomatov and Moresi, 2002; Schott and Yuen, 2004), small-wavelength thermal structure is generated within the layer. These numerical experiments also show that even in 100% internally-heated cases, entrainment exists at cusps anticorrelated with where the downwellings are, and larger amounts of internal heating reduce the buoyancy ratio needed for stability. Temperature-dependent viscosity decreases the density contrast needed for stable layering (Tackley, 1998; Schott et al., 2002), and when the layer is marginally stable, can lead to complicated schlieren structures of entrained material, and complicated layer topography (Schott et al., 2002). For reasonable Earth parameters, (Tackley, 1998) found for an internally-heated case that ~1% density contrast was sufficient to maintain a layer over reasonable timescales.

Thick, large-topography lower layer. With a lowish buoyancy ratio like 0.6 (Montague et al., 1998), the topography on the layer interface is large (Davaille, 1999a; Kellogg et al., 1999), which may result in discontinuous 'piles' or 'hills' if the layer thickness is less than the topography. In 2-D calculations at low Rayleigh number, this results in wide stable 'hills' below the upwelling, which cause strong (~several km) negative topography on the CMB (Davies and Gurnis, 1986; Hansen and Yuen, 1989), with temperature-dependent viscosity decreasing the magnitude of this negative topography (Hansen and Yuen, 1989). The topography on a layer interface decreases with increasing Rayleigh number, approximately as $Ra^{-1/3}$ (Davies and Gurnis, 1986; Tackley, 1998), which predicts relatively little topography at the Earth's convective vigor (Montague and Kellogg, 2000). If, however, the increase of viscosity and thermal conductivity and decrease of thermal expansivity with depth is taken into account, they lead to a low effective Ra for the deep mantle, so large interface fluctuations can still occur, as shown in 3D (Tackley, 1998; Tackley, 2002). It has

been argued that such structures may account for the superplumes observed in seismic tomography, discussed in section 1.8. An important point shown by (van Thienen et al., 2005) is that any layering around 660 km induced by the post-spinel phase transition makes the layer more stable over long time periods, presumably because it reduces the temperature drop across the layer and the convective velocities.

Regarding the three-dimensional structure of a strongly undulating layer, Cartesian calculations (Tackley, 1998; Tackley, 2002), either Boussinesq or compressible with either constant, depth-dependent or depth-and temperature-dependent viscosity, found that the long-term solution of piles tend to be ridges/spokes. In spherical geometry Boussinesq calculations (Oldham and Davies, 2004) there appears to be a greater tendency for the piles to be isolated. A viscosity contrast between the layers makes a major difference to the planform: (McNamara and Zhong, 2004b) show that temperature-dependent viscosity leads to linear piles that are swept around and spread through the entire lower mantle, whereas compositional-dependent viscosity in which the dense material is more viscous leads to isolated round 'superplumes', particularly with contrasts as large as factor 500. This seems to be consistent with the 'domes' in the laboratory results of (Davaille, 1999a), except that they also observe domes when the dense layer is less viscous. The reconciliation of these is that such domes are transient features- for long-lived features domes are only observed when the lower layer is more viscous (McNamara and Zhong, 2004b).

Applying the specific geometry and motion of Earth's plates to a spherical thermo-chemical convection model, (McNamara and Zhong, 2005) found that structures similar to those seismologically observed under Africa and the Pacific were generated. Specifically, Earth's subduction history tends to focus dense material into a ridge-like pile beneath Africa and a relatively more rounded pile under the Pacific ocean, which they argue is consistent with seismic observations.

3.1.3 Influence of a dense layer on plume dynamics

Temperature. The presence of a dense layer reduces the temperature anomaly of plumes (Farnetani, 1997; Zhong, 2006), which may help to explain why the inferred temperature anomaly of plumes close to the lithosphere is much lower than the estimated temperature drop across the lower thermal boundary layer (TBL) for whole-mantle convection.

Stability: Laboratory experiments find that plumes rising from cusps of a dense layer are stable over longer time periods than plumes rising from the lower TBL of whole-mantle convection. In particular (Davaille et al., 2002) finds that the dense layer acts as a 'floating anchor', reducing the lateral migration of plumes, which then have a scaled drift velocity of 1-2 mm/year-larger than simple scalings predict for thermal plumes. In addition the dense layer enables them to survive for 100s Myrs,. The plume spacing is proportional to the stratified boundary layer thickness. In the laboratory experiments of (Jellinek and Manga, 2002), the dense, low-viscosity material forms a network of ridges (embayment and divides) and they delineate the trade-off between viscosity contrast and layer topography in the stabilization of plumes. They found that if the dense material has a similar viscosity, the topography required to stabilize plumes is >2-3 times the thermal boundary layer thickness (to overcome viscous stresses), but this required topography decreases as the layer viscosity decreases, because the lower layer then acts as a free-slip boundary. Indeed, with >2.5 orders of magnitude viscosity contrast, only minimal topography is needed. With no dense layer present, upwellings are in the form of intermittent thermals.

This laboratory finding that a dense layer stabilizes plumes is, however, seemingly contradicted by numerical experiments (McNamara and Zhong, 2004a). In these numerical experiments, plume stability was quantified as the ratio of horizontal plume velocity to average surface velocity. (McNamara and Zhong, 2004a) found this to be about the same in layered calculations as it is in isochemical calculations with a rigid lower boundary, regardless of the viscosity contrast of the dense material. They also found that layer topography doesn't influence fixity, but can lead to longer-lived plume conduits that follow the topographic peaks around. The

reconciliation of these apparently contradictory findings is not clear. One possibility is that the dense layer reduces the convective vigor and that the laboratory experiments didn't take this into account. Another is that there is a difference in the dynamics of downwellings (for example they might be stronger in the numerical experiments), which push the lower layer and associated hot plumes around. More study is needed to reconcile laboratory and numerical results on this issue.

Starting plumes: Despite the effect that a dense layer can have on increasing plume stability as discussed above, some studies have found that for starting plumes, the presence of a dense layer can add complexity and modes of time-dependence that are not present with purely thermal plumes. (Lin and Van Keken, 2006b; Lin and Van Keken, 2006a) investigated axisymmetric models set up to produce a plume at the axis, various temperature-dependences of viscosity and a dense layer with various thicknesses, buoyancy ratios and viscosity contrasts. They found that entrainment commonly becomes a transient process for models with variable viscosity. In models where a large fraction of the dense layer was entrained, variable viscosity could lead to secondary instabilities developing after the initial plume head, whereas in models with only a thin filament entrained, variable viscosity could lead to an initial pulse of entrainmant. In general, the dense material led to a wider range of plume morphologies than observed with purely thermal plumes. As with results discussed elsewhere, they found that decreasing the viscosity of the layer made it more stable.

Even greater morphological variability and complexity was found in the 3-D models of (Farnetani and Samuel, 2005), in which thermo-chemical plume formation was modeled in a compressible mantle with no imposed symmetry, an initially 200 km thick layer with buoyancy ratio B=0.1, T- and depth-dependent viscosity. Plume morphologies were much less regular than 'classical' plumes, and included plumes with blob-like or irregular heads, tilted plumes, ~1000 km wide 'megaplumes', broad plumes without heads, as well as 'classical' head plus narrow tail plumes, often with several types coexisting. The buoyancy flux of conduits varied widely, and some structures ponded under the 660 km discontinuity. Plume conduits were founds to be laterally heterogeneous (i.e., without concentric zonation), but as with previous results (Farnetani et al., 2002) the only material hot enough to melt underneath the lithosphere is from the source region.

3.1.4 Entrainment of surrounding material by mantle plumes

As discussed above, plumes clearly entrain material from a dense layer at their base. A long-standing question is how much this composition is diluted by material entrained from the upper layer as they rise. The initial plume head and subsequent conduit have different structure and so are expected to be different in their entrainment characteristics.

Depending on the viscosity contrast, rising hot diapirs, analogous to plume heads, thermally entrain surrounding material as they rise, forming a folded structure (Griffiths, 1986). It was demonstrated that this structure also occurs in plume conduits if they are sheared by the surrounding material (Richards and Griffiths, 1989), to such an extent that "small plumes or narrow plume conduits may consist of only a small fraction of original source material" (Richards and Griffiths, 1989). (Hauri et al., 1994) presented analytic solutions for plume conduits, finding that they entrain significant amounts of ambient mantle due to lateral thermal conduction from the plume. They found a huge range of possible entrainment, depending on the buoyancy flux, with most of the entrained material coming from the lower half of the layer they are passing through.

Although plumes may entrain a significant amount of surrounding material, (Farnetani and Richards, 1995) found that the entrained material does not contribute significantly to the melt produced by the plume, with >90% of the primary plume magmas being composed of primary plume material. The first-order reason for this is that the entrained material has a much lower temperature than the core of the original plume, and so is much less likely to melt underneath the lithosphere. Reinforcing and extending this finding, (Farnetani et al., 2002) analyzed entrainment by a thermal plume with temperature-dependent viscosity contrast 100, and found that the material that melts is from the thermal boundary layer at the base of the mantle. The material in the plume

head was found to be much more extensively stretched and stirred than that in the plume conduit, implying greater homogenization of geochemical anomalies. At that viscosity contrast, the plume head did not entrain surrounding material, although a substantial amount of lower mantle material was advected upwards with the plume into the upper mantle.

Entrainment of the dense layer by plumes is further discussed in the next section.

3.2 Long-Term Entrainment of Stable Layers

In a system with stable compositional layering, the system nevertheless evolves with time because the thermal convection in each layer causes entrainment of material from the other layer, in the form of thin schlieren, thereby diminishing the density contrast (Olson, 1984). There are two possible outcomes to this evolution: (i) If the entrainment is asymmetric (typically due to the lower layer being thinner than the other, e.g., (Samuel and Farnetani, 2003)) then one layer may eventually disappear due to complete entrainment into the other layer. Indeed, it is likely that in the long term there is substantial entrainment of any dense material residing above the CMB, which may be balanced by addition of material by segregation or core reactions, as discussed later. (ii) The density contrast decreases to the point where the layering is no longer stable and large-scale overturn and stirring occurs. Numerical calculations and laboratory experiments have been useful in elucidating the details of these processes, while mathematical analysis has been useful in developing scaling laws for entrainment.

3.2.1 Comparison of entrainment laws and estimates

Several authors have obtained expressions for the entrainment rate as a function of parameters such as density contrast, viscosity contrast, and so forth. Studies usually focus on one of two situations: a thin layer at the base of the mantle, or two layers of substantial thickness. While the same laws might apply, the former case obviously has much greater asymmetry and the lower layer might not be convecting.

Laboratory experiments

From studying the entrainment in laboratory experiments with two layers of equal depths, (Olson, 1984) found that the mixing rate of the two layers, defined as the rate of change of their density divided by the density difference (i.e., the fractional volume flux), scales as:

$$\dot{M}/\dot{\varepsilon} \approx 0.046 Ri^{-1} \qquad (37)$$

where the Richardson $Ri = \Delta\rho g D/\tau$ with τ being the average viscous stress within each layer. Eliminating Ri leads to:

$$\dot{M}/\dot{\varepsilon} \approx 0.046 \frac{\tau}{\Delta\rho g D} \qquad (38)$$

For two thick stable layers where the lower layer is more viscous by a factor of 1.0 to 6.4×10^4, (Davaille, 1999b) found that the scaling for entrainment by linear sheets (typically found in the more viscous layer) is different from that for axisymmetric plumes (found in the less viscous layer). For entrainment by linear sheets:

$$Q_{21} = C_1 \frac{\kappa h_0}{B} Ra^{1/5} \qquad (39)$$

whereas for columnar plumes:

$$Q_{12} = C_2 \frac{\kappa h_0}{B^2} Ra^{1/3} \qquad (40)$$

where Q=flux of material, h_0=initial thickness of lower layer, κ=thermal diffusivity, and C_1 and C_2 are two experimentally-determined constants. The "plume" law has the same $1/B^2$ form as the one proposed by (Sleep, 1988) (discussed below). When the lower layer is substantially more viscous than the upper layer, it is difficult for the upper layer to entrain it, requiring an additional factor (Davaille, 1999a):

$$Q = C_1 \frac{\kappa H}{B^2} Ra^{1/3} \frac{1}{1 + \Delta\eta/B} \qquad (41)$$

where $\Delta\eta$ is the viscosity contrast. This additional factor applies for $\Delta\eta$>1, i.e., for entrainment of the more viscous layer into the less viscous layer. If the layer being entrained is substantially less viscous than the entraining layer then Q could also be reduced due to draining of the less viscous material back into the layer it came from, but this was not observed by (Davaille, 1999a; Davaille et al., 2002) at $\Delta\eta$ as low as 0.01. This entrainment law was subsequently verified for the case of a thin layer with plume entrainment (Davaille et al., 2002). Depending on parameters, a mantle plume would entrain chemically dense material at a rate of 0.1-15% of its total volume flux. (Davaille et al., 2002) present graphs of layer survival time versus thickness and density contrast, based on thermal expansivity 10^{-5} K^{-1} and 'temperature heterogeneity' of 500K. As an example, entrainment of 100 km over 4.5 Gyr corresponds to a 3.5% density contrast if the layers are the same viscosity or ~2% density contrast if the dense material is ten times more viscous.

Several other authors have conducted laboratory experiments to study entrainment and long-term evolution. In experiments with an initial layer thickness of 0.2 (600 km) and similar viscosity materials, (Gonnermann et al., 2002) find vigorous convection in both layers and entrainment consistent with the scaling laws of (Davaille, 1999a). They estimate that an initially 300 km thick layer can survive over Earth history if it has a 2% density contrast, but if initially thicker then it can survive initial density contrast <2%. In some cases the dynamics changed from stable layering to doming.

The strong influence of viscosity contrast on entrainment of a thin layer was demonstrated by (Namiki, 2003) using viscosity ratios from 0.1 to 400. It was found that when the lower layer is more viscous it grows in size due to asymmetric entrainment of the upper layer. When the lower layer is less viscous, an interfacial layer developed and the volumes of the layers did not change because plumes entrained the interfacial layer, not the lower layer. This interfacial layer is a novel finding not observed in any other mantle-related studies, so it is worth considering what causes it. The layer might develop because of incomplete entrainment of the lower, less viscous layer by the upper layer due to reduced viscous coupling. It might form as a result of double-diffusive convection which helps to transport material across the boundary (M. Manga, personal communication). If the latter explanation is correct, it would not form in Earth because the chemical diffusion rate is very low. In any case, by considering stresses (as in (Olson, 1984)) (Namiki, 2003) derives an entrainment law that is consistent with those discussed above:

$$\dot{E}_i \sim \frac{\kappa_i}{B_i^2 \delta_{th_i}} \qquad (42)$$

where $\dot{E}_i$ is the entrainment rate of layer i, δ is the thermal boundary layer thickness, related to the Rayleigh number as $\delta_{th} \sim 5 L_i Ra^{-1/3}$ leading to an overall scaling of

$$\dot{E}_i \sim 0.2 \frac{\kappa_i}{B_i^2 L_i} Ra^{1/3} \quad (43)$$

In this parameterization the effect of a viscosity difference is to alter the ΔT for each layer, hence B and Ra. The survival time of a 200 km thick layer was calculated as a function of its density difference, assuming the total ΔT=4000 K, the viscosity of D" is 10^{19} Pa s, the viscosity of the mantle is 10^{21} or 10^{22} Pa s, and thermal expansivity is 2×10^{-5} K^{-1}. It was estimated that a density difference of at least 300 kg/m^2 (5.5%) is needed for the layer to survive over geological time (ignoring the possible presence of an interfacial layer). With a more realistic thermal expansivity of 1×10^{-5} K^{-1}, this would be reduced to 2.75% contrast, comparable with other estimates.

A scaling law that explicitly includes viscosity contrast was proposed by (Jellinek and Manga, 2002) on the basis of laboratory experiments:

$$q = 0.49 \frac{\kappa}{H} \frac{Ra^{1/3}}{\Delta\eta B} \quad (44)$$

where H=depth of tank and $\Delta\eta$>1 is the ratio of upper to lower layer viscosity. This is similar to the expression of (Davaille, 1999a) given above, in the limit of $\Delta\eta >> B$. It is interesting that in this limit, the dependence on B is 1/B rather than 1/B^2.

Mathematical or numerical approaches

Gradual entrainment of thin chemical layer at the base of the mantle by either 2D upwelling sheets or axisymmetric plumes was analyzed by (Sleep, 1988) to determine the fraction of entrained material in the upwelling as a function of chemical density contrast. The analysis did not consider the details of the entrainment process, but rather the carrying capacity of the plume conduit. Thus, a 1-D section across the upwelling was considered, with the entrained material in the form of a thin filament in the center of the upwelling. To determine the thickness of this filament, it was assumed that the thickness adjusts so as to maximize entrainment rate (e.g., if it is too thick then the upwelling velocity decreases). The models included temperature-dependent viscosity. While a general scaling law for all parameter combinations was not explicitly stated, the general form was found to be

$$F = C / B^2 \quad (45)$$

where C is a constant and B is the chemical buoyancy ratio. Based on these models, (Sleep, 1988) estimated that a chemical density contrast of 6% is necessary for a 100 km thick, non-convecting layer to survive over the age of the Earth if the thermal expansivity is 2×10^{-5} K^{-1}. Subsequent mineral physics data (e.g., (Anderson et al., 1992; Chopelas, 1996)) indicates a thermal expansivity closer to 1×10^{-5} K^{-1} at the CMB, so this estimate of density contrast should be adjusted to 3%. Additionally, if the initial layer thickness were larger, then a higher entrainment rate could be tolerated. In any case, this density contrast corresponds to B~3 based on the temperature drop over the lower boundary layer, or B~1.5 using the temperature drop over the entire system- both substantially larger than that required to stabilize the layer against rapid overturn. (Sleep, 1988) also considered the case of an internally-convecting layer and concluded that the above estimate is still reasonable.

The entrainment process at the base of the plume (not considered by (Sleep, 1988)) was included in the high-resolution 2-D numerical models of (Zhong and Hager, 2003). They found that treating the lateral flow at the bottom of the plume makes some significant differences compared to

the 1-D analysis of (Sleep, 1988), with the 1-D model overestimating entrainment by up to more than a factor of 4 compared to their 2-D calculations. They found that the entrainment rate Q is mainly controlled by the buoyancy ratio B and the radius of the thermal plume r_T but insensitive to the thickness of the dense layer, with a relationship:

$$Q \sim B^{-2.48} r_T^{3.80} \quad (46)$$

Because their model was set up to produce a plume with prescribed parameters, they did not obtain a scaling law for a full convective system. They did, however, apply the scaling to estimate the survival time of a 1000 km thick layer, and it was estimated that more than 90% of a 1000 km thick dense layer can survive for 4.5 Gyr if the dense material has a net negative buoyancy of ~1% . It is important to note that this is the "net" buoyancy (thermal + chemical) and not the chemical buoyancy! For a thermal expansivity of 2.5×10^{-5} K^{-1} and the dense material 800 K hotter, the chemical density contrast would have to be 3%. This could be reduced by a factor of ~2 using a more realistic deep mantle thermal expansivity.

Recently (Lin and Van Keken, 2006a; Lin and Van Keken, 2006b) revisited the transient dynamics of a plume forming from a boundary layer with an included dense chemical layer, first studied by (Christensen, 1984). The dynamics are discussed in section 3.1.3. Although the short-lived (250 Ma) nature of their simulations was not intended to study long-term entrainment, they did compare short-term entrainment with existing laws and also found some interesting behavior that is worth noting here. In particular, they found two behaviors that are not accounted for in standard entrainment theory: (i) A very thin layer, i.e., much thinner than the thermal boundary layer, could be entrained very rapidly despite having B=2 or 3, (ii) For B~1, a new starting plume head caused a 'pulse' in entrainment, bringing into question the applicability of stead-state entrainment laws for a dynamic, time-dependent mantle. As expected, temperature-dependent viscosity resulted in much lower entrainment, for example with a factor of 1000, even a layer with B<0.5 was stable. Regarding entrainment rate, their results were consistent with $F = C / B^2$ found by (Sleep, 1988) with C=0.07, and the scaling law of (Davaille, 1999b) with C=1.1, although there was some deviation from the latter when B>1, which they suggested is due to the effective B and Ra adapting with time in the laboratory experiments. They estimate that a layer with temperature-dependent viscosity can survive if it is thicker than 75 km and its compositional density contrast is larger than 1.5% assuming thermal expansivity is 3×10^{-5}, which would be reduced to ~0.5% with an Earth-like thermal expansivity.

Summary of layer survival estimates. As several studies discussed above have estimated the density contrast required for a dense layer to survive over geological time in the face of continuous entrainment, it is useful to consider whether these estimates are consistent with each other. In general, the published estimates assume a deep mantle thermal expansivity at least a factor of 2 higher than realistic, so in Table 2 they have been rescaled if necessary to a thermal expansivity of 1×10^{-5} K^{-1}:

Table 2. Scaled estimates of density contrast required for long-term survival

Study	Thickness (km)	$\Delta\rho$	η
(Sleep, 1988)	100	3.0%	1
(Davaille et al., 2002)	100	3.5%	1
(Davaille et al., 2002)	100	2.0%	10
(Gonnermann et al., 2002)	300	2.0%	1
(Namiki, 2003)	200	2.75%	0.01
(Zhong and Hager, 2003)	1000	1.5%	1
(Lin and Van Keken, 2006a)	>75	>0.5%	0.001

In general the rescaled estimates are consistent, with thinner layers increasing the required density contrast and a viscosity contrast (either higher or lower) reducing the required density contrast. Perhaps the exception is (Lin and Van Keken, 2006a), whose density estimate is very low. This could be because they have a larger viscosity contrast than any other study, and this is certainly worth exploring further. Another factor might be that they consider a single plume with ΔT=750 K rather than a full convective system as in the laboratory studies, and convective downwellings could help to destabilize the layer. On the other hand, (Sleep, 1988) and (Zhong and Hager, 2003) also consider isolated plumes. In summary, this issue requires investigation in a fully-convecting system with large viscosity contrast.

3.3 Evolution of a Mantle with Ongoing Differentiation

3.3.1 General evolution

So far the discussion has focused on the evolution of a system with preexisting layering. However, while the possibility of primordial layering exists, most of the observed heterogeneity appears to be related to recycled material, so several models have studied the evolution of a mantle in which heterogeneity is continuously introduced over time, generally to simulate the differentiated components in subducted slabs (Gurnis, 1986a; Ogawa, 1988; Christensen, 1989b; Ogawa, 1993; Christensen and Hofmann, 1994; Kameyama et al., 1996; Ogawa, 1997; Ogawa and Nakamura, 1998; Walzer and Hendel, 1999; Ogawa, 2000b; Davies, 2002; Tackley and Xie, 2002; Ogawa, 2003; Nakagawa and Tackley, 2004b; van Thienen et al., 2004; Xie and Tackley, 2004c; Xie and Tackley, 2004b; Nakagawa and Tackley, 2005b; Nakagawa and Tackley, 2005a; Tackley et al., 2005). Some of these have already been discussed to a certain extent, in the context of the effect on residence time for example.

In this section, models in which active heterogeneity is introduced are discussed. Some of the models track trace elements as well as crust-residue differentiation; the trace element aspects of them is discussed in section 4. One of the main differences between studies is how they treat the secular evolution of the planet, in which the mantle and core cools and heat producing elements produce less heat. While some studies attempt to directly include this (e.g., (Ogawa, 2003; Xie and Tackley, 2004b; Nakagawa and Tackley, 2005a)), others have parameterized the faster earlier evolution as a longer run time at a constant convective vigor (Davies, 2002). Other differences are how crustal production is treated (self-consistent melting criterion or assumed thickness crust) and how plate tectonics is treated (kinematic plates or using a yield-stress approach).

While there are substantial variations in the assumptions and results amongst different calculations, it is possible to generalize the typical evolution.

(i) Initial condition: chemically homogeneous.
(ii) Vigorous early melting occurs. If subducted crust and residue components are able to separate at some depth, then depleted residue rises to the top and crust sinks to the bottom, forming a depleted upper mantle and layer of subducted crust at the bottom. Rapid formation of a depleted upper mantle was observed in some of the calculations of (Ogawa and Nakamura, 1998; Davies, 2002; Ogawa, 2003; Nakagawa and Tackley, 2005b), but particularly in the calculation presented by (Davies, 2006) because of its high convective vigor (internally heated Ra=7.7×10^{11}) designed to represent the early Earth. (Davies, 2006) argues that this depletion helps plate tectonics to operate early on.
(iii) Increasing chemical stratification (depending on parameters), possibly including above the CMB and around 660 km (see later sections for discussion). Increasing heterogeneity as more recycled material gets subducted and stirred. It is possible that the phase changes around 660 km depth play a much larger role than they do now, because of the basic scaling with convective vigor (Christensen and Yuen, 1985; Ogawa, 2003).

(iv) Transition to a slowly-evolving long-term state, in which a dynamic equilibrium may be set up between segregation and entrainment, and between the generation (by melting) and destruction (by mixing and/or remelting) of heterogeneity. The mantle is highly heterogeneous, consisting of a large fraction of recycled material. At this point most of the mantle may be depleted relative to the start condition if subducted crust is able to form a layer in the deep mantle (e.g., (Ogawa, 1997; Xie and Tackley, 2004a)).
(v) Possible switches in the regime can occur, such as remixing of previously formed layers (Ogawa, 1994; Ogawa, 1997). Other possible changes are a reduction in stratification at 660 km depth (Ogawa, 2003), or changes in the plate tectonic regime (e.g., as proposed by (Vlaar, 1986; Davies, 1992; Sleep, 2000)), although the latter possibility has not been observed in models yet.

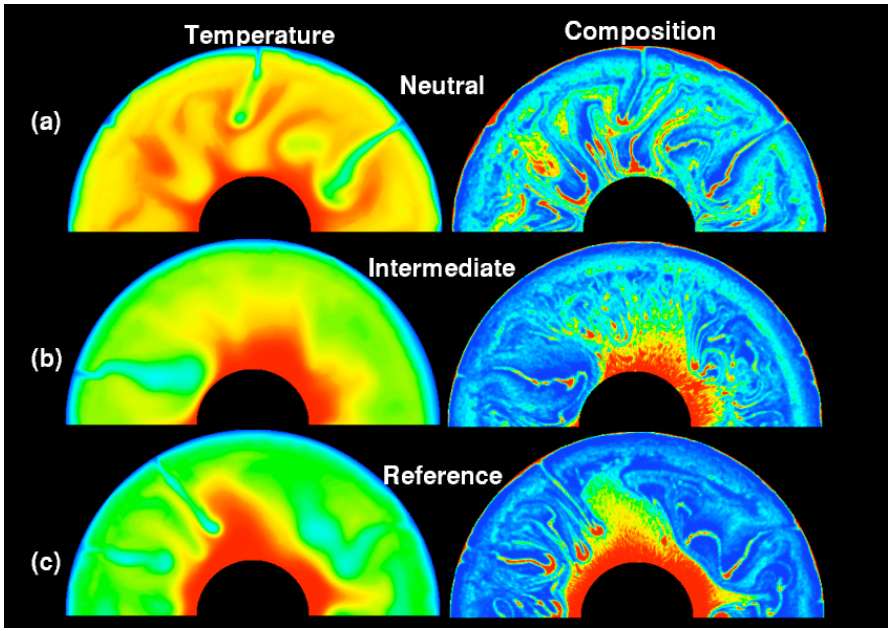

Figure 7. Laterally heterogeneous mantle and 'messy' layering resulting from continuous oceanic differentiation and recycling of MORB and residue for billions of years, from (Nakagawa and Tackley, 2005a). MORB=red, harzburgite=blue. All models include composition-dependent depth of the transition to perovskite (deeper for MORB) and the same compositional density contrasts in the upper mantle and top of lower mantle. The density contrast of MORB relative to pyrolite at the CMB is either (a) zero, (b) 1.1% or (c) 2.2%. When MORB is dense at the CMB, some of it segregates into a layer, which is intermittent in the intermediate-density case. In all cases, the transition zone is enriched and the top of the upper mantle is depleted, due to the different depths of the perovskite phase transition.

It is worth noting some findings of such calculations. Firstly, layers that form from segregation and settling of dense material (as discussed in the next section) tend not to have sharp boundaries like layers that modelers introduce a priori (Figure 7). This affects the ability of plumes to form at their interfaces and should also effect entrainment. Secondly, in models that include secular cooling, melting can be a very important transporter of heat early on. For example, in the calculations of (Xie and Tackley, 2004b), heat transported by melting, which is the sum of energy transport due to latent heat and energy loss to rapid cooling of the newly-formed crust at the surface, is about equally important as conductive heat loss early in the calculation, but later on subsides to a small fraction of the total heat transport as is the case on present-day Earth. The vigorous melting that

occurs early on was found in the calculations of (Ogawa, 1997; Ogawa and Nakamura, 1998) to cause a compositionally layered internal structure, whereas when the melting rate decreased due to cooling the internal structure became well mixed. The early, layered mode occurred when the average temperature no longer intersected the solidus. (Dupeyrat et al., 1995) also obtained a switch between layered and well-mixed modes, from a homogeneous start.

Shallow mantle depletion can cause some dynamical effects, as found by (Dupeyrat et al., 1995) modeling upper mantle convection. A layer of depleted residue building up under the lithosphere reduces convective velocity, and increases the wavelength of convective cells. When plates are included, they carry the buoyant residue down to the bottom where it can subsequently rise in the form of diapirs, which increases mixing rate.

3.3.2 Development of a dense layer by gravitational settling of subducted crust

The idea that subducted oceanic crust might settle at the CMB was initially proposed by (Hofmann and White, 1982) as a way of separating the subducted crust from convective mixing for long enough for it to develop the isotopic age observed in OIBs. Long-term storage of subducted oceanic crust may also help to explain other geochemical signatures- for example the positive Nd anomaly of Archaean rocks (Chase and Patchett, 1988). This section discusses constraints on the plausibility of this process. The possibility of a layer building up over time due to reactions with the core is discussed in another section.

MORB density contrast. A key parameter in this process is the density contrast of the MORB assemblage at the pressure and temperature range of the CMB. Unfortunately, this is still uncertain due to uncertainties in the properties of the mineral phases present in MORB at these pressures, although there are ongoing improvements in our knowledge of these. Historically, (Ringwood, 1990b) proposed that basalt remains 2–4% denser than peridotite throughout the whole mantle, with the exception of the depth range 660–720 km, where it is less dense, the consequences of which are discussed in section 3.3.3. Other mineral physicists have, however, calculated that MORB might actually be less dense than pyrolite at CMB pressures, in particular (Kesson et al., 1998) and (Ono et al., 2001). According to (Kesson et al., 1998), MORB is intrinsically 0.9% denser than pyrolite at 1100 km depth but -0.5% (28 kg/m^3) less dense than pyrolite at the CMB, while depleted peridotite is less dense than pyrolite at all depths: -0.8 and -0.7% at 1100 km and the CMB respectively. At face value this implies that MORB would be positively buoyant at the CMB, but what may matter is the density relative to residue, rather than relative to pyrolite, which is +0.2% (11 kg/m^3). This is because it seems likely that 95-99% of the mantle has been processed through MOR melting, and thus has been differentiated into residue and MORB, with very little pyrolite remaining. In any case, 11 kg/m^3 density difference is not enough to have a significant dynamical effect. More recently, (Ono et al., 2001) calculated that although MORB is ~100 kg/m^3 denser at the top of the lower mantle, its density profile intersects an average mantle density at around 1500–2000 km depth in the lower mantle, making MORB neutrally buoyant at ~1600 km depth and positively buoyant at greater depths.

The most recent estimates of MORB density, however, appear to be moving back in the direction of it being more dense than pyrolite at CMB pressures. From in situ x-ray observations of peridotite and NMORB and K-rich basalts at up to CMB pressures and temperatures (Ono et al., 2005b) estimated that MORB is still 40-80 kg/m^3 denser than the average mantle at a depth of 1800 km, at which depth he had previously estimated MORB to have ~zero density anomaly (Ono et al., 2001). (Guignot and Andrault, 2004) refined the equation of state of phases containing Na, K and Al, and calculated MORB to be denser than pyrolite by 100-160 kg/m^3 at the top of the lower mantle reducing to 25-95 kg/m^3 at the CMB, which corresponds to 0.45% to 1.7% of the density at the CMB, and results in a buoyancy parameter B of 0.2-0.7 (assuming a thermal expansivity of 1.0×10^{-5} K^{-1} and superadiabatic temperature contrast of 2500 K), or 0.4-1.4 (assuming a local temperature contrast of 1200 K). Most recently, (Hirose et al., 2005) measured physical properties of MORB samples at pressure and temperatures up to those near the CMB, and found that MORB

is substantially denser than PREM throughout the lower mantle and by about 200 kg/m^3 (3.6%) near the CMB, corresponding to a buoyancy ratio B of 1.4 (ΔT=2500 K) or 3.0 (ΔT=1200 K). Results from several studies can be used to estimate whether settling is possible at these density contrasts.

Modeling studies. The earliest results on this issue (Gurnis, 1986a) found that with B=2, although basaltic tracers that were already separated from the residue component of the slab could aggregate into piles under upwellings for completely internally-heated flows, with basal heating they got rapidly swept back into the main flow, and if accompanied by complementary depleted tracers did not settle at all. One way of understanding this result is in terms of the Stokes velocity of a sinking blob of crust: at high lower mantle viscosities this is extremely low, for example 0.1 mm/year for a 5 km blob with mantle viscosity=10^{21} Pa s. If, however, the strong temperature-dependence of viscosity of mantle rocks is taken into account, then relatively low viscosities may be present in the hot lower thermal boundary layer, which allow the crust to settle from the residue fast enough, and several studies that have included this have found significant crustal settling is possible.

The laboratory study of (Olson and Kincaid, 1991) is particularly enlightening because there are no questions of resolution, artificial diffusion or other issues that plague numerical treatments of composition. They introduced compositionally-stratified slabs with equally-thick layers of 1% denser and 1% less dense material (B~+-0.6) and initially 3.5 orders of magnitude higher viscosity to the bottom of their tank, and found that after a period of warming, the buoyant component of the slab underwent a Rayleigh-Taylor instability in which the low-density 'depleted' material rose through the high-density 'crustal' material, which then remained above the CMB in a 'spoke' pattern and subsequently got entrained over time, as discussed later. The scaled time from slab incidence to dense spokes was 1.8 Ga. In this experiment, which has a buoyancy ratio in the range discussed above, almost all of the dense 'crust' settled to the CMB, but this may be exaggerated because the 'crust' and 'residue' layers were assumed to be equally thick, whereas in reality the crustal layer is much thinner.

A similar process has been obtained in numerical experiments, but with a smaller fraction of the crustal material remaining at the CMB. (Christensen, 1989b) included temperature-dependent viscosity as well as a decrease in thermal expansivity with depth in a calculation with the continuous introduction of slabs containing crust and residue layers, taking care to scale the thickness of the compositional layers in proportion to the thermal thickness of the slab. He found that for a buoyancy ratio ~1, between 5% and 25% of the basaltic crust settled at the CMB. Again, the observed process was a Rayleigh-Taylor instability of the residue component, leaving behind some fraction of the crust. With constant viscosity, no segregation occurred, consistent with (Gurnis, 1986a). Interestingly, if a layer of dense crustal material already existed, a larger fraction of the incoming basalt was able to segregate and settle. These calculations were greatly developed in (Christensen and Hofmann, 1994) in which it was found that for B=1.5, ~14% of the total amount of crust in the mantle was in 'pools' (similar to piles) above the CMB, implying that ~1/6 of the subducted crust initially settled into a layer at bottom. Higher Rayleigh number decreased the size of the bottom 'pools', but higher B increased them (e.g., 26% of the total crust for B=2.25). Making the viscosity less temperature-dependent reduced the amount of settling, as with previous results. Interestingly, the bottom pools were not 100% crust- rather their crustal content was ~60%.

The first models of the discussed type that are at an Earth-like convective vigor were presented by (Davies, 2002), who assumed a density difference of up to 100 kg/m^3 but a constant α=2×10^{-5} K^{-1}, about a factor of 2 higher than realistic at the CMB. In contrast to the models of (Christensen and Hofmann, 1994), the model was heated entirely from within, with no hot thermal boundary layer and hence no low viscosity region at the bottom (the fraction of basal heating was arguably higher than realistic in the models of (Christensen and Hofmann, 1994)). Nevertheless, despite the absence of a low viscosity TBL and high α, a significant amount of basalt settled above the CMB, although less than obtained by (Christensen and Hofmann, 1994). (Davies, 2002) suggested other mechanisms that assist crustal settling, such as thickening of the crust due to slab

buckling (the Stokes velocity increases as size^2), and the fact that the vertical velocity approaches zero towards the lower boundary (making it more difficult for the convective flow to entrain sinking blobs). All these mechanisms may play a role, but as (Christensen, 1989b; Christensen and Hofmann, 1994) clearly demonstrated the strong influence of temperature-dependent viscosity on crustal settling above the CMB, it is likely that (Davies, 2002) would have obtained more crustal settling, if the lower boundary region were less viscous.

The studies discussed in this section so far have controlled the surface velocities (to make them plate-like) and the rate at which compositionally-distinct material is injected. A number of other studies (e.g., (Ogawa, 2000a; Ogawa, 2003; Xie and Tackley, 2004a) (Nakagawa and Tackley, 2005c)) attempted to treat these aspects self-consistently, with the crustal production rate determined by melting induced when the temperature reaches the solidus, and the surface velocities determined by solution of the governing equations, often using a rheology that facilitates a 'plate-like' behavior (e.g., (Moresi and Solomatov, 1998; Yoshida and Ogawa, 2004)). It is not clear that this makes the resulting calculations more representative of Earth, but they are different from the previously-discussed studies in other ways that make it instructive to discuss the results here.

The 2D box calculations of (Ogawa, 2003), building on a series of earlier papers (Ogawa, 1988; Ogawa, 1993; Ogawa, 1994; Kameyama et al., 1996; Ogawa, 1997; Ogawa and Nakamura, 1998; Ogawa, 2000a; Ogawa, 2000b), include self-consistent differentiation, a plate treatment involving hysteresis (Yoshida and Ogawa, 2004), and a cooling mantle with decaying heat sources. With MORB having a density anomaly of 120 kg/m^3 and a somewhat high constant thermal expansivity of 3×10^{-5} K^{-1}, subducted MORB settles into a layer above the core-mantle boundary that accumulates with time, while subducted residue undergoes diapir-like instabilities raising it back through the mantle. The basaltic layer has large undulations and is typically has a thickness of ~1/4 of the domain depth, which scales to 500 km.

The 2D cylindrical calculations of (Tackley and Xie, 2002; Xie and Tackley, 2004a; Xie and Tackley, 2004b) (Nakagawa and Tackley, 2004b; Nakagawa and Tackley, 2005a; Nakagawa and Tackley, 2005c) include self-consistent magmatism, temperature- and depth-dependent viscosity and yielding-induced plate tectonics, and decreasing convective vigor due to decaying heat-producing elements and a cooling core. The material properties such as thermal expansivity have reasonable depth-dependences. Various density profiles for the MORB component relative to the residue component in the lower mantle are considered, and the density of the average composition ('pyrolite') is assumed to be a weighted average of the densities of the two endmembers, consistent with the small-scale structure being a heterogeneous mixture of the two endmembers, but not primitive never-melted pyrolite. These calculations show that even for a relatively small density contrast for MORB in the deep mantle (e.g., 62 kg/m^3 (Nakagawa and Tackley, 2005a)), subducted MORB settles at the base and builds up into large discontinuous 'piles' of material extending up to ~700 km into the mantle. With double this density contrast (123 kg/m^3 (Xie and Tackley, 2004a; Xie and Tackley, 2004b; Nakagawa and Tackley, 2005a)), a continuous undulating layer of dense material is formed, again up to 500-700 km thick. When basalt is neutrally buoyant at CMB pressures, the CMB region is still heterogeneous because subducted crust and residue reside at the bottom for some period while they heat up sufficiently to be stirred back in to the convective flow (Xie and Tackley, 2004a). If there is crossover in density, with MORB positively buoyant at the CMB, then a layer of depleted residue can build up above the CMB, with blobs of MORB residing in the mid lower mantle where it is neutrally buoyant (Xie and Tackley, 2004a; Xie and Tackley, 2004b).

In these calculations (Ogawa, 2003; Tackley et al., 2005) the layer of dense material can become much thicker than observed in the calculations of (Christensen and Hofmann, 1994; Davies, 2002), a major reason being that the total amount of MORB that can be produced by melting of primitive material is higher. (Christensen and Hofmann, 1994; Davies, 2002) limit the total amount of MORB in the system to 10%, whereas the other authors assume, based on the fraction of garnet+pyroxene in pyrolite being 30-40%, that up to 30% or 40% basalt fraction can be generated by melting. The true situation is probably between these extremes: melting by more than

10% probably did occur in the hotter, early Earth, and re-melting of once-depleted pyrolite could produce additional basalt, but petrological considerations indicate that the bulk composition changes depending on the degree of melting (.e.g., (McKenzie and Onions, 1992; Asimow et al., 2001))

A recent factor that decreases the stability of a deep, dense layer is the recently-discovered post-perovskite phase transition (Murakami et al., 2004; Oganov and Ono, 2004). The positive Clapeyron slope of this transition acts to slightly destabilize the lower thermal boundary layer (Nakagawa and Tackley, 2004a), and any resulting chemical layering (Nakagawa and Tackley, 2005b). The destabilization effect is however relatively small, and seems to be lower than the uncertainties in MORB density discussed earlier, and uncertainties due to composition-dependence of the PPV transition (e.g., (Murakami et al., 2005; Ono et al., 2005a)). In any case, because dense material tends to accumulate under hot upwellings, and the positive Clapeyron slope leads to an anticorrelation between the phase transition depth and temperature, the occurrence of a thick PPV layer is anticorrelated with the occurrence of thick pile of dense material.

An uncertain factor in all of the above calculations is the influence of 2-D geometry on quantitative entrainment rates, and hence long-term stability. As discussed in section 3.2.1, in the laboratory experiments of (Davaille, 1999b), different scaling laws were found (i.e., with different exponents for B and Ra) for entrainment by 2-D sheets and 3-D plumes. This is something that will have to be addressed in the future.

3.3.3 Chemical layering induced by phase transitions

The intriguing possibility exists that one or more phase transitions near or below 660 km depth could enforce or enhance chemical layering. Some research has focused on the effect of a single phase transition- the endothermic spinel to perovskite+magnesiowüstite transition at around 660 km depth, which, according to dynamical models that assume this transition applies to all mantle material, can cause partial layering of thermal convection, with the degree of flow stratification very sensitive to the value of the Clapeyron slope (e.g., (Christensen and Yuen, 1985; Machetel and Weber, 1991; Peltier and Solheim, 1992; Weinstein, 1993; Tackley et al., 1994)). In reality, however, olivine makes up only ~60% of the mantle assemblage, and the phase changes in the other, pyroxene-garnet system, occur at different pressures. In particular, the transition to the perovskite phase occurs with a positive Clapeyron slope and probably at a greater depth such as 750 km. This has two effects: (i) the effect of the combined phase transitions on purely thermal convection is much reduced relative to what would occur if the olivine transitions applied to all mantle material, and (ii) subducted oceanic crust might be positively buoyant (less dense than other compositions) in a region ~10s km thick below the 660 km discontinuity, whereas it is negatively buoyant (more dense) at other pressures (Irifune and Ringwood, 1993). This has been suggested to cause the separation of slab components in the vicinity of 660 km, with the accumulation of "megaliths" (Ringwood and Irifune, 1988; Ringwood, 1991).

Estimates of depth extent over which this anomalous buoyancy occurs have varied widely: a recent study of (Ono et al., 2001) puts it at 660-720 km. A possible intermediate transition to ilmenite (Chudinovskikh and Boehler, 2002) would reverse this picture and increase the layering (van den Berg et al., 2002), but it is doubtful whether ilmenite occurs in a pyrolite composition (S. Ono, personal communication).

A single endothermic phase transition. If a chemical boundary already exists at a similar depth to the 660 km phase transition, (Christensen and Yuen, 1984) showed that their effects on deflecting a subducting slab and therefore causing flow layering can be added linearly. For the parameters they assumed, flow layering required a 4.5% chemical contrast or a Clapeyron slope of –5 MPa/K or a linear combination of the two. If chemical stratification does not, however, already exist, can an endothermic phase transition dynamically induce it? For a long-wavelength initial chemical heterogeneity, (Weinstein, 1992) showed that it can for certain combinations of chemical buoyancy ratio and Clapeyron slope. The endothermic phase was shown to act as a filter, trapping

chemically dense material below it and chemically less dense material above it, because the total buoyancy (thermal+chemical) of these types of material is insufficient to overcome the phase change buoyancy. For this mechanism to operate, the required chemical buoyancy contrasts were in the range 1.1-1.5% (assuming alpha=$2x10^{-5}$ K^{-1}) - much lower than those required to cause layering on their own. The required Clapeyron slope was, however, larger than realistic, in the range –5 to –8.6 MPa/K, though this is partly because the calculations were performed at a low convective vigor (Ra=10^5), and would be substantially reduced if an Earth-like vigor could be reached (Christensen and Yuen, 1985). For small-scale heterogeneities introduced by the continuous injection of compositionally-layered slabs, (Mambole and Fleitout, 2002) showed that small but measurable chemical stratification can be introduced by Clapeyron slopes as weak as –1 MPa/K, with the amount of chemical stratification increasingly steadily with the magnitude of the Clapeyron slope. With only the endothermic transition active, the dense component, which is the enriched, subducted MORB, is more prevalent in the lower mantle, while depleted, relatively buoyant material is more prevalent in the upper mantle. This result was confirmed by (Nakagawa and Buffett, 2005) in the case where the compositional anomalies were generated by melting-indiced differentiation. If the full system of phase transitions is considered the sense of layering is reversed, as discussed below.

Composition-dependent phase transitions and subducted slabs. An important question is whether the enriched basaltic crust and depleted harzburgitic residue can separate out due to the density inversions that occur around and below 660 km depth, as suggested by Ringwood (Ringwood, 1994). Three studies have demonstrated that this does not occur for slabs with a simple rheology, due to the strong viscous coupling between crust and rest of the slab (Richards and Davies, 1989; Gaherty and Hager, 1994; Christensen, 1997), whereas (van Keken et al., 1996) showed that if a weak layer separates the crust from the rest of the slab, crustal separation may be possible. While (Richards and Davies, 1989) investigated constant-viscosity slabs, (Gaherty and Hager, 1994) studied slabs with temperature-dependent viscosity falling vertically onto a viscosity increase at 660 km depth and a local density inversion below this depth, but their model did not include density anomalies due to phase change deflection or net compositional buoyancy of the slab below 660 km, which was an important component of the proposal of (Ringwood and Irifune, 1988). Thus, (Christensen, 1997) included these effects as well as a more realistic slab angle associated with trench migration at the subduction zone, with basaltic rock buoyant between 680-900 km, but still found that compositional effects are negligible for 100 Myr old plates, and although they could cause younger plates to stagnate at lower trench velocity they did not prevent eventual slab penetration into the lower mantle. The rheology of the slab is more complicated than simple temperature-dependence. (van Keken et al., 1996) considered a slab with an idealized rheological sandwich containing a soft (low viscosity) layer between the 'hard garnet' crust and the cold viscous slab interior, and showed that the crust can separate once the slab passes below 660 km depth, if most of the slab is ten times more viscous than the surrounding material and the weak peridotitic layer is 10 or 100 times less viscous than the rest of the slab. This model underestimates the viscosity of the slab based on simple viscosity laws, but once the peridotitic part of the slab passes through the spinel to perovskite+magnesiowüstite transition, it may be considerably weakened due to transformational superplasticity associated with grain-size reducing by the phase transition (Karato, 1995), whereas the crustal component would not. In summary, with 'conventional' rheology, compositional effects play only a minor role in slab interaction with the 660-800 km region and separation of slab components at 660 km depth is not possible, but if there is substantial weakening of the sub-crustal layer due to transformation superplasticity or other effects, then separation of the basaltic crust might occur.

Composition-dependent phase transitions in a convecting system. Regardless of the viability of slab components separating at around 660 km depth, several studies have shown that once slabs reach the bottom thermal boundary layer and heat up, the compositionally-distinct components can indeed separate (Olson and Kincaid, 1991; Christensen and Hofmann, 1994); thus the question of how separated crust and residue components interact with the phase transitions is of

great relevance. The stability of a transition layer (consisting of an inseparable mixture of eclogite and harzburgite) that has already formed in the 660 region to thermal convection was studied by (Christensen, 1988), who found that it could only survive for a few hundred million years, but this model did not allow for separate basalt and harzburgite components, nor the possibility of recharge of these components. Models in which differentiated components are constantly introduced by subduction (Fleitout et al., 2000; Ogawa, 2000a) show the development of a strong compositional gradient across the 660, with depleted harzburgitic material accumulating at the top of the lower mantle, enriched basaltic material accumulating at the bottom of the upper mantle and a chemical gradient present throughout the entire mantle, as evident in the later calculations of (Tackley and Xie, 2002; Xie and Tackley, 2004a; Xie and Tackley, 2004b). This entrapment of distinct components typically does not occur when a downwelling first encounters the region, but rather after the crust and residue components have separated in the deep mantle and are subsequently circulating as 'blobs'. That the chemical and flow stratification is due mainly to the different depths of the perovskite transition in garnet and olivine systems rather than Clapeyron slope effects was demonstrated by (Tackley et al., 2005). (Nakagawa and Buffett, 2005) found that slab penetration into the lower mantle is accompanied by an upwelling counter flow of depleted material in the area surrounding the slab, which is a mechanism for generating depleted regions in the upper mantle.

Multicomponent phase transitions is is not the only mechanism that can cause an accumulation of subducted basalt above 660 km: (Davies, 2002; Davies, 2006) showed that a low viscosity (high Rayleigh number) upper mantle in combination with a viscosity jump at 660 km depth can also be cause this.

In summary, it is quite likely that local chemical stratification exists across the 660 km interface caused by differing depths of the perovskite transition in the olivine and pyroxene-garnet systems. There is, however, still uncertainty as to these depths. This local chemical stratification around 660-720 km is a prediction that could be tested seismically, which would help to determine whether the currently-estimated depths of these phase transitions are indeed correct. For additional information on phase transitions see (Oganov, Treatise volume 2).

3.3.4 The effect of chemical layering on core heat flow and planetary thermal evolution

As was noted early on (e.g., (Christensen and Hofmann, 1994)), the presence of a compositionally-dense layer above the CMB reduces the heat flow out of the core. This reduction can be dramatic if the dense layer completely covers the core, and should be taken into account in thermal evolution calculations (e.g., (McNamara and Van Keken, 2000)). Unfortunately, when the layer undulates greatly and is discontinuous, such that some patches of the core are not covered, the appropriate parameterization of core heat flux is unknown, so direction numerical simulation becomes the preferred approach.

A long-standing paradox in modeling Earth's thermal evolution is explaining how the heat flux out of the core can have stayed large enough over billions of years to maintain the geodynamo, without growing the inner core to a much larger size than observed. Parameterized models of core-mantle evolution in which no complexities are present predict a final inner core size that is much larger than that observed (e.g., (Labrosse et al., 1997; Labrosse, 2003; Nimmo et al., 2004). As the heat conducted out of the core is determined by what is happening in the mantle, the time history of CMB heat flow is an important quantity to investigate using numerical models, both from the point of view of understanding core evolution and in providing an additional constraint on mantle models.

(Nakagawa and Tackley, 2004b) used a thermo-chemical convection model similar to those already presented but with a parameterized core heat balance based on (Buffett et al., 1992; Buffett et al., 1996) to show that the presence of a layer of dense material above the CMB, either primordial or arising from segregated crust, substantially reduces the CMB heat flow hence inner core growth. A problem is, CMB heat flow can be reduced so much that it is insufficient to facilitate dynamo action, and can even become zero or negative. Because of this, a discontinuous

layer, rather than a global layer, was found to be the most promising scenario. (Nakagawa and Tackley, 2005a) subsequently found that it is difficult to match the constraints of correct inner core size and enough heat flow out of the core, unless there is radioactive potassium in the core (e.g., (Nimmo et al., 2004)), in that case viable evolution solutions were obtained, with a tradeoff found between crustal density and core K content.

As was discussed in an earlier section, chemical layering has a strong influence on plume temperature and dynamics. A systematic study of the effect of chemical layering on plume heat flux, plume excess temperature, and upper mantle temperature was conducted by (Zhong, 2006) in 3-D spherical geometry, assuming a sharp chemical interface and a global layer, and moderately temperature-dependent viscosity. The possible range of parameters (layer depth, internal heating rates) was constrained by comparing to observations. The preferred model is one in which the dense layer was relatively thin (<350 km) and the internal heating rate in the upper layer is ~3 times higher than that inferred for the MORB source region, which, curiously, is similar to the heating deficit inherent in the "heat-helium paradox" (Ballentine et al., 2002).

3.4 On the accuracy of numerical thermochemical convection calculations

A fundamental problem with treating chemical variations numerically is the negligible diffusivity of chemical variations, which leads to the possibility of sharp interfaces and very narrow lamella (e.g., less than one grid spacing), both of which are very difficult to treat numerically. Two major classes of method are used in the mantle dynamics community to track compositional variations: field-based approaches on a fixed (Eulerian) grid, and Lagrangian particles/tracers that are advected through the grid. Various benchmark tests of these have been performed in the mantle convection community (van Keken et al., 1997; Tackley and King, 2003). Further discussion might be found in the Chapter by Zhong et al. (this volume).

Field-based approaches have the advantage of computational speed and little additional computational complexity, but the disadvantages of numerical diffusion, which smears out sharp features, and numerical dispersion, which causes artifacts like overshoots and ripples. Other research communities that employ computational fluid dynamics techniques (e.g., the atmospheric science community) face similar problems and there is much ongoing research into improving advection methods, a small sampling of which is: (Muller, 1992; Xu-Dong and Osher, 1996; Smolarkiewicz and Margolin, 1998; Yabe et al., 2002). In the mantle dynamics community, the relatively straightforward interface-sharpening scheme of (Lenardic and Kaula, 1993) can yield a dramatic improvement in the advection of interfaces (e.g., (Tackley and King, 2003)).

Tracer-based approaches have the advantage of minimal numerical diffusion (a small amount does exist because of finite error in updating each tracer's position), thus the apparent ability to represent discontinuities and sub grid-scale features, but the disadvantage that one needs 5-50 times as many tracers as grid points to prevent statistical noise from unduly influencing the solution (e.g., (Christensen and Hofmann, 1994; Tackley and King, 2003)), which adds a considerable computational burden. This noise arises because in order to calculate the buoyancy caused by compositional variations, some averaging must be done over tracers in the vicinity of each grid or nodal point. It has been found that taking a local average of the C value of each tracer (as exemplified by the 'ratio method') is far less noisy than methods that rely on a number count of tracers (the so-called 'absolute method'), regardless of the underlying numerical scheme (Tackley and King, 2003). Another type of tracer method tracks only the interface between two compositions, and is thus far more computationally efficient than methods where tracers exist everywhere (e.g., (Schmalzl and Loddoch, 2003; Lin and Van Keken, 2006a)), though it is not suited for continuously-varying chemical fields, and the computational needs increase up to exponentially with time as the interface becomes more complex, unless interface simplification algorithms are applied (Schmalzl and Loddoch, 2003).

Benchmarks of these various methods for cases with an active compositional layer (van Keken et al., 1997; Tackley and King, 2003), indicate a sensitivity of the results to the details of the

method being used, including a strong sensitivity of the entrainment rate of a stable compositional layer to resolution (both grid and number of tracers) (Tackley and King, 2003). This means that in the various numerical results reviewed in this section may not be quantitatively correct in the amount of entrainment that exists as a function of density contrast except in calculations where the grid is greatly refined in the region of entrainment (e.g., (Zhong and Hager, 2003; Lin and Van Keken, 2006a)), although convergence tests suggest that they are qualitatively correct in the general planforms and features that arise. This is an issue that will require more attention in the future, particularly as more calculations are performed in 3-D.

4. CONVECTION MODELS TRACKING TRACE ELEMENT EVOLUTION

4.1 Passive Heterogeneity

4.1.1 Helium and argon

The evolution of noble gases in a mantle that included outgassing and radiogenic ingrowth but not major-element differentiation was studied by (van Keken and Ballentine, 1998; van Keken and Ballentine, 1999). These studies investigated various proposed mechanisms for maintaining a relatively undegassed lower mantle over billions of years, finding that neither high deep-mantle viscosity, a strongly endothermic phase transition at 660 km depth, or temperature-dependent viscosity, are capable of causing a relatively undegassed deep mantle, in contrast to earlier modeling at lower convective vigor (Gurnis and Davies, 1986a). They did find that the observed total amount of ^{40}Ar outgassing is consistent with whole-mantle convection over geological history, although the convective vigor in their models was constant with time. In that case, 50% degassing of radiogenic ^{40}Ar implies ~70% degassing of primitive isotopes.

(van Keken et al., 2001) extended the analysis to the heat-helium imbalance, tracking the relationship between the rate of helium outgassing and the heat flux. Large fluctuations in the helium outgassing were obtained, but only the most extreme fluctuations would explain the 'heat-helium' issue as it is currently understood, i.e., with a ^{4}He concentration 3.5 times higher than current estimates (Ballentine et al., 2002).

The helium ratio evolution caused by subduction of differentiated oceanic plates was studied by Ferrachat and Ricard (2001), who tracked the evolution of oceanic crust and residue and showed that if oceanic crust segregates at the CMB, a large region of recycled oceanic lithosphere with high ^{3}He/^{4}He can form above it. However, in their model compositional variations were also purely passive, not influencing the flow, whereas models that account for the density anomalies of differentiated components have found that depleted material tends to rise.

4.1.2 Continent formation

The melting-induced differentiation of the continental crust and depleted mantle from primitive mantle was the focus of models by (Walzer and Hendel, 1997b; Walzer and Hendel, 1997a; Walzer and Hendel, 1999). In (Walzer and Hendel, 1997b; Walzer and Hendel, 1997a) the 670 km discontinuity was impermeable, and upon melting, trace-element ratios in the crust and depleted mantle were taken to be those in (Hofmann, 1988) rather than calculated using partition coefficients. As a result of these model assumptions, the lower mantle remained primitive while the upper mantle rapidly differentiated into continental crust and depleted mantle with exactly the trace element ratios of (Hofmann, 1988). This approach was extended in (Walzer and Hendel, 1999) to include a permeable 660 km discontinuity with phase changes at 410 and 660 and a plate model that allowed continents to aggregate. Curiously, despite the lack of compositional density contrasts their models typically developed an average (but very irregular) vertical stratification with primitive material in the deepest mantle and depleted material above it. This could be related to extremely high viscosities in their model mid lower mantle, typically in the range 10^{24}-10^{26} Pa s,

much higher than is assumed in other models or obtained in inversions of postglacial rebound or geoid and topography.

4.2 Active Heterogeneity

4.2.1 U-Pb and HIMU

The hypothesis that segregation and sequestering of subducted MORB is responsible for the HIMU component and related Pb-Pb isochron (Hofmann and White, 1982) was investigated in pioneering calculations by (Christensen and Hofmann, 1994) using a numerical mantle convection model that included tracking of crust-residue differentiation and isotopes of trace elements U, Pb, Sm and Nd, which partitioned between crust and residue on melting. The model was partly heated from within and partly from below and had a kinematic time-dependent plate-like upper boundary condition. As discussed earlier, a fraction of the subducted crust segregated into a layer above the CMB, and with some parameter combinations, realistic Pb-Pb isotope diagrams and ''ages'' were obtained. The isotope age depended on the length of time subducted MORB resided near the CMB. However, they found it necessary to run the calculations for only 3.6 Gyr instead of the full age of the Earth, otherwise the age was too high, contrary to previous expectations from mixing time estimates (reviewed in section 2.6) that it would be difficult to obtain a large enough age. This would be appropriate if the mantle were completely mixed 3.6 Gyr before present. Furthermore, their model mantle had a constant convective vigor (e.g., velocities, rate of melting), rather than, as discussed earlier, a vigor that decreases with time as the mantle temperature and radiogenic heat production decrease.

The calculations of (Xie and Tackley, 2004b) followed a similar approach to those of (Christensen and Hofmann, 1994), but with a convective vigor that decreases with time due to secular cooling and the decay of heat-producing elements, and the investigation of 4.5 Gyr run times as well as 3.6 Gyr. Technical differences were the use of a visco-plastic rheology to allow plate-like behavior of the lithosphere (Moresi and Solomatov, 1998) rather than kinematic velocity boundary conditions, and a more self-consistent treatment of melting and crustal generation based on comparing the temperature to a solidus. The higher convective vigor early in the calculations plus the longer evolution resulted in a lot of differentiation early in the modeled evolution, which resulted in Pb-Pb ages that are much too large (3.39 Gyr for the reference case). This large age is not surprising, because the rate of melting is much higher earlier in the evolution, so early differentiating material dominates the isotopic signature. Additionally, early differentiated material has developed a more radiogenic signature so influences the least squares fit more than recently differentiated material. This finding is consistent with previous attempts at modeling lead isotope ratios starting from 4.5 Gyr ago that obtained unrealistically high slopes in $^{207}Pb/^{204}Pb$–$^{206}Pb/^{204}Pb$ space (Armstrong and Hein, 1973; Allegre et al., 1980). It is also consistent with the numerical models of (Davies, 2002), in which although Pb-Pb ages were not calculated, found mean ages (since melting) of ~2.7 Gyr for MORB. (Christensen and Hofmann, 1994) attributed this 'too old' problem to the rapid decay of ^{235}U into ^{207}Pb in the early stage of the model, also finding that the early differentiation has a strong effect on the isotopic signatures at the end of the run. Thus they chose to start their models 3.6 Gyr ago with uniform Pb composition, which assumes that any earlier differentiation in the mantle has been completely homogenized by the convection.

Several possible explanations for the discrepancy between models and data were investigated by (Xie and Tackley, 2004b). These are that HIMU material may not have been subducted into the mantle prior to 2.0–2.5 Gyr B.P., that melting is not rapid enough in the model (i.e., too low processing rate meaning too high residence time), that stretching of heterogeneities is inadequately represented, that the ''sampling volume'' over which isotopic ratios are calculated is incorrect, that the deep-mantle density of crustal material is incorrect, or that the Pb-Pb slope is made artificially large by noise associated with tracer discretization. The most successful and straightforward explanation was found to be the first, which is discussed in more detail below, but

it is worth briefly discussing the others. Regarding the melting-induced processing rate, this was found to be within the range of possibilities for the Earth (see discussion in 1.5.3). A parameterized box model indicated that only the most extreme assumptions would lead to a low enough residence time. Inadequate treatment of stretching highlights a problem with tracer treatments: whereas in reality a tracer should get exponentially stretched into a long tendril that extends over an area much wider than the sampling volume thereby reducing its contribution to the isotopic signature of a melt, in fact it remains as a localized entity. (Xie and Tackley, 2004b) tested one approximation of this: tracking the integrated strain as in (McKenzie, 1979; Kellogg and Turcotte, 1990), then ignoring high-strain tracers when calculating the isotopic signature of a sampling volume. This was found to reduce the Pb-Pb somewhat, but not enough to match observations. Changing the sampling volume over which heterogeneities are averaged does not change the Pb-Pb slope, only the amount of scatter.

One possible reason for the ~1.8 Ga Pb-Pb age is that HIMU material did not enter the mantle before 2.0–2.5 Gyr ago, for which there are two possible explanations. One of these is that higher subduction zone temperatures in the past may have caused essentially all Pb, U, and other trace elements to be stripped from the subducted crust by melting (Martin, 1986). Supporting this explanation is eclogite xenoliths from the upper mantle under western Africa that are highly depleted in incompatible elements and have been interpreted as the melting residue of Archaean subducted crust (Barth et al., 2001). Another possible explanation is that the HIMU end-member was not produced prior to the rise in atmospheric oxygen about 2.2 Gyr ago. In this latter scenario, HIMU is produced by addition of continental U to oceanic crust by hydrothermal circulation at ridges (Michard and Albarède, 1985; Elliott et al., 1999), with efficient stripping of U from continents being accomplished by an oxygen-rich atmosphere oxidizing U to its 6+ state (Holland, 1984; Holland, 1994). This is not the only process that has been proposed to produce HIMU: the other is preferential stripping of Pb (relative to U) from the subducted crust to the overlying mantle in subduction zones (Newsom et al., 1986; Hofmann, 1988; Chauvel et al., 1995). It is possible that both of these processes may operate. In the numerical model of (Xie and Tackley, 2004b), as in that of (Christensen and Hofmann, 1994), HIMU was produced by artificially changing the partition coefficients of U and Pb so that they fractionate on melting. In order to evaluate the effect of it not being produced prior to some point in the past, (Xie and Tackley, 2004b) ran cases in which the U and Pb partition coefficients are set equal for the first part of the model run, then changed to their default values at a specified point in the past. Setting the transition to 2.5 Gyr before present caused a Pb-Pb isotopic age of 1.75 Gyr, whereas setting it to 2.0 Gyr before present caused an isotopic age of 1.4 Gyr. Thus, from a modeling perspective a lack of HIMU production prior to 2–2.5 Gyr ago is an appealing mechanism for explaining the effective age of the Pb-Pb isotope diagrams, although it needs to be shown that this fits other isotope systems too.

A mathematical analysis of the relationship between the probability distribution of heterogeneity age (i.e., time since last melting), and the pseudo-isochron age, was conducted by (Rudge, 2006), superceding an earlier box model approach by (Allegre and Lewin, 1995). He obtained simple relationships between mean remelting time and isochron age for a constant melting rate, which closely fit the Pb-Pb pseudo-isochron ages in the numerical simulations of (Christensen and Hofmann, 1994). His more general theory was also able to fit the isochron ages of the time-dependent melting histories in the simulations and calculations of (Xie and Tackley, 2004b). An important finding is that for constant melting rate, the Pb-Pb pseudo-isochron age is substantially higher than the mean time before remelting- in particular fitting a 2.0 Gyr Pb-Pb pseudo-isochron age with a constant melting rate over Earth's history requires a time interval of only 0.5 Gyr before material remelts, much shorter than seems reasonable.

4.2.2 $^{3}He/^{4}He$

The origin of the high $^{3}He/^{4}He$ endmember is discussed in section 1.6.1. The two most commonly cited origins have both been the foci of numerical investigations: (Samuel and Farnetani, 2003)

demonstrated the dynamical viability of the "primitive" explanation, while (Ferrachat and Ricard, 2001; Xie and Tackley, 2004a) demonstrated the viability of the "recycled" explanation. In any case, it is important to recall that the ratio of $^3He/^4He$ constantly decreases with time due to radiogenic ingrowth of ^4He from U and Th decay. Elemental fractionation between He and (U+Th) upon melting, and outgassing of He to the atmosphere influence He/(U+Th) in the crust and residue, which over time can then develop $^3He/^4He$ different from primitive material. Thus the present-day distribution of He isotope ratios reflects a combination of ingrowth, fractionation and outgassing.

Primitive. (Samuel and Farnetani, 2003) used a fully dynamical convection model (e.g., with no imposed surface velocities) to demonstrate that a thick basal layer of primitive material, consistent with the proposal of (Kellogg et al., 1999; van der Hilst and Karason, 1999), is capable of generating $^3He/^4He$ histograms similar to those observed for MORB and OIB. Isotopes of U, Th, K and He were tracked in three different components: primitive, subducted MORB and subducted residue, with the primitive layer being the 'mass balance' reservoir of U, Th and K as well as the high $^3He/^4He$ component. Partitioning of trace elements between crust and residue was based on an assumed melt fraction. With a compositional density contrast of 2.4% (100 kg/m^3), depth-dependent thermal expansivity, temperature-dependent viscosity and a primitive layer making up 25% of the mantle volume, it was found that $^3He/^4He$ values in MORB cluster in the observed range, whereas OIB samples, which were associated with plumes forming from the layer interface, display a much wider spread because they contain a heterogeneous mixture of the three different components. Heterogeneity dispersed more rapidly in the upper layer than in the lower layer due to the higher convective vigor there. Lower layer material was entrained into the upper layer much more rapidly than upper layer into the lower layer: after 2.1 Gyr the percentages were 25% and 3% respectively.

Recycled. As discussed in section 4.1.1, (Ferrachat and Ricard, 2001) found that a high $^3He/^4He$ repository of subducted residue built up in the deep mantle in a steady-state flow with no compositional buoyancy. Studies that do include compositional buoyancy find, however, that the depleted residue tends to rise to the shallow mantle, as in the preliminary calculations of (Tackley and Xie, 2002), in which high $^3He/^4He$ residue aggregates near the top due to its buoyancy, where it is sampled by mid-ocean ridge volcanism. Thus, (Xie and Tackley, 2004a) investigated the possibility that active (buoyant) compositional variations caused by crustal production may play an important role in the evolution of noble gas isotopes and the generation and maintenance of distinct endmembers, using numerical convection models with a self-consistent melting criterion and plate-like dynamics. The distribution of $^3He/^4He$ ratios in the modeled MORB source region was found to be highly dependent on the density contrasts between the different components (primitive, residue and basalt) and compatibility of He relative to U and Th. While in most cases the $^3He/^4He$ was scattered to too high values. Two parameter combinations were identified that led to a 'realistic' MORB-like distribution of $^3He/^4He$ (i.e., clustered around 8-10 times atmospheric): (i) He less compatible then U, Th and crust dense in the deep mantle. In this case, the shallow mantle contained a large proportion of depleted residue, which had MORB-like $^3He/^4He$, and the high $^3He/^4He$ component was primitive material. (ii) He equally compatible as U, Th and crust buoyant in the deep mantle. In this case, subducted crust in the shallow mantle brought the $^3He/^4He$ into the correct range; both primitive material and residue had the same 'primitive' $^3He/^4He$.

These calculations demonstrate that a MORB-like shallow mantle $^3He/^4He$ and the existence of a high $^3He/^4He$ endmember are consistent with whole-mantle convection from a homogeneous start, but with the ambiguity of two alternative explanations. Indeed there may be a continuum of 'successful' solutions in (partition coefficient, buoyancy) space, which would require the consideration of additional constraints to constrain further. These calculations did not attempt to distinguish between MORB and OIB melting signatures. Thus, more investigations are necessary, preferably in 3-D.

5. NEW CONCEPTS AND FUTURE OUTLOOK

5.1 Revisiting Noble Gas Constraints

Ar and He budget. Noble gas constraints were reviewed in section 1.6.1. As discussed in that section, the "50% ^{40}Ar degassing" constraint is straightforward to match with whole mantle convection, even with substantially higher processing rates in the past. A much more troubling constraint from the point of view of whole mantle convection models, is that the Argon concentration in the MORB source is much lower than it would be if the Ar thought to be in the mantle were evenly distributed, which has been taken as evidence of layered convection with the lower layer containing the "missing" argon. Along similar lines is the "heat-helium imbalance", i.e., the concentration of He in the MORB source region seems to be too low relative to concentrations of U and Th. Recently, (Ballentine et al., 2002) noted that both of these constraints are based on fluxes of ^3He through the oceans that represent an average over 1000 years, and if the true long-term average were a factor of 3.5 higher, both constraints would be removed. He argues that two other indicators of ^3He concentration in the MORB source- the concentration in the 'popping rock' and the estimate of carbon concentration in MORBs based on graphite-melt equilibrium, give estimates of ^3He concentration up to several times higher than obtained from the He flux through the oceans. On the other hand, (Saal et al., 2002) obtain rather lower ^3He concentrations by considering carbon concentrations in undegassed melt inclusions. Numerical models of convection that track the relevant isotopes (van Keken et al., 2001) obtain considerable variation in the outgassing rate over timescales much longer than 1000 years.

The 'standard' reconciliation of the heat-Helium imbalance invokes the concept that He and heat have different transport mechanisms, i.e., heat is transported across a thermal boundary layer at 660 km depth whereas He is not. (Castro et al., 2005) found that a similar concept occurs to He transport in continental aquifers, which, when applied to the oceans, suggests that the He flux into the ocean may be much lower than the flux out of the mantle, due to the action of seawater circulating through the oceanic crust (see (Albarède, 2005a) for further discussion).

The "missing ^{40}Ar" constraint would also be eased if the total amount of ^{40}K in the mantle were lower than commonly assumed, which is based on bulk silicate Earth abundances (e.g., (McDonough and Sun, 1995)) combined with the K/U ratio observed in MORB (Jochum et al., 1983). It has been shown that this difficulty could be resolved if the amount of ^{40}K in the mantle were a factor ~2 than commonly estimated (Albarède, 1998; Davies, 1999), which would be the case if the K/U ratio were lower than that observed in MORB, perhaps due to fractionation of K from U (Albarède, 1998). (Lassiter, 2004) suggests that K/U could be significantly lower than normally assumed, if the K depletion of oceanic crust in subduction zones is taken into account. Then, subducted MORB in the mantle would have a relatively low K/U, lowering the mantle average.

As a result of these various arguments, it seems plausible that the "missing ^{40}Ar" and "heat-Helium imbalance" constraints are less robust than previously thought.

High 3He/4He. Although the high $^3He/^4He$ endmember (C or FOZO) is often assumed to be primitive and undegassed, several authors (e.g., (Albarède, 1998; Anderson, 1998; Coltice and Ricard, 1999; Coltice et al., 2000b; Ferrachat and Ricard, 2001; Coltice and Ricard, 2002)) have suggested that it could instead be generated by recycling, as was discussed in detail in section 1.6.1 and investigated by the numerical models of (Ferrachat and Ricard, 2001; Xie and Tackley, 2004a) discussed in section 4.2.2. If high $^3He/^4He$ is caused by low [U+Th] rather than high [^3He] then an inverse correlation is expected between [U+Th] and $^3He/^4He$, and such a correlation was found in the data plotted by (Coltice and Ricard, 1999). (Meibom et al., 2003) point out that the unfiltered $^3He/^4He$ dataset for MORB has a Gaussian distribution similar to that for $^{187}Os/^{188}Os$, and propose that both are due to mixing of radiogenic and nonradiogenic components (associated with basalt and residue respectively) with varying amounts of partial melting. They propose that residue can retain substantial He due to the capture of He-rich bubbles in magma chambers. Further reinforcing this interpretation is a recent compilation of OIB isotope data which shows that high

^{3}He source has the same isotopic and major element composition as depleted mantle, therefore represents already-melted material (Class and Goldstein, 2005). (Hauri et al., 1994) had earlier concluded that the FOZO represented differentiated material. (Class and Goldstein, 2005) find an inverse correlation between ^{3}He/^{4}He and Th abundance consistent with He being a mixture of a small amount (~2%) primitive material plus ingrown ^{4}He. Based on the difference between plumes and OIBs they infer that amount of time the high ^{3}He/^{4}He material has remained separate from the rest of the mantle is ~1-2 Gyr.

5.2 Improved Recipes for Marble Cakes and Plum Puddings

5.2.1 Two recipes

Extreme compositional heterogeneity of the mantle, building on the "marble cake" proposal of (Allegre and Turcotte, 1986), is a common theme in recent attempts to explain mantle geochemistry, and contrasts with earlier views of a relatively homogeneous upper mantle, with the necessary OIB heterogeneity supplied by plumes from the deep mantle. The proposed mantle assemblage typically consists of a mostly depleted residue with ~few % primitive material, ~10-20% recycled MORB and ~few % recycled sediment (derived from continental crust) and possibly continental lithosphere and/or OIB.

One possible recipe is that the assemblage in the MORB source region is different from that in the plume (hence OIB) source region, but both assemblages are derived mostly by recycling processes. This is consistent with the proposal of (Hofmann and White, 1982; Christensen and Hofmann, 1994) that HIMU and perhaps EM components arise from subducted crust that has segregated into a layer above the CMB. This recycled deep layer can also be the location for storing incompatible elements that are "missing" according to mass budget calculations (Coltice and Ricard, 1999), and have higher concentrations in MORB than in primitive material, requiring a smaller storage area. The high ^{3}He/^{4}He component might be caused by strips of former oceanic lithosphere (Coltice and Ricard, 1999; Coltice and Ricard, 2002) as discussed in the previous section. In the marble cake of (Coltice and Ricard, 1999; Coltice and Ricard, 2002), this subducted lithosphere forms a layer above D", accounting for different MORB and OIB signatures, but it is not clear that such a layer would be stable. A deep layer of residue was obtained in the numerical calculations of (Ferrachat and Ricard, 2001), but compositional density contrasts were not accounted for in those calculations, and when they are, residue tends to rise into the upper part of the mantle (e.g., (Tackley and Xie, 2002; Ogawa, 2003; Xie and Tackley, 2004a)), although this depends on uncertain density relations in the deep mantle, as discussed earlier.

Another possible recipe is that OIB and MORB result from the same statistical distribution with their geochemical differences due entirely to melting processes, with the details of the melting processes varying in different proposals. In the original proposal (Allegre and Turcotte, 1986), enriched plums exist in a depleted matrix, and the higher heterogeneity of OIBs was ascribed to smaller sampling region and lower degrees of melt. More recent proposals tend to emphasize the heterogeneity of the entire mixture, with no ~uniform residue. Based on modeling the evolution of the distribution of trace element ratios in the differentiating continental crust – depleted mantle system, (Kellogg, 2004) proposed something of an inversion of this model, with depleted 'plums' consisting the residue from continental crust extraction, and a 'matrix' with a C/FOZO composition consisting of small-scale strips of everything else. (Meibom et al., 2003; Meibom and Anderson, 2004), proposed that MORB and OIB derive from the same source region (SUMA – the Statistical Upper Mantle Assemblage; the composition of the lower mantle was not specified) with the geochemical differences due to different statistical sampling of this highly heterogeneous source region- essentially, smaller melt fractions. A whole mantle consisting mainly of residue and strips of subducted crust was also favored by (Helffrich and Wood, 2001), who used various constraints to estimate plausible fractions of the different components that satisfy global heat budget constraints: for the mantle their model contained between 10-24% recycled oceanic crust, with the

rest mostly sterile mantle (i.e., zero heat-producing elements) and recycled continental material making up to 0.4%. The viability of this class of model is strongly supported by the recent modeling of (Ito and Mahoney, 2005b; Ito and Mahoney, 2005a; Ito and Mahoney, 2006) who calculated the melting of a heterogeneous 4 or 5-component mantle, and found that in most cases OIBs and MORBs could be drawn from the same source distribution, although different OIBs require different proportions of the components. This analysis is further discussed below.

A further proposed recipe is that large primitive 'blobs' exist throughout the mantle (Becker et al., 1999). The proposed blobs are larger than the sampling lengthscale and are not sampled by ridge volcanism. The dynamical feasibility of this model has not been established and it will not be further discussed here.

5.2.2 Two-stage melting

It was proposed by (Phipps Morgan and Morgan, 1999), that the OIB and MORB signatures can be explained by two-stage melting of a heterogeneous "plum pudding" source region. In this model, the OIB source is 'normal' mantle that includes lots of enriched basalt-pyroxenite veins, while the MORB source is produced from this by depletion associated with hotspot melting. Thus, the initial stage of melting is associated with plumes producing OIBs with low degree melting. The once-depleted plume material fills the asthenosphere, constituting the MORB source; subsequent second-stage melting underneath spreading centers produces the depleted MORB signature. A parameterized box model is presented to demonstrate the success of this model in explaining geochemical data. While the literal topology of this two-stage model is not widely accepted, it is useful to summarize the outcome of the parameterized model because the heterogeneous mixture of different components could have wider applicability. The model mantle contains the following components: PRIM (primitive material), ORES (residue from OIB melting), MRES (residue from MORB melting), recycled components ZOIB, ZMORB ad ZCONT and the continental crust. The rate of oceanic floor production is 2.7km^2/yr at the present day and increases in the past as (heat production)^2. By the end of the calculation, 95% of mantle has passed through MOR processing, and the proportions of the components are: PRIM=5%, ZCONT+ZOIB=2%, ZMORB=20%, ORES=5%, MRES=62.5%, with continental crust being 0.5% . A Rb-Sr pseudo-age of 1.3 Ga is obtained, which is much younger than whole-mantle pseudo-isochron of 3.5 Ga because it represents the average time between OIB melting and MORB melting. (Phipps Morgan and Morgan, 1999) also present an explanation for the Pb kappa conundrum (Th/U of MORB is 2.5 whereas lead ratios imply it should be 4) based on the different compatibilities of Th and U, and for the heat-He imbalance based on He being outgassed mainly by hotspots and continental flood basalts (as previously suggested by (Kellogg and Wasserburg, 1990)), which leads to the prediction that atmospheric He concentrations should be elevated after flood basalt events.

5.2.3 Source statistics and component fractions

A series of papers (Anderson, 2000; Anderson, 2001; Meibom et al., 2002; Meibom et al., 2003; Meibom and Anderson, 2004; Meibom et al., 2005) studied the statistical distributions of isotope ratios in MORB and OIB environments, and found that they support the idea that the upper mantle consists of a multiple-length-scale mixture of different ''plums'' with no uniform matrix, from long-term recycling of crustal and sedimentary components. Helium ratio distributions for the 'unfiltered' MORB dataset were plotted by (Anderson, 2000; Anderson, 2001) and found to be drawn from the same statistical distribution as OIB helium ratios but with smaller standard deviation, which was argued to be related to averaging over larger sampling regions and degrees of melting consistent with the central limit theorem in which "independent averaging of samples from any given distribution will approach a Gaussian distribution with a variance that becomes smaller as the sample volume increases" (Meibom et al., 2002). This random sampling model was subsequently found to be consistent with the observed Gaussian distribution of ^{187}Os/^{188}Os in

mantle-derived grains, implying random sampling between ancient radiogenic and unradiogenic mantle with relatively high degrees of partial melting (Meibom et al., 2002). The similarity between Os ratio distributions and He ratio distributions was discussed in (Meibom et al., 2003) and argued to be evidence for the same processes acting on both systems, with (Meibom and Anderson, 2004) further analyzing ratios of Pb, Sr, Nd, pointing out the Gaussian shape reflects the dominance of the homogenization during sampling process by partial melting and magma chamber mixing, rather than the nature of the source region. They argue that the dominant lengthscales are in the range 100m – 100 km, rather than the cm to meter scale implicit in the original marble cake proposal (Allegre and Turcotte, 1986), and that therefore the efficiency of convective stirring is limited, with the dominant homogenization processes occurring during the melting and magmatic stages. There are also larger-scale variations related to different plate tectonic histories.

A lengthscale constraint comes from the Os analysis of mantle-derived grains in (Meibom et al., 2002): as a single grain corresponds to about 1 m^3 of mantle, this is the minimum lengthscale of heterogeneity, and it is consistent with observations of Os variations in abyssal peridotites on lengthscales 10-100 m. (Parkinson et al., 1998; Brandon et al., 2000). An age constraint comes from the least radiogenic Os ratio they found, which indicates a depletion age of 2.6 Gyr.

Quantitative modeling of the distribution of isotope ratios by sampling a heterogeneous system was performed by (Kellogg et al., 2002) using a new type of "box model" that allows the distribution of isotope ratios to be calculated in addition to the mean values (Allegre and Lewin, 1995), as a function of melt fraction, sampling zone size, and evolution. Essentially, each melting event produces new "subreservoirs", which are stretched with time, evolve isotopically and can be statistically sampled at a particular lengthscale. The results showed that indeed, as the sampling lengthscale or melt fraction is increased, isotope ratio distributions tends towards Gaussian, as discussed above. The method was used to successfully match Rb-Sr and Sm-Nd isotope ratio diagrams by differentiation and recycling in the upper mantle – continental crust system, and subsequently extended to include the U-Th-Pb system (Kellogg, 2004), and later applied to the whole mantle system including the oceanic differentiation cycle (Kellogg, 2004).

A simpler mathematical model of mantle isotopic variability was developed by (Rudge et al., 2005). Their model considered the mantle to be a single reservoir that experiences ongoing melting events with a certain average time between remelting. They found that the best fit to the isotopic scatter was obtained with remelting timescale of 1.4-2.4 Ga and melt fraction of around 0.5%, the latter of which is similar to (Kellogg et al., 2002; Kellogg, 2004), although the latter study was intended to represent continental formation melting. This did not, however, fit Pb isotopic data.

5.2.4 Can OIB and MORB be produced by the same statistical distribution?

To answer this question, it is necessary to understand the composition that is obtained when a heterogeneous mixture is partially melted, and when it is melted in different environments-- in particular, underneath spreading centers (MORB) versus underneath the lithosphere (OIBs), and this is far from straightforward. Ito and van Keken (ch. 9, this volume) present a review of some of the relevant observation and explanations.

When a source region that is heterogeneous in major element chemistry is partially melted, it is likely that the enriched pyroxenite material melts at a lower temperature than depleted residue, which means that low degrees of melting will preferentially sample the enriched material, while high degrees of melting will average over the whole assemblage (Sleep, 1984). Whether this can quantitatively account for the differences between MORB and OIB compositions has not, until recently, been quantitatively assessed. Note that this is preferential sampling of enriched components is different from the proposal of (Anderson, 2001; Meibom and Anderson, 2004), in which the same material would be melted in MORB and OIB environments but with smaller melt fraction producing greater variability with the same mean. Based on quantitative modeling of trace element distributions, (Kellogg et al., 2002) find that OIB and MORB cannot be produced from the

same distribution simply by differences in sample volume (with smaller samples being more heterogeneous): differences in the melting processes and/or source regions are necessary.

If the depleted matrix (DM) and pyroxenite (PX) veins are at small enough lengthscales to be in thermal equilibrium, (Phipps Morgan, 2001) found that melting of the PX is greatly enhanced by heat flowing from the surrounding matrix. The details depend on the temperature-pressure gradient of PX solidus relative to DM solidus, consistent with other calculations (Hirschmann et al., 1999) and confirming the prediction of (Sleep, 1984).

Complicating interpretations of hotspot melting is that different basalts from the same hotspot do not generate the same composition, but rather elongate tube-like fields (Hart et al., 1992), a traditional interpretation of which is a mixing line between two end-member components present in the source region. (Phipps Morgan, 1999) finds, however, that such linear arrays are naturally generated by progressive melting of a heterogeneous source mixture, and remain linear independent of the number of distinct isotopic components in the initial source mixture.

Calculations with up to five components were performed by (Ito and Mahoney, 2005a; Ito and Mahoney, 2005b; Ito and Mahoney, 2006), who quantitatively modeled the different trace element compositions that arise as a result of differing OIB and MORB environments. Two key differences arise between OIB and MORB melting environments as a result of the differing mantle flow. Whereas flow beneath a spreading center rises at a roughly constant velocity to the surface, the vertical flow caused by plumes impinging on the base of a rigid lithosphere decreases towards the base of the lithosphere tens of kilometers deep. Hence the total amount of decompression melting that takes place in OIB environments is typically less, but even if the temperature is high enough to make it the same, the depth-distribution of OIB melting is concentrated towards greater depths whereas that of MORB melting is constant with depth. As the enriched components are assumed to melt at lower temperature (greater depth) due to their different lithologies and (sometimes) enrichment in volatiles, they make up a larger proportion of OIB-type melts, whereas MORB melting is diluted to a much larger extent by the depleted component, leading to a more enriched signature for OIBs. The details of the trace element are sensitive to the exact composition of enriched components in the melting zone, particularly for OIB melting.

(Ito and Mahoney, 2005a) study a heterogeneous mantle consisting of three components: DM=depleted mantle (similar to the DMM of (Hart et al., 1992)), PX=pyroxenite (essentially subducted MORB, and carrying the HIMU signature) and EM=enriched mantle (similar to EM1 and EM2). They calculate the trace element signature (La/Sm, Sr, Nd, Pb) of the resulting melt assuming perfect melt homogenization, as a function of the proportions of PX and EM (keeping DM fixed at 90%), the thickness of lithosphere, and the potential temperature. Their results reproduce many of the features observed in MORB and OIB data, particularly the difference between OIBs erupting over old (thick) seafloor and those erupting over young seafloor, which are that over young seafloor the compositions of hotspot islands are less variable and overlap with MORB observations, whereas over old seafloor, trace-element compositions are more enriched and highly variable due to sensitivity to exact proportions of PX and EM, and temperature, in the source region. The results are also able to reproduce some features of "arrays" in ratio-ratio space, the trajectories of which are often curved and have corners due to the transition from melting one component to melting another. Because the observed isotope ratios of each hotspot typically cover a wide range (an elongated "array"), the 'fit' must focus on fitting the scatter rather than precise values. Incomplete magma mixing during ascent, which is not treated, may cause melt batches to have more extreme isotopic signatures. Evidence for pressure being a most important sampling parameter is in correlated major element, trace element and isotope compositions in postglacial Icelandic basalts (Stracke et al., 2003).

This analysis is then applied to specific island chains in (Ito and Mahoney, 2005b), with the goal of answering the question of whether two distinct sources are needed to explain OIB and MORB. The authors use a simple grid search scheme to determine the range of mantle sources that can fit 13 specific hotspot island chains based on correlations in Sr, Nd, Pb isotopes space, then calculate the isotopic composition you would get if melting each one below mid-ocean ridges. The

variables are mantle temperature excess, mass fractions of components, and isotopic compositions of EM and PX. Most model OIB compositions produce MORB that is indistinguishable from observed MORB compositions, suggesting that the whole mantle could be made of the same statistical assemblage. The proportion of different components was different for different OIBs, indicating large-scale heterogeneity. However, some predicted MORB compositions lie outside the range of observed normal MORB data. The fit to MORB is optimal when DM fractions are 85-95%, with the rest being PX and EM. Regarding abundances of enriched components, on average PX is slightly more abundant than EM (by a factor 1.17). Regarding the global budget issue, they calculated that if the upper bound for U and Th in continents and upper bound for U and Th in model are assumed, an additional primitive or otherwise enriched source is not necessary, though in that case only 30% of the mantle+core heat budget is radiogenic.

This approach was extended to include He in (Ito and Mahoney, 2006), with the addition of a high $^{3}He/^{4}He$ component corresponding to C(Hanan and Graham, 1996) or FOZO (Hart et al., 1992; Hilton et al., 1999) and basically the same as HRDM (Stuart et al., 2003). It was found that OIB and MORB can arise out of the same heterogeneous source region if three conditions are met: (i) the high $^{3}He/^{4}He$ component starts melting deeper than DM, (ii) DM is >=85% of the mantle, and (iii) the concentration of He in C/FOZO is comparable to that in DM. The models are successful in matching the low variation in MORB $^{3}He/^{4}He$.

The requirement for C/FOZO to have the same He concentration as DM implies that it is not primitive but has already melted reinforces the findings of (Class and Goldstein, 2005) and earlier proposals and evidence discussed earlier (Albarède, 1998; Coltice and Ricard, 1999): it keeps a high He ratio due to strong depletion in U and Th while retaining relatively high ^{3}He, perhaps in olivine-rich lithologies (Meibom et al., 2005; Parman et al., 2005) or by mixing with primitive material, with the difference that (Ito and Mahoney, 2006) remove the requirement for this component to be distributed differently (e.g., located in the deep mantle and brought up by plumes or depleted by a two-stage melting process (Phipps Morgan and Morgan, 1999))- it can be part of the general upper mantle assemblage as proposed by (Meibom and Anderson, 2004). Still, C/FOZO and DM are distinct components despite their similarity in major and trace elements other than He, so it needs to be established how such similar material can evolve two quite different He ratios.

5.3 Transition Zone Water Filter Concept

As mentioned in section 1.10, water is a potentially very important constituent in Earth's mantle due to its effect on rheology (e.g., (Hirth and Kohlstedt, 1996)), and is cycled between the interior and the biosphere/exosphere. Despite this importance, only one study has attempted to track its transport around the mantle (Richard et al., 2002). Water is also thought to play an important role in transporting trace elements from the subducting slab through the mantle wedge region, and several studies have tried to calculate how much water leaves the slab and/or its influence on the mantle wedge region (e.g., (van Keken et al., 2002; Gerya and Yuen, 2003; Ruepke et al., 2004; Arcay et al., 2005)).

It has also been proposed that water plays an important role in trace element transport in the transition zone region. Due to different solubilities of water in different minerals, the transition zone between 410 and 660 km depth can contain 10-30 times higher water concentrations than the mantle above or below it. This has led to the idea (Bercovici and Karato, 2003) that some water may be trapped in the transition zone, and with it, incompatible trace elements. If so, this provides a way of maintaining a mantle that is layered in trace elements but still undergoing whole-mantle convection.

The high water content of enriched transition zone material rising through the 410 km discontinuity would cause it to partially melt, and the incompatible trace elements would enter the melt, leaving a depleted solid in the MORB source region. A requirement for this melt to be trapped is that it is denser than the surrounding solid, in which case a melt layer would build up

above 410 km, with the production of new melt being balanced by entrainment and solidification of melt near downwelling slabs. This mechanism applies to the slow passive upwelling return flow characteristic of a mainly internally-heated system. Plumes from the water-poor lower mantle could, however, escape being stripped of their trace elements because they have a relatively low water content and move through the transition zone too quickly for water to diffuse into them. Thus, plumes in the upper mantle appear enriched relative to the filtered MORB. Material traveling in the opposite direction and entering the lower mantle across the 660 km discontinuity would likely be too cold to melt but water could enter a free phase at grain boundaries and percolate back into the transition zone.

While appealing in its simplicity and ability to reconcile geochemical layering and whole-mantle convection, several aspects of the proposal require testing, as is presently happening. The existence of a partial melt layer above 410 km should be testable seismically, and some studies have indeed indicated such a zone (e.g., (Revenaugh and Sipkin, 1994; Song et al., 2004)). Mineral properties such as the density of melt above 410 km depth, the partition coefficients or relevant trace elements at this pressure, and the diffusivity of hydrogen need to be established. The detailed dynamical and geochemical consequences need to be worked out. A geochemical prediction of the model is that at steady state the average isotopic composition of the convecting upper mantle must be almost the same as that of the lower mantle, with modifications for radiogenic ingrowth, which implies that noble gas residence times in the upper mantle must be very long (C. J. Ballentine, personal communication, 2007).

Some of this research is in progress, as summarized in (Karato et al., 2006). For example, (Leahy and Bercovici, 2004) calculate the convective consequences of concentrating heat producing elements in the transition zone and/or lower mantle, and find that the exact distribution has a minor influence on the flow except in the extreme case where all heat-producing elements are concentrated in the transition zone. An analysis of electrical conductivity of the relevant phases compared to that inferred in the mantle implies the predicted amount of water in the transition zone (Huang et al., 2005; Huang et al., 2006), although this has been doubted (Hirschmann, 2006a). Further discussions of water transport in the mantle can be found in (Hirschmann, 2006b).

5.4 Outlook and Future Directions

5.4.1 Can geochemical and geophysical observations be reconciled with current paradigms?

Recent advances in paradigms and modelling bring us closer to an integrated model that is consistent with both geochemical and geophysical constraints, but several major questions remain.

Likely characteristics of an integrated geodynamical-geochemical model are:

- The turbulent (exponential) mixing regime, with a whole-mantle mixing time (to ~10s cm scale lengths) ~3 Gyr as discussed in section 2.6.4.
- The mantle is compositionally heterogeneous at all scales, from thousands of km to centimeters.
- The upper mantle that is not much better mixed than the lower mantle, as demonstrated by recent numerical results (Hunt and Kellogg, 2001; Stegman et al., 2002). ('Upper mantle' mixing time estimates are meaningless in whole-mantle convection, as discussed earlier).
- Almost all of the mantle (i.e., 95-99%) has been processed through mid-ocean ridge melting and so presumably been degassed of primordial noble gases. This is consistent with the constraint of only ~50% degassing of radiogenic ^{40}Ar.

Less certain, but looking increasingly feasible are:

- Many OIBs can arise from a statistically similar heterogeneous source as MORB, through differences in melting processes. It is also feasible, however, that plume-related volcanism could tap a different statistical assemblage.

- There may be some vertical stratification of incompatible trace elements due either to gravitational stratification of major elements (crust settling above the CMB, perhaps some of it generated very early on, and/or the composition-dependence of the depth of the perovskite phase transition, or effects of water (the transition zone water filter) or melting (possible entrapment in melt zones at the CMB).

Many geochemical issues remain to be explained, although hypotheses exist. These include the radiogenic heat budget of the mantle (where are the heat-producing elements missing from the MORB source region? – although recent silicate Earth models (Lyubetskaya and Korenaga, 2007a; Lyubetskaya and Korenaga, 2007b) suggest that there are no missing elements), the correct explanation of high $^{3}He/^{4}He$ ratios (the 'recycled' hypothesis has been gaining ground on the 'primitive' explanation recently), and the Pb paradox. In some cases, uncertainties arise because of uncertain physical properties such as partition coefficients and densities.

5.4.2 Quantitative modeling approaches

Recent years have seen the improvement of several modeling approaches that are capable of generating model geochemical data to compare to observations. These include improved 'box models' that treat the statistical distribution of isotope ratios as well as their mean values (Kellogg et al., 2002; Kellogg and Tackley, 2004; Rudge et al., 2005; Rudge, 2006), improved methods for calculating the trace element signatures that arise from melting in different environments (Phipps Morgan, 1999; Ito and Mahoney, 2005b; Ito and Mahoney, 2005a; Ito and Mahoney, 2006), and numerical thermo-chemical convection models that track trace elements and make quantitative predictions about trace element distributions and evolution, as well as the seismic structure of the mantle. These different methods are complementary and can be combined to enhance understanding. Several modeling challenges remain in the future. The global numerical models do not include continent formation, because the relevant processes are poorly understood; the complex mass transport occurring in subduction zones is an important part of this. Global numerical models cannot treat the smaller scales, which must therefore be done using some statistical approach.

Acknowledgements. The author thanks Chris Ballentine and Nicolas Coltice for thoughtful reviews, David Bercovici for his editorial comments and organization, and Yanick Ricard for providing Figure 4.

REFERENCES

Abe Y 1997 Thermal and chemical evolution of the terrestrial magma ocean. *Phys. Earth Planet. Int.* **100,** 27-39

Agranier A, Blichert-Toft J, Graham D W, Debaille V, Schiano P, Albarède F 2005 The spectra of isotopic heterogeneities along the Mid-Atlantic Ridge. *Earth Planet. Sci. Lett.* **238,** 96-109

Albarède F 1998 Time-dependent models of U-Th-He and K-Ar evolution and the layering of mantle convection. *Chem. Geol.* **145,** 413-429

Albarède F 2001 Radiogenic ingrowth in systems with multiple reservoirs: applications to the differentiation of the mantle-crust system. *Earth Planet. Sci. Lett.* **189,** 59-73

Albarède F 2005a Helium feels the heat in Earth's mantle. *Science* **310,** 1777-1778

Albarède F 2005b The survival of mantle geochemical heterogeneities. In: Van Der Hilst R D, Bass J D, Matas J, Trampert J (eds.) *Earth's Deep Mantle: Structure, Composition, and Evolution*. American Geophysical Union27-46

Albarède F, van der Hilst R D 2002 Zoned mantle convection. *Phil. Trans. R. Soc. Lond. A* **360,** 2569-2592

Allegre C J 1997 Limitation on the mass exchange between the upper and lower mantle: the evolving convection regime of the Earth. *Earth Planet. Sci. Lett.* **150,** 1-6

Allegre C J, Brevart O, Dupre B, Minster J F 1980 Isotopic and chemical effects produced in a continuously differentiating convecting Earth mantle. *Phil. Trans. R. Soc. Lond. A* **297,** 447-477

Allegre C J, Hart S R, Minster J F 1983a Chemical structure and evolution of the mantle and continents determined by inversion of Nd and Sr isotopic data. I. Theoretical methods. *Earth and Planetary Science Letters* **66,** 177-90

Allegre C J, Hofmann A, O'Nions K 1996 The argon constraints on mantle structure. *Geophys. Res. Lett.* **23,** 3555-3557

Allegre C J, Lewin E 1995 Isotopic Systems and Stirring Times Of the Earths Mantle. *Earth and Planetary Science Letters* **136,** 629-646

Allegre C J, Moreira M, Staudacher T 1995 $^{4}He/^{3}He$ Dispersion and Mantle Convection. *Geophysical Research Letters* **22,** 2325-2328

Allegre C J, Sarda P, Staudacher T 1993 Speculations About the Cosmic Origin Of He and Ne In the Interior Of the Earth. *Earth and Planetary Science Letters* **117,** 229-233

Allegre C J, Staudacher T, Sarda P, Kurz M D 1983b Constraints on evolution of Earth's mantle from rare gas systematics. *Nature* **303,** 762-766

Allegre C J, Turcotte D L 1986 Implications of a 2-component marble-cake mantle. *Nature* **323,** 123-127

Anderson D L 1993 He-3 From the Mantle - Primordial Signal or Cosmic Dust. *Science* **261,** 170-176

Anderson D L 1995 Lithosphere, Asthenosphere, and Perisphere. *Reviews Of Geophysics* **33,** 125-149

Anderson D L 1998 A Model to Explain the Various Paradoxes Associated with Mantle Noble Gas Geochemistry. *Proceedings of the National Academy of Sciences of the United States of America* **95,** 9087-9092

Anderson D L 2000 The statistics of helium isotopes along the global spreading ridge system and the central limit theorum. *Geophys. Res. Lett.* **27,** 77-82

Anderson D L 2001 A statistical test of the two reservoir model for helium isotopes. *Earth Planet. Sci. Lett.* **193,** 77-82

Anderson O L, Oda H, Isaak D 1992 A model for the computation of thermal expansivity at high compression and high temperatures - MgO as an example. *Geophys. Res. Lett.* **19,** 1987-1990

Arcay D, Tric E, Doin M-P 2005 Numerical simulations of subduction zones. Effect of slab dehydration on the mantle wedge dynamics. *Phys. Earth Planet. Int.* **149,** 133-153

Armstrong R L, Hein S M 1973 Computer simulation of Pb and Sr isotope evolution of the Earth's crust and upper mantle. *Geochim. Cosmochim. Acta* **37,** 1-18

Asimow P D, Hirschmann M M, Stolper E M 2001 Calculation of peridotite partial melting from thermodynamic models of minerals and melts, IV. Adiabatic decompression and the composition and mean properties of mid-ocean ridge basalts. *Journal of Petrology* **42,** 963-998

Ballentine C J 2002 Geochemistry - Tiny tracers tell tall tales. *Science* **296,** 1247-1248

Ballentine C J, Barford D N 2000 The origin of air-like noble gases in MORB and OIB. *Earth Planet. Sci. Lett.* **180,** 39-48

Ballentine C J, Marty B, Lollar B S, Cassidy M 2005 Nean isotopes constrain convection and volatile origin in the Earth's mantle. *Nature* **433,** 33-38

Ballentine C J, van Keken P E, Porcelli D, Hauri E H 2002 Numerical models, geochemistry and the zero-paradox noble-gas mantle. *Philosophical Transactions of the Royal Society of London Series A-Mathematical Physical & Engineering Sciences* **360,** 2611-2631

Barth M G, Rudnick R L, Horn I, McDonough W F, Spicuzza M J, Valley J W, Haggerty S E 2001 Geochemistry of xenolithic eclogites from west Africa, part I: A link between low MgO eclogites and Archean crust formation. *Geochim. Cosmochim. Acta* **65,** 1499-1527

Batchelor G K 1952 The effect of homogeneous turbulence on material lines and surfaces. *Proc. R. Soc. A.* **213,** 349-366

Batchelor G K 1959 Small-scale variation of convected quantities like temperature in a turbulent fluid. *J. Fluid Mech.* **5,** 113-133

Becker T W, Kellogg J B, O'Connell R J 1999 Thermal constraints on the survival of primitive blobs in the lower mantle. *Earth Planet. Sci. Lett.* **171,** 351-365

Benz W, Cameron A G W 1990 Terrestrial effects of the giant impact. In: Newsom H E, Jones J H (eds.) *Origin of the Earth*. Oxford University Press,New York,61-68

Bercovici D, Karato S 2003 Whole-mantle convection and the transition-zone water filter. *Nature* **425,** 39-44

Boehler R, Chopelas A, Zerr A 1995 Temperature and Chemistry Of the Core-Mantle Boundary. *Chemical Geology* **120,** 199-205

Bolton H, Masters G 2001 Travel times of P and S from the global digital seismic networks: Implications for the relative variation of P and S velocity in the mantle. *Journal of Geophysical Research-Solid Earth* **106,** 13527-13540

Boyet M, Carlson R W 2006 A new geochemical model for the Earth's mantle inferred from ^{146}Sm-^{142}Nd systematics. *Earth Planet. Sci. Lett.* **250,** 254-268

Brandon A, Snow J E, Walker R J, Morgan J W, Mock T D 2000 ^{190}Pt-^{186}Os and ^{187}Re-^{187}Os systematics of abyssal peridotites. *Earth Planet. Sci. Lett.* **177,** 319-335

Brandon A D, Walker R J 2005 The debate over core-mantle interaction. *Earth Planet. Sci. Lett.* **232,** 211-225

Brandon A D, Walker R J, Morgan J W, Norman M D, Prichard H M 1998 Coupled 186Os and 187Os evidence for core-mantle interaction. *Science* **280,** 1570-1573

Brandon A D, Walker R J, Puchtel I S, Becker H, Humayun M, Revillon S 2003 186Os-187Os systematics of Gorgona Island komatiites: implications for early growth of the inner core. *Earth Planet. Sci. Lett.* **206,** 411-426

Buffett B A, Huppert H E, Lister J R, Woods A W 1992 Analytical Model For Solidification Of the Earths Core. *Nature* **356,** 329-331

Buffett B A, Huppert H E, Lister J R, Woods A W 1996 On the thermal evolution of the Earth's core. *Journal of Geophysical Research* **101,** 7989-8006

Bunge H P, Richards M A, Baumgardner J R 1997 A sensitivity study of 3-dimensional spherical mantle convection at 10^8 Rayleigh number - Effects of depth-dependent viscosity, heating mode, and an endothermic phase change. *J. Geophys. Res.* **102,** 11991-12007

Bunge H P, Richards M A, Lithgowbertelloni C, Baumgardner J R, Grand S P, Romanowicz B A 1998 Time Scales and Heterogeneous Structure in Geodynamic Earth Models. *Science* **280,** 91-95

Caffee M W, Hudson G B, Velsko C, Huss G R, Alexander E C, Chivas A R 1999 Primordial noble gases from Earth's mantle: Identification of a primitive volatile component. *Science* **285,** 2115-2118

Carlson R W 1987 Geochemical evolution of the crust and mantle. *Rev. Geophys.* **25,** 1011-1020

Carlson R W 1994 Mechanisms Of Earth Differentiation - Consequences For the Chemical-Structure Of the Mantle. *Reviews Of Geophysics* **32,** 337-361

Castillo P 1988 The Dupal anomaly as a trace of the upwelling lower mantle. *Nature* **336,** 667-70

Castle J C, van der Hilst R D 2003a Searching for seismic scattering off mantle interfaces between 800 km and 2000 km depth. *J. Geophys. Res.* **108,** doi:10.1029/2001JB000286

Castle J C, van der Hilst R D 2003b Using ScP precursors to search for mantle structures beneath 1800 km depth. *Geophys. Res. Lett.* **30,** doi:10.1029/2002GL016023

Castro M C, Patriarche D, Goblet P 2005 2-D numerical simulations of groundwater flow, heat transfer and 4He transport - implications for the He terrestrial budget and the mantle helium-heat imbalance. *Earth Planet. Sci. Lett.* **237,** 893-910

Chase C G 1981 Oceanic island Pb: Two-stage histories and mantle evolution. *Earth Planet. Sci. Lett.* **52,** 277-284

Chase C G, Patchett P J 1988 Stored mafic/ultramafic crust and early Archean mantle depletion. *Earth Planet. Sci. Lett.* **91,** 66-72

Chauvel C S, Goldstein S L, Hofmann A W 1995 Hydration and dehydration of oceanic crust controls Pb evolution in the mantle. *Chem. Geol.* **126,** 65-75

Chopelas A 1996 Thermal Expansivity Of Lower Mantle Phases Mgo and Mgsio3 Perovskite At High-Pressure Derived From Vibrational Spectroscopy. *Physics Of the Earth and Planetary Interiors* **98,** 3-15

Christensen U 1984 Instability of a hot boundary layer and initiation of thermo-chemical plumes. *Annales Geophysicae* **2,** 311-319

Christensen U 1988 Is subducted lithosphere trapped at the 670-km discontinuity? *Nature* **336,** 462-463

Christensen U 1989a Mixing by time-dependent convection. *Earth Planet. Sci. Lett.* **95,** 382-394

Christensen U 1990 Mixing By Time-Dependent Mantle Convection - Reply. *Earth and Planetary Science Letters* **98,** 408-410

Christensen U R 1989b Models of mantle convection - one or several layers. *Phil. Trans. R. Soc. London A* **328,** 417-424

Christensen U R 1997 Influence of chemical buoyancy on the dynamics of slabs in the transition zone. *J. Geophys. Res.* **102,** 22435-22433

Christensen U R, Hofmann A W 1994 Segregation of subducted oceanic crust In the convecting mantle. *J. Geophys. Res.* **99,** 19867-19884

Christensen U R, Yuen D A 1984 The Interaction Of a Subducting Lithospheric Slab With a Chemical or Phase-Boundary. *Journal Of Geophysical Research* **89,** 4389-4402

Christensen U R, Yuen D A 1985 Layered convection induced by phase transitions. *J. Geophys. Res.* **90,** 10291-10300

Chudinovskikh L, Boehler R 2002 The MgSi)3 Ilmenite-Perovskite phase boundary: Evidence for strongly negative Clapeyron slope.

Cizkova H, Cadek O, Van Den Berg A P, Vlaar N J 1999 Can lower mantle slab-like seismic anomalies be explained by thermal coupling between the upper and lower mantles? *Geophys. Res. Lett. (USA)* **26,** 1501-4

Class C, Goldstein S L 2005 Evolution of helium isotopes in the Earth's mantle. *Nature* **436,** 1107-1112

Coltice N 2005 The role of convective mixing in degassing the Earth's mantle. *Earth Planet. Sci. Lett.* **234,** 15-25

Coltice N, Albarède F, Gillet P 2000a ^{40}K-^{40}Ar constraints on recycling continental crust into the mantle. *Science* **288,** 845-7

Coltice N, Ferrachat S, Ricard Y 2000b Box modeling the chemical evolution of geophysical systems: case study of the Earth's mantle. *Geophys. Res. Lett.* **27,** 1579-1582

Coltice N, Ricard Y 1999 Geochemical observations and one layer mantle convection. *Earth Planet. Sci. Lett.* **174,** 125-37

Coltice N, Ricard Y 2002 On the origin of noble gases in mantle plumes. *Philosophical Transactions of the Royal Society of London Series A-Mathematical Physical & Engineering Sciences* **360,** 2633-2648

Coltice N, Schmalzl J 2006 Mixing times in the mantle of the early Earth derived from 2-D and 3-D numerical simulations of convection. *Geophys. Res. Lett.* **33,** doi:10.1029/2006GL027707

Corrsin S 1961 The reactant concentration spectrum in turbulent mixing with a first order reaction. *J. Fluid Mech.* **11,** 407-416

Creager K C, Jordan T H 1984 Slab Penetration Into the Lower Mantle. *Journal Of Geophysical Research* **89,** 3031-3049
Creager K C, Jordan T H 1986 Slab Penetration Into the Lower Mantle Beneath the Mariana and Other Island Arcs Of the Northwest Pacific. *Journal Of Geophysical Research Solid Earth and Planets* **91,** 3573-Continues
Cserepes L, Rabinowicz M 1985 Gravity and Convection In a 2-Layer Mantle. *Earth Planet. Sci. Lett.* **76,** 193-207
Cserepes L, Rabinowicz M, Rosembergborot C 1988 3-Dimensional Infinite Prandtl Number Convection In One and 2 Layers With Implications For the Earths Gravity-Field. *Journal Of Geophysical Research Solid Earth and Planets* **93,** 12009-12025
Davaille A 1999a Simultaneous generation of hotspots and superswells by convection in a heterogeneous planetary mantle. *Nature* **402,** 756-60
Davaille A 1999b Two-layer thermal convection in miscible viscous fluids. *J. Fluid Mech.* **379,** 223-53
Davaille A, Girard F, Le B M 2002 How to anchor hotspots in a convecting mantle? *Earth & Planetary Science Letters* **203,** 621-34
Davies G F 1980 Thermal histories of convective Earth models and constraints on radiogenic heat production in the Earth. *J. Geophys. Res.* **85,** 2517-2530
Davies G F 1981 Earth's neodynium budget and structure and evolution of the mantle. *Nature* **290,** 208-213
Davies G F 1983 Viscosity Structure Of a Layered Convecting Mantle. *Nature* **301,** 592-594
Davies G F 1984 Geophysical and isotopic constraints on mantle convection - an interim synthesis. *J. Geophys. Res.* **89,** 6017-6040
Davies G F 1988 Ocean Bathymetry and Mantle Convection.1. Large-Scale Flow and Hotspots. *Journal Of Geophysical Research Solid Earth and Planets* **93,** 10467-10480
Davies G F 1990 Heat and mass transport in the early Earth. In: Newsome H E, Jones J H (eds.) *Origin of the Earth*. Oxford University Press,New York,175-194
Davies G F 1992 On the Emergence Of Plate-Tectonics. *Geology* **20,** 963-966
Davies G F 1999 Geophysically constrained mantle mass flows and the ^{40}Ar budget: a degassed lower mantle? *Earth Planet. Sci. Lett.* **166**
Davies G F 2002 Stirring geochemistry in mantle convection models with stiff plates and slabs. *Geochem. Cosmochem. Acta* **66,** 3125-3142
Davies G F 2006 Depletion of the ealy Earth's upper mantle and the viability of early plate tectonics. *Earth Planet. Sci. Lett.* **243,** 376-382
Davies G F, Gurnis M 1986 Interaction of mantle dregs with convection - lateral heterogeneity at the core-mantle boundary. *Geophys. Res. Lett.* **13,** 1517-1520
Delano J W 2001 Redox history of the Earth's interior since similar to 3900 Ma: Implications for prebiotic molecules [Review]. *Origins of Life & Evolution of the Biosphere* **31,** 311-341
Deparis V, Legros H, Ricard Y 1995 Mass anomalies due to subducted slabs and simulations of plate motion since 200 My. *Phys. Earth Planet. Inter.* **89,** 271-80
Deschamps F, Trampert J, Tackley P J 2005 Thermo-chemical structure of the lower mantle: seismological evidence and consequences for geodynamics. In: Yuen D A, Maruyama S, Karato S I, Windley B F (eds.) *Superplume: Beyond Plate Tectonics*. Springersubmitted
Dixon E T, Honda M, McDougall I, Campbell I H, Sigurdsson I 2000 Preservation of near-solar isotopic ratios in Icelandic basalts. *Earth Planet. Sci. Lett.* **180,** 309-324
Drake M J, Righter K 2002 Determining the composition of the Earth [Review]. *Nature* **416,** 39-44
du Vignaux N M, Fleitout L 2001 Stretching and mixing of viscous blobs in Earth's mantle. *Journal of Geophysical Research-Solid Earth* **106,** 30893-30908
Dubrovinsky L, Annersten H, Dubrovinskaia N, Westman F, Harryson H, Fabrichnaya O, Carlson S 2001 Chemical interaction of Fe and Al_2O_3 as a source of heteroeneity at the Earth's core-mantle boundary. *Nature* **412,** 527-529

Dubrovinsky L, Dubrovinskaia N, Langenhorst F, Dobson D, Rubie D, Gessmann C, Abrikosov I A, Johansson B, Baykov V I, Vitos L, Le B T, Crichton W A, Dmitriev V, Weber H P 2003 Iron-silica interaction at extreme conditions and the electrically conducting layer at the base of Earth's mantle. *Nature* **421,** 58-61
Dupeyrat L, Sotin C, Parmentier E M 1995 Thermal and chemical convection in planetary mantles. *Journal of Geophysical Research, B, Solid Earth and Planets* **100**. 497-520
Dupre B, Allegre C J 1983 Pb-Sr variation in Indian Ocean basalts and mixing phenomena. *Nature* **303,** 142-146
Elliott T, Zindler A, Bourdon B 1999 Exploring the kappa conundrum: the role of recycling in the lead isotope evolution of the mantle. *Earth & Planetary Science Letters* **169,** 129-145
Farley K A, Natland J H, Craig H 1992 Binary Mixing Of Enriched and Undegassed (Primitive?) Mantle Components (He, Sr, Nd, Pb) In Samoan Lavas. *Earth and Planetary Science Letters* **111,** 183-199
Farley K A, Neroda E 1998 Noble gases in the Earth's mantle. *Annual Review of Earth & Planetary Sciences* **26,** 189-218
Farnetani C G 1997 Excess Temperature Of Mantle Plumes - the Role Of Chemical Stratification Across D". *Geophysical Research Letters* **24,** 1583-1586
Farnetani C G, Legras B, Tackley P J 2002 Mixing and deformations in mantle plumes. *Earth and Planetary Science Letters* **196,** 1-15
Farnetani C G, Samuel H 2003 Lagrangian structures and stirring in the Earth's mantle. *Earth and Planetary Science Letters* **206,** 335-348
Farnetani C G, Samuel H 2005 Beyond the thermal plume paradigm. *Geophys. Res. Lett.* **32,** doi:10.1029/2005GL022360
Farnetani D G, Richards M A 1995 Thermal Entrainment and Melting In Mantle Plumes. *Earth and Planetary Science Letters* **136,** 251-267
Ferrachat S, Ricard Y 1998 Regular vs. chaotic mantle mixing. *Earth Planet. Sci. Lett.* **155,** 75-86
Ferrachat S, Ricard Y 2001 Mixing properties in the Earth's mantle: Effects of the viscosity stratification and of oceanic crust segregation. *Geochem. Geophys. Geosyst.* **Volume 2,** Paper number 2000GC000092 [7490 words, 10 figures, 2 animations, 1 table]
Fleitout L, Mambole A, Christensen U 2000 Phase changes around 670 km depth and segregation in the Earth's mantle. *EOS Trans. AGU, Fall Meeting Suppl.* **81,** Abstract T12E-11
Forte A M, Mitrovica J X 2001 Deep-mantle high-viscosity flow and thermochemical structure inferred from seismic and geodynamic data. *Nature* **410,** 1049-56
Fukao Y 1992 Seismic Tomogram Of the Earths Mantle - Geodynamic Implications. *Science* **258,** 625-630
Fukao Y, Obayashi M, Inoue H, Nenbai M 1992 Subducting Slabs Stagnant In the Mantle Transition Zone. *Journal Of Geophysical Research-Solid Earth* **97,** 4809-4822
Gable C W, O'Connell R J, Travis B J 1991 Convection in 3 dimensions with surface plates - Generation of toroidal flow. *J. Geophys. Res.* **96,** 8391-8405
Gaherty J B, Hager B H 1994 Compositional Vs Thermal Buoyancy and the Evolution Of Subducted Lithosphere. *Geophysical Research Letters* **21,** 141-144
Galer S J G, O'Nions R K 1986 Magmagenesis and the mapping of chemical and isotopic variations in the mantle. *Chem. Geol.* **56,** 45-61
Gerya T V, Yuen D A 2003 Rayleigh-Taylor instabilities from hydration and melting propel `cold plumes' at subduction zones. *Earth & Planetary Science Letters* **212,** 47-62
Glatzmaier G A, Schubert G 1993 3-Dimensional Spherical-Models Of Layered and Whole Mantle Convection. *J. Geophys. Res.* **98,** 21969-21976
Goarant F, Guyot F, Peyronneau J, Poirier J P 1992 High-pressure and high-temperature reactions between silicates and liquid iron alloys, in the diamond anvil cell, studied by analytical electron microscopy. *J. Geophys. Res.* **97,** 4477-4487
Gonnermann H M, Manga M, Jellinek A M 2002 Dynamics and longevity of an initially stratified mantle - art. no. 1399. *Geophysical Research Letters* **29,** 1399

Graham D, Lupton J, Albarède F, Condomines M 1990 Extreme temporal homogeneity of Helium isotopes at Piton de la Fournaise, Reunion Island. *Nature* **347,** 545-548

Graham D W 2002 Noble gas isotope geochemistry of mid-ocean ridge and ocean island basalts; characterizazion of mantle source reservoirs. In: Porcelli D, Wieler R, Ballentine C J (eds.) *Noble Gases in Geochemistry and Cosmochemistry, Reviews in Mineralogy and Geochemistry*. Mineral. Soc. Amer.,Washington, D. C.,247-318

Graham D W, Blichert-Toft J, Russo C J, Rubin K H, Albarède F 2006 Cryptic striations in the upper mantle revealed by hafnium isotopes in southest Indian ridge basalts. *Nature* **440,** 199-202

Graham D W, Lupton J E, Spera F J, Christle D M 2001 Upper-mantle dynamics revealed by helium isotope variations along the Southeast Indian Ridge. *Nature* **409,** 701-3

Grand S P 1994 Mantle Shear Structure Beneath the America and Surrounding Oceans. *Journal Of Geophysical Research-Solid Earth* **99,** 11591-11621

Griffiths R W 1986 Dynamics of mantle thermals with constant buoyancy or anomalous internal heating. *Earth and Planetary Science Letters* **78,** 435-446

Guignot N, Andrault D 2004 Equations of state of Na-K-Al host phases and implications for MORB density in the lower mantle. *Phys. Earth Planet. Int.* **143-144,** 107-128

Gurnis M 1986a The effects of chemical density differences on convective mixing in the Earth's mantle. *J. Geophys. Res.* **91,** 1407-1419

Gurnis M 1986b Quantitative Bounds On the Size Spectrum Of Isotopic Heterogeneity Within the Mantle. *Nature* **323,** 317-320

Gurnis M 1986c Stirring and Mixing In the Mantle By Plate-Scale Flow - Large Persistent Blobs and Long Tendrils Coexist. *Geophysical Research Letters* **13,** 1474-1477

Gurnis M, Davies G F 1986a The effect of depth-dependent viscosity on convective mixing in the mantle and the possible survival of primitive mantle. *Geophys. Res. Lett.* **13,** 541-544

Gurnis M, Davies G F 1986b Mixing In Numerical-Models Of Mantle Convection Incorporating Plate Kinematics. *Journal Of Geophysical Research Solid Earth and Planets* **91,** 6375-6395

Hager B H, Clayton R W, Richards M A, Comer R P, Dziewonski A M 1985 Lower Mantle Heterogeneity, Dynamic Topography and the Geoid. *Nature* **313,** 541-546

Hager B H, Richards M A 1989 Long-wavelength variations in Earths geoid - Physical models and dynamical implications. *Phil. Trans. R. Soc. London A* **328,** 309-327

Hanan B B, Graham D W 1996 Lead and helium isotope evidence from oceanic basalts for a common deep source of mantle plumes. *Science* **272,** 991-995

Hansen U, Yuen D A 1988 Numerical simulations of thermal-chemical instabilities at the core mantle boundary. *Nature* **334,** 237-240

Hansen U, Yuen D A 1989 Dynamical influences from thermal-chemical instabilities at the core-mantle boundary. *Geophys. Res. Lett.* **16,** 629-632

Hansen U, Yuen D A 2000 Extended-Boussinesq thermal-chemical convection with moving heat sources and variable viscosity. *Earth and Planetary Science Letters* **176,** 401-11

Harrison D, Burnard P, Turner G 1999 Noble gas behaviour and composition in the mantle: constraints from the Iceland plume. *Earth Planet. Sci. Lett.* **171,** 199-207

Harrison T M, Blichert-Toft J, Mueller W, Albarade F, Holden P, Mojzsis S J 2005 Heterogeneous hadean hafnium: Evidence of continental crust at 4.4 to 4.5 Gyr. *Science* **310,** 1947-1950

Hart S R 1984 A large-scale isotope anomaly in the Southern Hemisphere mantle. *Nature* **309,** 753-7

Hart S R, Hauri E H, Oschmann J A, Whitehead J A 1992 Mantle plumes and entrainment: isotopic evidence. *Science* **256,** 517-520

Hauri E 2002 SIMS analysis of volatiles in silicate glasses: 2. Isotopes and abundances in Hawaiian melt inclusions. *Chem. Geol.* **183,** 115-141

Hauri E H, Whitehead J A, Hart S R 1994 Fluid Dynamic and Geochemical Aspects Of Entrainment In Mantle Plumes. *Journal Of Geophysical Research Solid Earth* **99,** 24275-24300

Hedlin M A H, Shearer P M 2000 An analysis of large-scale variations in small-scale mantle heterogeneity using global seismographic network recordings of precursors to PKP. *Journal of Geophysical Research* **105,** 13655-73

Hedlin M A H, Shearer P M, Earle P S 1997 Seismic evidence for small-scale heterogeneity throughout the Earth's mantle. *Nature* **387,** 145-150

Helffrich G R, Wood B J 2001 The Earth's mantle [Review]. *Nature* **412,** 501-507

Hilton D R, Fischer T P, Marty B 2002 Noble gases and volatile recycling at subduction zones. *Rev. Mineral. Geochem.* **47,** 319-370

Hilton D R, Gronvold K, Macpherson C G, Castillo P R 1999 Extreme 3He/4He ratios in northwest Iceland: Constraining the common component in mantle plumes. *Earth Planet. Sci. Lett.* **173,** 53-60

Hilton D R, Porcelli D 2003 Noble gases as mantle tracers. In: Carlson R W (ed.) *Treatise on Geochemistry, Vol 2: The mantle and core*. Elsevier,Amsterdam,277-318

Hirose K, Kushiro I 1993 Partial melting of dry peridotites at high pressures: Determination of compositions of melts segregated from peridotite using aggregates of diamond. *Earth Planet. Sci. Lett.* **114,** 477-489

Hirose K, Shimizu N, van Westeren W, Fei Y 2004 Trace element partitioning in Earth's lower mantle and implications for geochemical consequences of partial melting at the core-mantle boundary.

Hirose K, Takafuji N, Sata N, Ohishi Y 2005 Phase transition and density of subducted MORB crust in the lower mantle. *Earth Planet. Sci. Lett.* **237,** 239-251

Hirschmann M 2006a A wet mantle conductor? *Nature* **439,** E3

Hirschmann M M 2006b Water, melting, and the deep Earth H_2O cycle. *Ann. Rev. Earth Planet. Sci.* **34,** 629-653

Hirschmann M M, Asimow P D, Ghiorso M S, Stolper E M 1999 Calculation of peridotite partial melting from thermodynamic models of minerals and melts. III. Controls on isobaric melt production and the effect of water on melt production. *Journal of Petrology* **40,** 831-851

Hirth G, Kohlstedt D L 1996 Water in the Oceanic Upper-Mantle - Implications For Rheology, Melt Extraction and the Evolution of the Lithosphere. *Earth and Planetary Science Letters* **144,** 93-108

Hoffman N R A, McKenzie D P 1985 The Destruction Of Geochemical Heterogeneities By Differential Fluid Motions During Mantle Convection. *Geophysical Journal Of the Royal Astronomical Society* **82,** 163-206

Hofmann A W 1988 Chemical differentiation of the Earth: The relationship between mantle, continental crust, and oceanic crust. *Earth Planet. Sci. Lett.* **90,** 297-314

Hofmann A W 1997 Mantle geochemistry: the message from oceanic volcanism. *Nature* **385,** 219-29

Hofmann A W 2003 Sampling mantle heterogeneity through oceanic basalts: Isotopes and trace elements. In: Carlson R W (ed.) *Treatise on Geochemistry*. Elsevier61-101

Hofmann A W, Hart S R 1978 An assessment of local and regional isotopic equilibrium in the mantle. *Earth Planet. Sci. Lett.* **38,** 44-62

Hofmann A W, White W M 1982 Mantle Plumes From Ancient Oceanic-Crust. *Earth and Planetary Science Letters* **57,** 421-436

Hoink T, Schmalzl J, Hansen U 2006 Dynamics of metal-silicate separation in a terrestrial magma ocean. *Geochem. Geophys. Geosyst.* **7,** doi:10.1029/2006GC001268

Holland G, Ballentine C J 2006 Seawater subduction controls the heavy noble gas composition of the mantle. *Nature* **441,** 186-191

Holland H D 1984 *The chemical evolution of the atmosphere and oceans*, Princeton Univ. Press, Princeton, N. J.

Holland H D 1994 Early Proterozoic atmospheric change. In: Bengtson S (ed.) *Early life on Earth*. Columbia University Press,New York,237-244

Honda M, McDougall I, Patterson D B, Doulgeris A, Clague D A 1999 Noble gases in submarine pillow basalt glasses from Loihi and Kilauea, Hawaii: A solar component in the Earth. *Geochem. Cosmochem. Acta* **57,** 859-874

Hopp J, Trieloff M 2005 Refining the noble gas record of the Reunion mantle plume source: Implications on mantle geochemistry. *Earth Planet. Sci. Lett.* **240,** 573-588

Huang X, Xu Y, Karato S 2005 Water content in the transition zone from electrical conductivity of wadsleyite and ringwoodite. *Nature* **434,** 746-749

Huang X, Xu Y, Karato S 2006 A wet mantle conductor? Reply. *Nature* **439,** E3-E4

Humayun M, Qin L, Norman M D 2004 Geochemical evidence for excess iron in the mantle beneath Hawaii. *Science* **306,** 91-94

Hunt D L, Kellogg L H 2001 Quantifying mixing and age variations of heterogeneities in models of mantle convection: Role of depth-dependent viscosity. *J. Geophys. Res.* **106,** 6747-6760

Irifune T, Ringwood A E 1993 Phase-Transformations In Subducted Oceanic-Crust and Buoyancy Relationships At Depths Of 600-800 Km In the Mantle. *Earth and Planetary Science Letters* **117,** 101-110

Ishii M, Tromp J 1999 Normal-mode and free-air gravity constraints on lateral variations in velocity and density of Earth's mantle. *Science* **285,** 1231-5

Ito G, Mahoney J J 2005a Flow and melting of a heterogeneous mantle: 1.Method and importance to the geochemistry of ocean island and mid-ocean ridge basalts. *Earth Planet. Sci. Lett.* **230,** 29-46

Ito G, Mahoney J J 2005b Flow and melting of a heterogeneous mantle: 2. Implications for a chemically nonlayered mantle. *Earth Planet. Sci. Lett.* **230,** 47-63

Ito G, Mahoney J J 2006 Melting a high $^{3}He/^{4}He$ source in a heterogeneous mantle. *Geochem. Geophys. Geosyst.* **7,** Q05010, doi:10.1029/2005GC001158

Jacobsen S B, Wasserburg G J 1979 The mean age of mantle and crustal reservoirs. *J. Geophys. Res.* **84,** 7411-7427

Jellinek A M, Manga M 2002 The influence of a chemical boundary layer on the fixity and lifetime of mantle plumes. *Nature* **418,** 760-763

Jochum K, Hofmann A W, Ito E, Seufert H M, White W M 1983 K, U and Th in mid-ocean ridge basalt glasses and heat production, K/U and K/Rb in the mantle. *Nature* **306,** 431-436

Jordan T H, Puster P, Glatzmaier G A, Tackley P J 1993 Comparisons between seismic Earth structures and mantle flow models based on radial correlation functions. *Science* **261,** 1427-1431

Kameyama M, Fujimoto H, Ogawa M 1996 A thermo-chemical regime in the upper mantle in the early Earth inferred from a numerical model of magma-migration in a convecting upper mantle. *Physics of the Earth and Planetary Interiors* **94,** 187-215

Kanda R V S, Stevenson D J 2006 Suction mechanism for iron entrainment into the lower mantle. *Geophys. Res. Lett.* **33,** doi:10.1029/2005GL025009

Kaneshima S, Helffrich G 1999 Dipping low-velocity layer in the mid-lower mantle:Evidence for geochemical heterogeneity. *Science* **283,** 1888-1891

Karato S 1995 Interaction Of Chemically Stratified Subducted Oceanic Lithosphere With the 660 Km Discontinuity. *Proceedings Of the Japan Academy Series B Physical and Biological Sciences* **71,** 203-207

Karato S, Bercovici D, Leahy G, Richard G, Jing Z 2006 The transition zone water filter model for global material circulation: where do we stand? In: Jacobsen S D, Van Der Lee S (eds.) *Earth's Deep Water Cycle, AGU Monograph Series, 168.* American Geophysical Union289-314

Karato S, Murthy V R 1997 Core Formation and Chemical-Equilibrium In the Earth.1. Physical Considerations. *Physics Of the Earth and Planetary Interiors* **100,** 61-79

Karato S, Wang Z C, Liu B, Fujino K 1995 Plastic-Deformation Of Garnets - Systematics and Implications For the Rheology Of the Mantle Transition Zone. *Earth and Planetary Science Letters* **130,** 13-30

Karato S, Wu P 1993 Rheology of the upper mantle - a synthesis. *Science* **260,** 771-778

Kasting J F, Eggler D H, Raeburn S P 1993a Mantle redox evolution and the oxidation state of the Archean atmosphere. *J. Geol* **101,** 245-257

Kasting J F, Whitmore D P, Reynolds R T 1993b Habitable zones around main sequence stars. *Icarus* **101,** 108-28

Kellogg J B (2004) Towards and understanding of chemical and isotopic heterogeneity in the Earth's mantle. Cambridge, Massachussetts, Harvard University

Kellogg J B, Jacobsen S B, O'Connell R J 2002 Modeling the distribution of isotopic ratios in geochemical reservoirs. *Earth and Planetary Science Letters* **204,** 183-202

Kellogg J B, Tackley P J 2004 A comparison of methods for modeling geochemical variability in the Earth's mantle. *EOS Trans. AGU, Fall Meeting Suppl.* **85,** Abstract U41A-0728

Kellogg L H 1997 Growing the Earth's D" layer: Effect of density variations at the core-mantle boundary. *Geophys. Res. Lett.* **24,** 2749-2752

Kellogg L H, Hager B H, van der Hilst R D 1999 Compositional stratification in the deep mantle. *Science* **283,** 1881-4

Kellogg L H, Stewart C A 1991 Mixing By Chaotic Convection In an Infinite Prandtl Number Fluid and Implications For Mantle Convection. *Physics Of Fluids a Fluid Dynamics* **3,** 1374-1378

Kellogg L H, Turcotte D L 1986 Homogenization of the mantle by convective mixing and diffusion. *Earth Planet. Sci. Lett.* **81,** 371-378

Kellogg L H, Turcotte D L 1990 Mixing and the Distribution Of Heterogeneities In a Chaotically Convecting Mantle. *Journal Of Geophysical Research Solid Earth and Planets* **95,** 421-432

Kellogg L H, Wasserburg G J 1990 The Role Of Plumes In Mantle Helium Fluxes. *Earth and Planetary Science Letters* **99,** 276-289

Kennett B L N, Widiyantoro S, Vanderhilst R D 1998 Joint Seismic Tomography For Bulk Sound and Shear-Wave Speed in the Earths Mantle. *Journal of Geophysical Research Solid Earth* **103,** 12469-12493

Kesson S E, Gerald J D F, Shelley J M 1998 Mineralogy and dynamics of a pyrolite lower mantle. *Nature* **393,** 252-255

Klein E M, Langmuir C H, Zindler A, Staudigel H, Hamelin H 1988 Isotope evidence of a mantle convection boundary at the Australian-Antarctic Discordance. *Nature* **333,** 623-9

Knittle E, Jeanloz R 1989 Simulating the core-mantle boundary - an experimental study of high-pressure reactions between silicates and liquid iron. *Geophys. Res. Lett.* **16,** 609-612

Knittle E, Jeanloz R 1991 Earths Core-Mantle Boundary - Results Of Experiments At High-Pressures and Temperatures. *Science* **251,** 1438-1443

Korenaga J 2003 Energetics of mantle convection and the fate of fossil heat. *Geophysical Research Letters* **30,** 1437

Kramers J D, Tolstikhin I N 1997 Two terrestrial lead isotope paradoxes, forward transport modelling, core formation and the history of the continental crust. *Chem. Geol.* **139,** 75-110

Kump L R, Kasting J F, Barley M E 2001 Rise of atmospheric oxygen and the "upside-down" Archean mantle. *Geochemistry Geophysics Geosystems* **2,** doi:10.1029/2000GC000114

Kurz M D, Jenkins W J, Hart S R, Clague D 1983 Helium isotopic variations in volcanic rocks from Loihi seamount and the island of Hawaii. *Earth Planet. Sci. Lett.* **66,** 388-406

Kyvalova H, Cadek O, Yuen D A 1995 Correlation analysis between subduction in the last 180 Myr and lateral seismic structure of the lower mantle: geodynamical implications. *Geophys. Res. Lett.* **22,** 1281-4

Labrosse S 2003 Thermal and magnetic evolution of the Earth's core. *Phys. Earth Planet. Int.* **140,** 127-143

Labrosse S, Poirier J P, Le Mouel J L 1997 On cooling of the Earth's core. *Physics of the Earth and Planetary Interiors* **99,** 1-17

Lassiter J C 2004 Role of recycled oceanic crust in the potassium and argon budget of the Earth: Toward a resolution of the "missing argon" problem. *Geochem. Geophys. Geosyst.* **5,** Q11012, doi:10.1029/2004GC000711

Lay T, Garnero E J 2004 Core-mantle boundary structures and processes. In: Sparks R S J, Hawkesworth C J (eds.) *The State of the Planet: Frontiers and Challenges in Geophysics*. AGU,Washington, D. C.,doi:10.1029/150GM04

Lay T, Garnero E J, Williams Q 2004 Partial melting in a thermo-chemical boundary layer at the base of the mantle. *Phys. Earth Planet. Int.* **146,** 441-467

Le Bars M, Davaille A 2002 Stability of thermal convection in two superimposed miscible viscous fluids. *Journal of Fluid Mechanics* **471,** 339-63

Le Bars M, Davaille A 2004a Large interface deformation in two-layer thermal convection of miscible viscous fluids. *Journal of Fluid Mechanics* **499,** 75-110

Le Bars M, Davaille A 2004b Whole layer convection in a heterogeneous planetary mantle. *Journal of Geophysical Research* **109,** 23 pp

Leahy G M, Bercovici D 2004 The influence of the transition zone water filter on convective circulation in the mantle. *Geophys. Res. Lett.* **31,** doi:10.1029/2004GL021206

Lecuyer C, Ricard Y 1999 Long-term fluxes and budget of ferric iron: implication for the redox states of the Earth's mantle and atmosphere. *Earth Planet. Sci. Lett.* **165,** 197-211

Lenardic A, Kaula W M 1993 A Numerical Treatment Of Geodynamic Viscous-Flow Problems Involving the Advection Of Material Interfaces. *Journal Of Geophysical Research-Solid Earth* **98,** 8243-8260

Lin S-C, Van Keken P E 2006a Dynamics of thermochemical plumes: 1. Plume formation and entrainment of a dense layer. *Geochem. Geophys. Geosyst.* **7,** doi:10.1029/2005GC001071

Lin S-C, Van Keken P E 2006b Dynamics of thermochemical plumes: 2. Complexity of plume structures and its implications for mapping of mantle plumes. *Geochem. Geophys. Geosyst.* **7,** doi:10.1029/2005GC001072

Lithgow-Bertelloni C, Richards M A, Ricard Y, O'Connell R J, Engebretson D C 1993 Toroidal-poloidal partitioning of plate motions since 120 Ma. *Geophys. Res. Lett.* **20,** 375-378

Luo S-N, Ni S, Helmberger D V 2001 Evidence for a sharp lateral variation of velocity at the core-mantle boundary from multipathed PKPab. *Earth and Planetary Science Letters* **189,** 155-64

Lyubetskaya T, Korenaga J 2007a Chemical composition of Earth's primitive mantle and its variance, 1, Method and results. *J. Geophys. Res.* **in press**

Lyubetskaya T, Korenaga J 2007b Chemical composition of Earth's primitive mantle and its variance, 2, Implications for global geodynamics. *J. Geophys. Res.* **in press**

Machetel P, Weber P 1991 Intermittent Layered Convection In a Model Mantle With an Endothermic Phase-Change At 670 Km. *Nature* **350,** 55-57

Malvern L E 1969 *Introduction to the mechanics of a continuous medium*, Prentice Hall, Englewood Cliffs, New Jersey

Mambole A, Fleitout L 2002 Petrological layering induced by an endothermic phase transition in the Earth's mantle - art. no. 2044. *Geophysical Research Letters* **29,** 2044

Manga M 1996 Mixing of heterogeneities in the mantle - Effect of viscosity differences. *Geophys. Res. Lett.* **23,** 403-406

Manga M, Jeanloz R 1996 Implications Of a Metal-Bearing Chemical-Boundary Layer In D" For Mantle Dynamics. *Geophysical Research Letters* **23,** 3091-3094

Martin H 1986 Effect of steeper archean geothermal gradient on geochemistry of subduction zone magmas. *Geology* **14,** 753-756

Masters G, Laske G, Bolton H, Dziewonski A 2000 The relative behavior of shear velocity, bulk sound speed, and compressional velocity in the mantle: Implications for chemical and thermal structure. In: Karato S, Forte a M, Liebermann R C, Masters G, Stixrude L (eds.) *Geophysical Monograph on Mineral Physics and Seismic Tomography fom the atomic to the global scale*. Americal Geophysical Union63-87

Matsuda J M S, Ozima M, Ito K, Ohtaka O, Ito E 1993 Noble gas partitioning between metal and silicate under high pressures. *Sience* **259,** 788-790

McDonough W F, Sun S-S 1995 The composition of the Earth. *Chem. Geol.* **120,** 223-253

McKenzie D 1979 Finite deformation during fluid flow. *Geophys. J. R. astr. Soc.* **58,** 689-715

McKenzie D, Onions R K 1992 Partial Melt Distributions From Inversion Of Rare-Earth Element Concentrations (J Petrol, Vol 32, Pg 1021, 1991). *Journal Of Petrology* **33,** 1453-1453

McNamara A K, Van Keken P E 2000 Cooling of the Earth: A parameterized convection study of whole versus layered models. *Geochem., Geophys., Geosys.* **Volume 1,** Paper number 2000GC000045 [7408 words, 5 figures, 3 tables]

McNamara A K, Zhong S 2004a The influence of thermochemical convection on the fixity of mantle plumes. *Earth Planet. Sci. Lett.* **222,** 485-500

McNamara A K, Zhong S 2004b Thermochemical structures within a spherical mantle: Superplumes or piles? *J. Geophys. Res.* **109,** doi:10.1029/2003JB00287

McNamara A K, Zhong S 2005 Thermochemical piles beneath Africa and the Pacific Ocean. *Nature* **437,** 1136-1139

Megnin C, Bunge H P, Romanowicz B, Richards M A 1997 Imaging 3-D Spherical Convection Models - What Can Seismic Tomography Tell Us About Mantle Dynamics. *Geophysical Research Letters* **24,** 1299-1302

Meibom A, Anderson D L 2004 The statistical upper mantle assemblage. *Earth & Planetary Science Letters* **217,** 123-139

Meibom A, Anderson D L, Sleep N H, Frei R, Chamberlain C P, Hren M T, Wooden J L 2003 Are high He-3/He-4 ratios in oceanic basalts an indicator of deep-mantle plume components? *Earth and Planetary Science Letters* **208,** 197-204

Meibom A, Sleep N H, Chamberlain C P, Coleman R G, Frei R, Hren M T, Wooden J L 2002 Re-Os isotopic evidence for long-lived heterogeneity and equilibration processes in the Earth's upper mantle. *Nature* **419,** 705-708

Meibom A, Sleep N H, Zahnle K, Anderson D L 2005 Models for noble gases in mantle geochemistry: Some observations and alternatives. *Plumes, Plates, and Paradigms, Spec. Pap. Geol. Soc. Am.* **388,** 347-363

Melosh H J 1990 Giant impacts and the thermal state of the early Earth. In: Newsom H E, Jones J H (eds.) *Origin of the Earth*. Oxford University Press,New York,

Metcalfe G, Bina C R, Ottino J M 1995 Kinematic Considerations For Mantle Mixing. *Geophysical Research Letters* **22,** 743-746

Michard A, Albarède F 1985 Hydrothermal uranium uptake at ridge crests. *Nature* **317,** 61-88

Montague N L, Kellogg L H 2000 Numerical models for a dense layer at the base of the mantle and implications for the geodynamics of D". *J. Geophys. Res.* **105,** 11101-11114

Montague N L, Kellogg L H, Manga M 1998 High Rayleigh number thermo-chemical models of a dense boundary layer in D". *Geophys. Res. Lett.* **25,** 2345-2348

Montelli R, Nolet G, Dahlen F A, Masters G, Engdahl E R, Hung S H 2004 Finite-frequency tomography reveals a variety of plumes in the mantle. *Science* **303,** 338-343

Moreira M, Breddam K, Curtice J, Kurz M D 2001 Solar nean in the Icelandic mantle: new evidence for an undegassed lower mantle. *Earth Planet. Sci. Lett.* **185,** 15-23

Moresi L, Solomatov V 1998 Mantle convection with a brittle lithosphere - Thoughts on the global tectonic styles of the Earth and Venus. *Geophys. J. Int.* **133,** 669-682

Muller R 1992 The Performance Of Classical Versus Modern Finite-Volume Advection Schemes For Atmospheric Modeling In a One-Dimensional Test-Bed. *Monthly Weather Review* **120,** 1407-1415

Murakami M, Hirose K, Kawamura K, Sata N, Ohishi Y 2004 Post-perovskite phase transition in $MgSiO_3$. *Science* **304,** 855-858

Murakami M, Hirose K, Sata N, Ohishi Y 2005 Post-perovskite phase transition and mineral chemistry in the pyrolitic lowermost mantle. *Geophys. Res. Lett.* **32,** doi:10.1029/2004GL021956

Murphy D T, Kamber B S, Collerson K D 2003 A refined solution to the first terrestrial Pb-isotope paradox. *J. Petrol.* **44,** 39-53

Murthy V R, Karato S 1997 Core Formation and Chemical-Equilibrium In the Earth.2. Chemical Consequences For the Mantle and Core. *Physics Of the Earth and Planetary Interiors* **100,** 81-95

Nakagawa T, Buffett B A 2005 Mass transport mechanism between the upper and lower mantle in numerical simulations of thermochemical mantle convection with multicomponent phase changes. *Earth Planet. Sci. Lett.* **230,** 11-27

Nakagawa T, Tackley P J 2004a Effects of a perovskite-post perovskite phase change near the core-mantle boundary on compressible mantle convection. *Geophys. Res. Lett.* **31, L16611,** doi:10.1029/2004GL020648

Nakagawa T, Tackley P J 2004b Effects of thermo-chemical mantle convection on the thermal evolution of the Earth's core. *Earth Planet. Sci. Lett.* **220,** 107-119

Nakagawa T, Tackley P J 2005a Deep mantle heat flow and thermal evolution of Earth's core in thermo-chemical multiphase models of mantle convection. *Geochem., Geophys., Geosys.* **6,** doi:10.1029/2005GC000967

Nakagawa T, Tackley P J 2005b The interaction between the post-perovskite phase change and a thermo-chemical boundary layer near the core-mantle boundary. *Earth Planet. Sci. Lett.* **238,** 204-216

Nakagawa T, Tackley P J 2005c Three-dimensional numerical simulations of thermo-chemical multiphase convection in Earth's mantle. *Proceedings of the Third MIT Conference on Computational Fluid and Solid Mechanics*

Namiki A 2003 Can the mantle entrain D"? *J. Geophys. Res.* **108,** doi:10.1029/2002JB002315

Newsom H E, White W M, Jochum K P, Hofmann A W 1986 Siderophile and chalcophile element abundances in oceanic basalts. *Earth Planet. Sci. Lett.* **80,** 299-313

Ni S, Tan E, Gurnis M, Helmberger D V 2002 Sharp sides to the African superplume. *Science* **296,** 1850-1852

Nimmo F, Price G D, Brodholt J, Gubbins D 2004 The influence of potassium on core and geodynamo evolution. *Geophys. J. Int.* **156,** 363-376

O'Nions R K, Evensen N M, Hamilton P J 1979 Geochemical modeling of mantle differentiation and crustal growth. *J. Geophys. Res.* **84,** 6091-6101

O'Nions R K, Oxburgh E R 1983 Heat and helium in the Earth. *Nature* **306,** 429

O'Nions R K, Tolstikhin I N 1996 Limits on the mass flux between lower and upper mantle and stability of layering. *Earth Planet. Sci. Lett.* **139,** 213-222

Oganov A R, Ono S 2004 Theoretical and experimental evidence for a post-perovskite phase of $MgSiO_3$ in Earth's D" layer. *Nature* **430,** 445-8

Ogawa M 1988 Numerical Experiments On Coupled Magmatism-Mantle Convection System - Implications For Mantle Evolution and Archean Continental Crusts. *Journal Of Geophysical Research Solid Earth and Planets* **93,** 15119-15134

Ogawa M 1993 A Numerical-Model Of a Coupled Magmatism Mantle Convection System In Venus and the Earths Mantle Beneath Archean Continental Crusts. *Icarus* **102,** 40-61

Ogawa M 1994 Effects Of Chemical Fractionation Of Heat-Producing Elements On Mantle Evolution Inferred From a Numerical-Model Of Coupled Magmatism Mantle Convection System. *Physics Of the Earth and Planetary Interiors* **83,** 101-127

Ogawa M 1997 A bifurcation in the coupled magmatism-mantle convection system and its implications for the evolution of the Earth's upper mantle. *Physics of the Earth and Planetary Interiors* **102,** 259-76

Ogawa M 2000a Coupled magmatism-mantle convection system with variable viscosity. *Tectonophysics* **322,** 1-18

Ogawa M 2000b Numerical models of magmatism in convecting mantle with temperature-dependent viscosity and their implications for Venus and Earth. *Journal of Geophysical Research* **105,** 6997-7012

Ogawa M 2003 Chemical stratification in a two-dimensional convecting mantle with magmatism and moving plates. *Journal of Geophysical Research* **108,** doi:10.1029/2002JB002205

Ogawa M, Nakamura H 1998 Thermochemical regime of the early mantle inferred from numerical models of the coupled magmatism-mantle convection system with the solid-solid phase transitions at depths around 660 km. *Journal of Geophysical Research* **103,** 12161-80

Oldham D, Davies J H 2004 Numerical investigation of layered convection in a three-dimensional shell with application to planetary mantles. *Geochem. Geophys. Geosyst.* **5,** doi:10.1029/2003GC000603

Olson P 1984 An Experimental Approach to Thermal-Convection In a 2-Layered Mantle. *J Geophys. Res.* **89,** 1293-1301

Olson P, Kincaid C 1991 Experiments on the interaction of thermal convection and compositional layering at the base of the mantle. *J. Geophys. Res.* **96,** 4347-4354

Olson P, Yuen D A, Balsiger D 1984a Convective Mixing and the Fine-Structure Of Mantle Heterogeneity. *Physics Of the Earth and Planetary Interiors* **36,** 291-304

Olson P, Yuen D A, Balsiger D 1984b Mixing Of Passive Heterogeneties By Mantle Convection. *Journal Of Geophysical Research* **89,** 425-436

Ono S, Ito E, Katsura T 2001 Mineralogy of subducted basaltic crust (MORB) from 25 to 37 GPa, and chemical heterogeneity of the lower mantle. *Earth Planet. Sci. Lett.* **190,** 57-63

Ono S, Oganov A R, Ohishi Y 2005a In situ observations of phase transition between perovskite and $CaIrO_3$-type phase in $MgSiO_3$ and pyrolitic mantle composition. *Earth Planet. Sci. Lett.* **236,** 914-932

Ono S, Oshishi Y, Isshiki M, Watanuki T 2005b In situ X-ray observations of phase assemblages in peridotite and basalt compositions at lower mantle conditions: Implications for density of subducted oceanic plate. *J. Geophys. Res.* **110,** doi:10.1029/2004JB0003196

Ottino J M 1989 *The kinematics of mixing: stretching, chaos, and transport*, Cambridge University Press,

Ozima M, Kudo K 1972 Excess argon in submarine basalts and an Earth-atmosphere evolution model. *Nature* **239,** 23-24

Palme H, O'Neill H S C 2003 Cosmochemical esimates of mantle composition. In: Carlson R W (ed.) *Treatise on Geochemistry*. Elsevier1-38

Parkinson I J, Hawkesworth C J, Cohen A S 1998 Ancient mantle in a modern arc: Osmium isotopes in Izu-Bonin-Mariana forearc peridotites. *Science* **281,** 2011-2013

Parman S W, Kurz M D, Hart S R, Grove T, L. 2005 Helium solubility in olivine and implications for high 3He/4He in ocean island basalts. *Nature* **437,** 1140-1143

Pearson D G, Davies G R, Nixon P H 1993 Geochemical constraints on the petrogenesis of diamond facies pyroxenites from the Beni Bousera peridotite massif, north Morocco. *J. Petrol.* **34,** 125-172

Peltier W R, Solheim L P 1992 Mantle Phase-Transitions and Layered Chaotic Convection. *Geophysical Research Letters* **19,** 321-324

Petford N, Yuen D, Rushmer T, Brodholt J, Stackhouse S 2005 Shear-induced material transfer across the core-mantle boundary aided by the post-perovskite phase transition. *Earth Planets Space* **57,** 459-464

Phipps Morgan J 1998 Thermal and rare gas evolution of the mantle. *Chemical Geology* **145,** 431-445

Phipps Morgan J 1999 Isotope topology of individual hotspot basalt arrays: Mixing curves or melt extraction trajectories? *Geochem. Geophys. Geosyst.* **1,** Paper Number 1999GC000004

Phipps Morgan J 2001 Thermodynamics of pressure release melting of a veined plum pudding mantle. *Geochem. Geophys. Geosyst.* **2,** Paper number 2000GC000049 [15,429 words, 10 figures, 1 table, 2 appendix figures, 1 appendix table]

Phipps Morgan J, Morgan J 1999 Two-stage melting and the geochemical evolution of the mantle: a recipe for mantle plum-pudding. *Earth Planet. Sci. Lett.* **170,** 215-239
Poirier J P 1993 Core-infiltrated mantle and the nature of the D'' layer. *J. Geomag. Geoelectr.* **45,** 1221-1227
Poirier J P, Le Mouel J L 1992 Does infiltration of core material into the lower mantle affect the observed geomagnetic field? *Phys. Earth Planet. Int.* **73,** 29-37
Poirier J P, Malavergne V, Le Mouel J L 1998 Is there a thin electrically conducting layer at the base of the mantle? In: Gurnis M, Wysession M E, Knittle E, Buffett B A (eds.) *The core-mantle boundary region*. American Geophysical Union,Washington, D. C.,131-137
Polve M, Allegre C J 1980 Orogenic lherzolite complexes studies by 87Rb-87Sr: A clue to understand the mantle convection processes? *Earth Planet. Sci. Lett.* **51,** 71-93
Porcelli D, Halliday A N 2001 The core as a possible source of mantle helium. *Earth Planet. Sci. Lett.* **192,** 45-56
Porcelli D, Wasserburg G J 1995 Mass Transfer of Helium, Neon, Argon, and Xenon through a Steady-State Upper Mantle. *Geochimica et Cosmochimica Acta* **59,** 4921-4937
Puster P, Jordan T H 1994 Stochastic-Analysis Of Mantle Convection Experiments Using 2-Point Correlation-Functions. *Geophysical Research Letters* **21,** 305-308
Puster P, Jordan T H 1997 How stratified is mantle convection? *J. Geophys. Res.* **102,** 7625-7646
Puster P, Jordan T H, Hager B H 1995 Characterization Of Mantle Convection Experiments Using 2-Point Correlation-Functions. *Journal Of Geophysical Research Solid Earth* **100,** 6351-6365
Reisberg l, Zindler A 1986 Extreme isotopic variability in the upper mantle: evidence from Ronda. *Earth Planet. Sci. Lett.* **81,** 29-45
Revenaugh J, Sipkin S A 1994 Seismic evidence for silicate melt atop the 410-km mantle discontinuity. *Nature* **369,** 474-476
Reymer A, Schubert G 1984 Phanerozioc addition rates to the continental crust and crustal growth. *Tectonics* **3,** 63-77
Ricard Y, Froidevaux C, Fleitout L 1988 Global Plate Motion and the Geoid - a Physical Model. *Geophysical Journal Oxford* **93,** 477-484
Ricard Y, Vigny C, Froidevaux C 1989 Mantle heterogeneities, geoid, and plate motion - a Monte-Carlo inversion. *J. Geophys. Res.* **94,** 13739-13754
Richard G, Monnereau M, Ingrin J 2002 Is the transition zone an empty water reservoir? Inferences from numerical models of mantle dynamics. *Earth. Plan. Sci. Lett.* **205,** 37-51
Richards M A, Davies G F 1989 On the Separation Of Relatively Buoyant Components From Subducted Lithosphere. *Geophysical Research Letters* **16,** 831-834
Richards M A, Engebretson D C 1992 Large-Scale Mantle Convection and the History Of Subduction. *Nature* **355,** 437-440
Richards M A, Griffiths R W 1989 Thermal Entrainment By Deflected Mantle Plumes. *Nature* **342,** 900-902
Richardson L F 1926 Atmospheric diffusion shown on a distance-neighbor graph. *proc. R. Soc. London* **110,** 709-?
Richter F M, Daly S F, Nataf H C 1982 A Parameterized Model For the Evolution Of Isotopic Heterogeneities In a Convecting System. *Earth and Planetary Science Letters* **60,** 178-194
Richter F M, Johnson C E 1974 Stability of a chemically layered mantle. *J. Geophys. Res.* **79,** 1635-1639
Richter F M, McKenzie D 1981 On some consequences and possible causes of layered mantle convection. *J. Geophys. Res.* **86,** 6133-6142
Richter F M, Ribe N M 1979 On the importance of advection in determining the local isotopic composition of the mantle. *Earth Planet. Sci. Lett.* **43,** 212-222
Righter K, Drake M J 2003 Partition coefficients at high pressure and temperature. In: Carlson C W (ed.) *Treatise on Geochemistry, Vol 2: The mantle and core*. Elsevier,Amsterdam,425-449

Ringwood A E 1990a Earliest history of the Earth-Moon system. In: Newsom H E, Jones J H (eds.) *Origin of the Earth*. Oxford University Press,New York,101-134
Ringwood A E 1990b Slab-mantleinteractions.3. Petrogenesis of intraplate magmas and structure of the upper mantle. *Chem. Geol.* **82,** 187-207
Ringwood A E 1991 Phase-Transformations and Their Bearing On the Constitution and Dynamics Of the Mantle. *Geochimica Et Cosmochimica Acta* **55,** 2083-2110
Ringwood A E 1994 Role Of the Transition Zone and 660 Km Discontinuity In Mantle Dynamics. *Physics Of the Earth and Planetary Interiors* **86,** 5-24
Ringwood A E, Irifune T 1988 Nature Of the 650-Km Seismic Discontinuity - Implications For Mantle Dynamics and Differentiation. *Nature* **331,** 131-136
Romanowicz B 2001 Can we resolve 3D density heterogeneity in the lower mantle? *Geophysical Research Letters* **28,** 1107-10
Rubie D C, Melosh H J, Reid, Liebske C, Righter K 2003 Mechanisms of metal-silicate equilibration in the terrestrial magma ocean. *Earth & Planetary Science Letters* **205,** 239-55
Rudge J F 2006 Mantle pseudo-isochrons revisited. *Earth Planet. Sci. Lett.* **249,** 494-513
Rudge J F, McKenzie D, Haynes P H 2005 A theoretical approach to understanding the isotopic heterogeneity of mid-ocean ridge basalt. *Geochim. Cosmochem. Acta* **69,** 3873-3887
Rudnick R L 1995 Making continental crust. *Nature (London)* **378,** 571-578
Rudnick R L, Fountain D M 1995 Nature and composition of the continental crust; a lower crustal perspective. *Reviews of Geophysics* **33,** 267-309
Ruepke L, Phipps Morgan J, Hort M, Connolly J A D 2004 Serpentine and the subduction zone water cycle. *Earth Planet. Sci. Lett.* **223,** 17-34
Saal A E, Hart S R, Shimizu N, Hauri E H, Layne G D 1998 Pb isotopic variability in melt inclusions from oceanic island basalts, Polynesia. *Science* **282,** 1481-4
Saal A E, Hauri E H, Langmuir C H, Perfit M R 2002 Vapour undersaturation in primitive mid-ocean-ridge basalt and the volatile content of Earth's upper mantle. *Nature* **419,** 451-455
Samuel H, Farnetani C G 2003 Thermochemical convection and helium concentrations in mantle plumes. *Earth and Planetary Science Letters* **207,** 39-56
Sarda P, Moreira M, Staudacher T 1999 argon-Lead isotopic correlation in mid-Atlantic ridge basalts. *Science* **283,** 666-668
Schersten A, Elliott T, Hawkesworth C, Norman M 2004 Tungsten isotope evidence that mantle plumes contain no contribution from the Earth's core. *Nature* **427,** 234-237
Schilling J-G 1973 Iceland mantle plume: Geochemical study of Reykjanes ridge. *Nature* **242,** 565-571
Schmalzl J, Hansen U 1994 Mixing the Earths mantle by thermal-convection - a scale-dependent phenomenon. *Geophys. Res. Lett.* **21,** 987-990
Schmalzl J, Houseman G A, Hansen U 1995 Mixing properties of three-dimensional (3-D) stationary convection. *Phys. Fluids* **7,** 1027-33
Schmalzl J, Houseman G A, Hansen U 1996 Mixing in vigorous, time-dependent three-dimensional convection and application to Earth's mantle. *J. Geophys. Res.* **101,** 21847-58
Schmalzl J, Loddoch A 2003 Using subdivision surfaces and adaptive surface simplification algorithms for modeling chemical heterogeneities in geophysical flows. *Geochem. Geophys. Geosyst.* **4,** doi:10.1029/2003GC000578
Schott B, Yuen D A 2004 Influences of dissipation and rheology on mantle plumes coming from the D"-layer. *Phys. Earth Planet. Int.* **146,** 139-145
Schott B, Yuen D A, Braun A 2002 The influences of composition-and temperature- dependent rheology in thermal-chemical convection on entrainment of the D "-layer. *Physics of the Earth & Planetary Interiors* **129,** 43-65
Schubert G, Masters G, Olson P, Tackley P 2004 Superplumes or plume clusters? *Physics of the Earth & Planetary Interiors* **146,** 147-162
Scrivner C, Anderson D L 1992 The Effect Of Post Pangea Subduction On Global Mantle Tomography and Convection. *Geophysical Research Letters* **19,** 1053-1056

Shaw D M 1970 Trace element fractionation during anatexis. *Geochim. Cosmochim. Acta* **34,** 237-242

Sleep N H 1984 Tapping Of Magmas From Ubiquitous Mantle Heterogeneities - an Alternative to Mantle Plumes. *Journal Of Geophysical Research* **89,** 10029-41

Sleep N H 1988 Gradual entrainment of a chemical layer at the base of the mantle by overlying convection. *Geophys. J. Oxford* **95,** 437-447

Sleep N H 1990 Hotspots and Mantle Plumes - Some Phenomenology. *Journal Of Geophysical Research Solid Earth and Planets* **95,** 6715-6736

Sleep N H 2000 Evolution of the mode of convection within terrestrial planets. *Journal of Geophysical Research* **105,** 17563-78

Sleep N H, Zahnle K 2001 Carbon dioxide cycling and implications for climate on ancient Earth. *Journal of Geophysical Research* **106,** 1373-99

Smolarkiewicz P K, Margolin L G 1998 MPDATA: a finite-difference solver for geophysical flows. *Journal of Computational Physics* **140,** 459-80

Sneeringer M, Hart S R, Shimizu N 1984 Strontium and samarium diffusion in diopside. *Geochim. Cosmochim. Acta* **48,** 1589-1608

Sobolev A V 1996 Melt inclusions in minerals as a source of principal petrological information. *Petrology* **4,** 209-220

Sobolev A V, Hofmann A W, Nikogosian I K 2000 Recycled oceanic crust observed in 'ghost plagioclase' within the source of Mauna Loa lavas. *Nature* **404,** 986-990

Sobolev A V, Shimizu N 1993 Ultra-depleted primary melt included in an olivine from the Mid-Atlantic Ridge. *Nature* **363,** 151-154

Solomatov V S 2000 Fluid dynamics of a terrestrial magma ocean. In: Canup R M, Righter K (eds.) *Origin of the Earth and Moon*. The University of Arizona Press,Tucson, AZ,

Solomatov V S, Moresi L N 2002 Small-scale convection in the D" layer. *Journal of Geophysical Research* **107,** doi:10.1029/2000JB000063

Solomatov V S, Olson P, Stevenson D J 1993 Entrainment From a Bed Of Particles By Thermal-Convection. *Earth and Planetary Science Letters* **120,** 387-393

Solomatov V S, Stevenson D J 1993a Nonfractional Crystallization Of a Terrestrial Magma Ocean. *Journal Of Geophysical Research-Planets* **98,** 5391-5406

Solomatov V S, Stevenson D J 1993b Suspension In Convective Layers and Style Of Differentiation Of a Terrestrial Magma Ocean. *Journal Of Geophysical Research-Planets* **98,** 5375-5390

Song T-R A, Helmberger D V, Grand S P 2004 Low-velocity zone atop the 410-km seismic discontinuity in the northwestern United States. *Nature* **427,** 530-533

Song X, Ahrens T J 1994 Pressure-Temperature Range Of Reactions Between Liquid-Iron In the Outer Core and Mantle Silicates. *Geophysical Research Letters* **21,** 153-156

Spence D A, Ockendon J R, Wilmott P, Turcotte D L, Kellogg L H 1988 Convective mixing in the mantle: The role of viscosity differences. *Geophys. J.* **95,** 79-86

Stacey F D 1992 *Physics of the Earth*, Brookfield Press, Kenmore, Queensland, Australia

Staudacher T, Allegre C J 1989 Recycling of oceanic crust and sediments: the noble gas subduction barrier. *Earth Planet. Sci. Lett.* **89,** 173-183

Stegman D R, Richards M A, Baumgardner J R 2002 Effects of depth-dependent viscosity and plate motions on maintaining a relatively uniform mid-ocean ridge basalt reservoir in whole mantle flow. *J. Geophys. Res.* **107,** 10.1029/2001JB000192

Stein M, Hofmann A W 1994 Mantle Plumes and Episodic Crustal Growth. *Nature* **372,** 63-68

Stevenson D J 1988 Infiltration, dissolution, and underplating: Rules for mixing core-mantle cocktails. *EOS Trans. AGU, Fall Meeting Suppl.* **69,** 1404

Stevenson D J 1990 Fluid dynamics of core formation. In: Newman H E, Jones J H (eds.) *Origin of the Earth*. Oxford University Press231-249

Stracke A, Hofmann A W, Hart S 2005 FOZO, HIMU, and the rest of the mantle zoo. *Geochem. Geophys. Geosyst.* **6,** doi:10.1029/2004GC000824

Stracke A, Zindler A, Salters V J M, McKenzie D, Blichert-Toft J, Albarade F, Gronvold K 2003 Theistareykir revisited. *Geochem. Geophys. Geosyst.* **4(2),** doi:10.1029/2001GC000201

Stuart F M, Lass-Evans S, Fitton J G, Ellam R M 2003 High 3He/4He ratios in picritic basalts from Baffin Island and the role of a mixed reservoir in mantle plumes. *Nature* **424,** 57-59

Suen C J, Frey F A 1987 Origins of mafic and ultramafic rocks in the Ronda peridotite. *Earth Planet. Sci. Lett.* **85,** 183-202

Tackley P J 1998 Three-dimensional simulations of mantle convection with a thermochemical CMB boundary layer: D"? In: Gurnis M, Wysession M E, Knittle E, Buffett B A (eds.) *The Core-Mantle Boundary Region.* American Geophysical Union231-253

Tackley P J 2000 Mantle convection and plate tectonics: towards an integrated physical and chemical theory. *Science* **288,** 2002

Tackley P J 2002 Strong heterogeneity caused by deep mantle layering. *Geochem. Geophys. Geosystems* **3,** 10.1029/2001GC000167

Tackley P J, King S D 2003 Testing the tracer ratio method for modeling active compositional fields in mantle convection simulations. *Geochem. Geophys. Geosyst.* **4,** doi:10.1029/2001GC000214

Tackley P J, Stevenson D J, Glatzmaier G A, Schubert G 1994 Effects of multiple phase transitions in a 3-dimensional spherical model of convection in Earth's mantle. *J. Geophys. Res.* **99,** 15877-15901

Tackley P J, Xie S 2002 The thermo-chemical structure and evolution of Earth's mantle: constraints and numerical models. *Phil. Trans. R. Soc. Lond. A* **360,** 2593-2609

Tackley P J, Xie S, Nakagawa T, Hernlund J W 2005 Numerical and laboratory studies of mantle convection: Philosophy, accomplishments and thermo-chemical structure and evolution. In: Van Der Hilst R D, Bass J, Matas J, Trampert J (eds.) *AGU Geophysical Monograph on Earth's Deep Mantle: Structure, Composition and Evolution*. AGU85-102

Tajika E, Matsui T 1992 Evolution Of Terrestrial Proto-Co2 Atmosphere Coupled With Thermal History Of the Earth. *Earth and Planetary Science Letters* **113,** 251-266

Tajika E, Matsui T 1993 Evolution Of Sea-Floor Spreading Rate-Based On Ar-40 Degassing History. *Geophysical Research Letters* **20,** 851-854

Taylor S R, McLennan S M 1995 The geochemical evolution of the continental crust. *Reviews of Geophysics* **33,** 241-265

Ten A, Yuen D A, Larsen T B, Malevsky A V 1996 The Evolution Of Material-Surfaces In Convection With Variable Viscosity As Monitored By a Characteristics-Based Method. *Geophysical Research Letters* **23,** 2001-2004

Ten A, Yuen D A, Podladchikov Y Y, Larsen T B, Pachepsky E, Malevsky A V 1997 Fractal Features In Mixing Of Non-Newtonian and Newtonian Mantle Convection. *Earth and Planetary Science Letters* **146,** 401-414

Ten A A, Podladchikov Y Y, Yuen D A, Larsen T B, Malevsky A V 1998 Comparison of mixing properties in convection with the particle-line method. *Geophys. Res. Lett.* **25,** 3205-8

Tolstikhin I N, Hofmann A W 2005 Early crust on top of the Earth's core. *Phys. Earth Planet. Int.* **148,** 109-130

Tolstikhin I N, Kramers J D, Hofmann A W 2006 A chemical Earth model with whole mantle convection: The importance of a core-mantle boundary layer (D") and its early formation. *Chem. Geol.* **226,** 79-99

Tonks W B, Melosh H J 1990 The physics of crystal settling and and suspension in a turbulent magma ocean. In: Newsom H E, Jones J H (eds.) *Origin of the Earth*. Oxford University Press,New York,151-174

Trampert J, Deschamps F, Resovsky J S, Yuen D 2004 Probabilistic tomography maps significant chemical heterogeneities in the lower mantle. *Science* **306,** 853-856

Trieloff M, Kunz J, Clague D A, Harrison D, Allegre C J 2000 The nature of pristine noble gases in mantle plumes. *Science* **288,** 1036-1038

Turcotte D L, Paul D, White W M 2001 Thorium-uranium systematics require layered mantle convection. *Journal of Geophysical Research* **106,** 4265-76
Turcotte D L, Schubert G 1982 *Geodynamics: Applications of Continuum Physics to Geological Problems*, Wiley, New York
Turner G 1989 The outgassing history of the Earth's atmosphere. *J. Geol. Soc. Lond.* **146,** 147-154
van den Berg A P, Jacobs M H, de Jong B H 2002 Numerical models of mantle convection based on thermodynamic data for the MgOSiO2 olivine-pyroxene system. *EOS Trans. AGU, Fall Meeting Suppl.* **83,** Abstract MR72B-1041
van der Hilst R D, Karason H 1999 Compositional heterogeneity in the bottom 1000 kilometers of Earth's mantle: toward a hybrid convection model. *Science (USA)* **283,** 1885-8
Van der Hilst R D, Widlyantoro S, Engdahl E R 1997 Evidence for deep mantle circulation from global tomography. *Nature* **386,** 578-84
van Keken P, Zhong S 1999 Mixing in a 3D spherical model of present-day mantle convection. *Earth Planet. Sci. Lett. (Netherlands)* **171,** 533-47
van Keken P E, Ballentine C J 1998 Whole-mantle versus layered mantle convection and the role of a high-viscosity lower mantle in terrestrial volatile evolution. *Earth Planet. Sci. Lett.* **156,** 19-32
van Keken P E, Ballentine C J 1999 Dynamical models of mantle volatile evolution and the role of phase transitions and temperature-dependent rheology. *J. Geophys. Res.* **104,** 7137-51
van Keken P E, Ballentine C J, Hauri E H 2003 Convective mixing in the Earth's mantle. In: Carlson R W (ed.) *Treatise on Geochemistry*. Elsevier471-491
van Keken P E, Ballentine C J, Porcelli D 2001 A dynamical investigation of the heat and helium imbalance. *Earth and Planetary Science Letters* **188,** 421-34
van Keken P E, Karato S, Yuen D A 1996 Rheological control of oceanic crust separation in the transition zone. *Geophys. Res. Lett.* **23,** 1821-1824
van Keken P E, Kiefer B, Peacock S M 2002 High-resolution models of subduction zones: Implications for mineral hydration reactions and the transport of water into the deep mantle. *Geochem. Geophys. Geosyst.* **3,** DOI 10.1029/2001GC000256
van Keken P E, King S D, Schmeling H, Christensen U R, Neumeister D, Doin M P 1997 A comparison of methods for the modeling of thermochemical convection. *J. Geophys. Res.* **102,** 22477-95
van Thienen P, van den Berg A P, Vlaar N J 2004 Production and recycling of oceanic crust in the early Earth. *Tectonophysics* **386,** 41-65
van Thienen P, van Summeren J, van der Hilst R D, van den Berg A P, Vlaar N J 2005 Numerical study of the origin and stability of chemically distinct reservoirs deep in Earth's mantle. In: Van Der Hilst R D, Bass J, Matas J, Trampert J (eds.) *The Structure, Evolution and Composition of Earth's Mantle, AGU Geophysical Monograph*. AGU117-136
Vidale J E, Schubert G, Earle P S 2001 Unsuccessful initial search for a midmantle chemical boundary layer with seismic arrays. *Geophys. Res. Lett.* **28,** 859-862
Vlaar N J 1985 Precambrian geodynamical constraints. In: Tobi a C, Touret J L R (eds.) *The Deep proterozoic crust in the North Atlantic provinces*. D. Riedel Publishing Company3-20
Vlaar N J 1986 Archaean global dynamics. *Dutch contributions to the International Lithosphere Program; Meeting* **65**. 91-101
Walker R J, Morgan J W, Horan M F 1995 187Os enrichment in some mantle plume sources: Evidence for core-mantle interation? *Science* **269,** 819-822
Walzer U, Hendel R 1997a Tectonic episodicity and convective feedback mechanisms. *Phys. Earth Planet. Int.* **100,** 167-188
Walzer U, Hendel R 1997b Time-dependent thermal convection, mantle differentiation and continental-crust growth. *Geophysical Journal International* **130,** 303-25
Walzer U, Hendel R 1999 A new convection-fractionation model for the evolution of the principal geochemical reservoirs of the Earth's mantle. *Physics of the Earth and Planetary Interiors* **112,** 211-56

Weinstein S A 1992 Induced compositional layering in a convecting fluid layer by an endothermic phase-transition. *Earth Planet. Sci. Lett.* **113,** 23-39
Weinstein S A 1993 Catastrophic Overturn Of the Earths Mantle Driven By Multiple Phase-Changes and Internal Heat-Generation. *Geophysical Research Letters* **20,** 101-104
Wen L 2001 Seismic evidence for a rapidly-varying compositional anomaly at the base of the Earth's mantle beneath the Indian ocean. *Earth Planet. Sci. Lett.* **194,** 83-95
Wen L X 2002 An SH hybrid method and shear velocity structures in the lowermost mantle beneath the central Pacific and South Atlantic Oceans - art. no. 2055. *Journal of Geophysical Research-Solid Earth* **107,** 2055
Wen L X, Anderson D L 1997 Layered Mantle Convection - a Model for Geoid and Topography. *Earth & Planetary Science Letters* **146,** 367-377
White W M 1985 Sources of oceanic basalts: radiogenic isotope evidence. *Earth Planet. Sci. Lett.* **115,** 211-226
Williams Q, Garnero E J 1996 Seismic Evidence For Partial Melt At the Base Of Earths Mantle. *Science* **273,** 1528-1530
Wolf A 1986 Quantifying chaos with Lyapunov exponents. In: Holden a V (ed.) *Chaos*. Princeton University Press,Princeton, N.J.,273-290
Wood B J, Blundy J D 2003 Trace element partitioning under crustal and uppermost mantle conditions: The influences of ionic radius, cation charge, pressure, and temperature. In: Carlson R W (ed.) *Treatise on Geochemistry, Vol 2: The mantle and core*. Elsevier,Amsterdam,395-424
Xie S, Tackley P J 2004a Evolution of helium and argon isotopes in a convecting mantle. *Phys. Earth Planet. Inter.* **146,** 417-439
Xie S, Tackley P J 2004b Evolution of U-Pb and Sm-Nd systems in numerical models of mantle convection. *J. Geophys. Res.* **109, B11204,** doi:10.1029/2004JB003176
Xie S, Tackley P J 2004c Seismic heterogeneity caused by oceanic crustal differentiation and segregation in the convecting mantle. *Earth Planet. Sci. Lett.* **in preparation**
Xu-Dong L, Osher S 1996 Nonoscillatory high order accurate self-similar maximum principle satisfying shock capturing schemes. I. *SIAM Journal on Numerical Analysis* **33,** 760-79
Yabe T, Ogata Y, Takizawa K, Kawai T, Segawa A, Sakurai K 2002 The next generation CIP as a conservative semi-Lagrangian solver for solid, liquid and gas. *Elsevier. Journal of Computational & Applied Mathematics* **149,** 267-77
Yamazaki D, Karato S 2001 Some mineral physics contraints on the rheology and geothermal structure of Earth's lower mantle. *Amer. Mineral.* **86,** 385-391
Yokochi R, Marty B 2004 A determination of the neon isotopic composition of the deep mantle. *Earth Planet. Sci. Lett.* **225,** 77-88
Yoshida M, Ogawa M 2004 The role of hot uprising plumes in the initiation of plate-like regime of three-dimensional mantle convection. *Geophysical Research Letters* **31,** 5607
Zhong S 2006 Constraints on thermochemical convection of the mantle from plume heat flux, plume excess temperature, and upper mantle temperature. *J. Geophys. Res.* **111,** doi:10.1029/2005JB003972
Zhong S J, Hager B H 2003 Entrainment of a dense layer by thermal plumes. *Geophysical Journal International* **154,** 666-676
Zindler A, Hart S 1986 Geochemical geodynamics. *Earth Planet. Sci. Lett.* **14,** 493-571